A Pre-clinical Study of a Therapy for Rett Syndrome by Using a Relevant Transgenic Mouse Model

By

Khatereh Saei Arezoumand

A Thesis submitted to the Faculty of Graduate Studies of

The University of Manitoba

In partial fulfillment of the requirements of the degree of

MASTER OF SCIENCE

Department of Biochemistry and Medical Genetics

Max Rady College of Medicine, Rady Faculty of Health Sciences

University of Manitoba

Winnipeg, Manitoba, Canada

Abstract

Rett Syndrome (RTT) is a severe neurodevelopmental disorder mainly affecting females. After a normal developmental period, symptoms appear at the age of 6-18 months, including developmental regression and loss of learned skills such as speech and purposeful hand movements. *De novo* mutations in the Methyl CpG Binding Protein 2 (*MECP2)* gene, which codes the MeCP2 protein are the underlying cause of over 95 % of RTT cases. MeCP2 is an epigenetic reader of methylated DNA, which controls gene expression in various cell types of the brain, mainly neurons. The control of *MECP2* gene dosage expression is critical since over-expression and under-expression, or genetic mutations lead to neurological deficits including *MECP2* Duplication Syndrome (MDS) and RTT, which currently do not have any cure. The two main RTT-associated molecular signaling abnormalities such as impaired *MECP2-BDNF-miR132* homeostasis and compromised mammalian Target of the Rapamycin (mTOR) pathway have been detected. Metformin (an anti-diabetic drug) is an inducer of *MECP2E1*/*BDNF* transcripts in brain cells *in vitro,* and an inhibitor of the hepatic mTOR pathway. However, it is unclear whether these effects of metformin can be detected in murine brain tissues. Furthermore, due to the drug safety profile, low price, and penetrability of metformin through the blood-brain barrier, it has been re-purposed in various neurodevelopmental disorders. As a result, metformin may regulate RTT-associated abnormalities and improve RTT-like phenotypes of an RTT mouse model. Consequently, in my thesis, I aim to reveal the gap in knowledge regarding the *Mecp2*-deficient abnormalities at the basal level as well as after metformin treatment for therapeutic purposes. To accomplish these aims, metformin, and vehicle treatments in Wild Type mice, monitoring of body weight, measurement of blood glucose level, and tissue collection for molecular analysis were completed. The results confirmed the safety of metformin treatment through intraperitoneal injection, and its sex- and region-dependent effects at the molecular level. Furthermore, metformin treatments in mutant mice showed an age- and sex-dependent improvement of the RTT-like symptoms at the phenotypical and behavioral levels. In conclusion, our study provides proof of principle for the effect of metformin on RTT-like abnormalities at the basal level and its therapeutic effects at the molecular, phenotypical, and behavioral levels in mice. These results offer an important insight for future re-purposing of metformin for the treatment of neurological disorders including RTT.

Acknowledgments

This dissertation is the result of over 3 years of constant effort and a mixture of experiences including victorious, achievements, learning, obstacles, frustrations, and failures which ultimately led to a stronger and superior version of me. I am grateful to all who assisted me and encouraged me during this journey.

Above all, my deepest appreciation is presented to my supervisor, Professor Mojgan Rastegar. You are one of the best Principal Investigators that any student could have. The opportunities you provided for me were priceless for my improvement as an international graduate student and it has been a pleasure working in your lab. You have tried to motivate me toward research by giving me enough time to adjust myself to my working environment and simultaneously overseeing my performance through your availability for guidance. I am extremely grateful for the training and endless support that you offered me in all aspects of my academic program. Your supervision and perceptions accelerated my learning process and assisted me to improve my critical thinking and reasoning skills. Furthermore, your patience encouraged me to constantly learn and develop my skills. Much grateful for your perpetual support and insightful comments throughout my program.

Secondly, I would like to express my most tremendous gratefulness to my Advisory Committee members, Dr. Jeffrey Wigle, and Dr. Tabrez Siddiqui for their encouragement, time, support, and insightful guidance in improving my project. During my program, your perceptive comments directed me through the right path of my thesis and broadened my horizon. I profoundly appreciate your kindness, support, and guidance. In addition, I am especially grateful to Dr. Siddiqui, who offered me the opportunity to perform behavioral tests in his behavioral room in BMSB and under his guidance.

Thirdly, in the case of teamwork in Prof. Rastegar's lab, I appreciate Carl Olson, our senior technician, for all his guidance during different steps of experiments including mice brain dissection, and tissue collection. Also, I appreciate Annan Ali Sher, a prior technician in our lab for training me in the Western blot technique. Besides, I am grateful for the assistance of our previous and current research associates including Dr. Shervin Pejhan, Dr. Mehran Nasr Esfahani, Dr. Arsalan Alizadeh, and Abbas Rezaian in terms of animal studies.

Likewise, I am grateful for the assistance of other lab members, including Marjorie Buist, a previous master's student in the case of animal studies, as well as Sandhini Lockman, and Nada El Tobgy in terms of the Western blot technique.

In the fourth place, I express my appreciation to the Biochemistry and Medical Genetics (BMG) Department at the University of Manitoba which supported me through different aspects of my program. All the facilities, equipment, resources, and interactions are provided in BMG to help students to thrive in different aspects including educational, occupational, and social life, and benefit from developing their theoretical and practical knowledge in their field of expertise.

Fifth, in the case of financial support, I highly appreciate my stipend from Prof. Rastegar grants (ORSA, NSERC-DG, CIHR-project grant, and the GETS) and the financial support of Research Manitoba through Maser's studentship award. Furthermore, I am grateful to the BMG and the Faculty of Graduate Studies (FGS) for the different awards that aided my tuition.

Next, I can not state my appreciation in words for my parents (Abbas and Mitra) who were supportive in all periods of my life. Without your endless love, support, faith, and sacrifice I would not be at this point. My brother (Aref) has always been a brilliant brother and had great support. Thank you, Aref for staying along with our parents when I was far from you. Now is the time to fulfill my dream of having my parents by my side and look forward to meeting you in Winnipeg.

Finally, I am forever grateful to my husband. This dissertation is an acknowledgment to you since, without you, this thesis would not have been feasible. You supported me as my precious love, my best friend, and my husband. I much appreciate you for loving me infinitely and motivating me each time I fell and have done your best to keep me happy in tough times. I am so blessed to have you in my life and forever appreciate your infinite love, unconditional support, and sacrifice, which was the greatest source of my inspiration and emotional support.

Dedication

Dedicated to my dearest family members

My husband, my lovely parents, and my brother

For their sacrifices, endless support, and belief in me and my abilities

The condition of your life is the reflection of your thoughts. You become the same person that you think about daily. Join these days and make a perfect person. You make your life, try to make the best one.

Do your best and God will do the rest!

Table of Contents

List of Figures

List of Tables

List of Abbreviations

AAV	Adeno-Associated Virus
Aβ	Amyloid-β
ACC	Acetyl-Coenzyme A Carboxylase
AD	Alzheimer's Disease
AMPK	AMP-Activated Protein Kinase
ASD	Autism Spectrum Disorders
ATRX	Alpha Thalassemia/mental Retardation Syndrome X-linked
BBB	Blood-Brain Barrier
BME	β-Mercaptoethanol
BMSB	Basic Medical Sciences Building
BSA	Bovine Serum Albumin
CACS	Central Animal Care Services
cAMP	cyclic Adenosine Monophosphate
CDK5	Cyclin-dependent kinase 5

CHRIM	Children's Hospital Research Institute of Manitoba
cKO	conditional KO
CNS	Central Nervous System
CRE	cAMP-Responsive Element
CREB	cAMP Response Element-Binding protein
CTD	C-Terminal Domain
4EBP	eIF4E Binding Protein
eEF2K	eukaryotic Elongation Factor 2 Kinase
eIF4B	eukaryotic Initiation Factor 4B
eIF4E	eukaryotic Initiation Factor 4E
EPM	Elevated Plus Maze
ER	Endoplasmic Reticulum
ERK	Extracellular-signal-Regulated Kinase
FBP	Fructose-1,6-Bisphosphatase
FTY720	Fingolimod (a sphingosine-1 phosphate analog)

FXS	Fragile X Syndrome
GMC	Genetic Model Center
HDACs	Histone Deacetylases
HD	Huntington's Disease
HFD	High-Fat Diet
HRP	Horseradish Peroxidase
ID	Intervening Domain
IGF1	Insulin-Like Growth Factor-1
IGF-1R	Insulin-Like Growth Factor-1 Receptor
IP	Intraperitoneal
MATE-1 and -2	Multidrug and Toxin Compound Extrusion-1 and -2
MBD	Methyl-Binding Domain
MDD	Major Depressive Disorder
MDS	*MECP2* Duplication Syndrome
MECP2	Methyl CpG Binding Protein 2 (human gene)

Mecp2	Methyl CpG Binding Protein 2 (mouse gene)
MeCP2	Methyl CpG Binding Protein 2 (protein)
MMP-9	Matrix Metalloproteinase-9
mTOR	mammalian Target of Rapamycin
NLS	Nuclear Localization Signal
NOR	New Objective Recognition
NTD	N-Terminal Domain
OCTs	Organic Cationic Transporters
OFT	Open Field Test
ORF	Open Reading Frame
P	Postnatal Day
PBS	Phosphate Buffer Saline
PD	Parkinson's Disease
PERK	Protein Kinase Endoplasmic Reticulum RNA-Like Kinase
PI	Preference Index

PKB	Protein Kinase B
PMAT	Plasma Membrane Monoamine Transporter
PTMs	Posttranslational Modifications
PVDF	Polyvinylidene Difluoride
rPS6	ribosomal Protein S6
RTT	Rett Syndrome
S6K1	p70S6 Kinase 1
SD	Standard Diet
siRNA	small interfering RNA
SK-1	Subtilisin/Kexin-isoenzyme-1
T2DM	Type 2 Diabetes Mellitus
THTR-2	Thiamine Transporter 2
TLE	Temporal Lobe Epilepsy
TrkB	Tropomyosin-related kinase B
TRAP1	Type 1 Receptor-Associated Protein

TRD	Transcription Repression Domain
TRIDs	Translational Readthrough-Inducing Drugs
TSC	Tuberous Sclerosis Complex
TSS	Transcription Start Site
ULK1/2	Unc-51-Like autophagy-activating Kinase ½
UPR	Unfolded Protein Response
UTR	Untranslated Region
WT	Wild Type
XCI	X-Chromosome Inactivation

Chapter 1. Introduction

1.1. Overview of Rett Syndrome

1.1.1. Etiology and Clinical Symptoms

Rett syndrome (RTT, MIM 312750) is a severe, X-linked, and rare neurodevelopmental disorder that happens in 1 in 10000 females [1-3]. After a normal developmental period of 6-18 months of age, symptoms appear through numerous steps (**Table 1.1**), including stagnation, rapid regression, plateau/pseudo-stationary, and late motor deterioration [4-6]. The first stage (stagnation) showed developmental regression in movement and speech abilities and reduced awareness. This stage is frequently ignored in diagnosis because parents and physicians may not detect these slight alterations. Throughout the rapid regression stage, the patients experience loss of hand movement and language skills, along with motor and breathing abnormalities [4]. Furthermore, the development of autistic-like characteristics such as social avoidance, and seizures are a possibility in patients. These conditions result in the plateau stage characterized by motor challenges and seizures, however the improvement of communication abilities. Finally, the entrance of children into the late motor descent stage happens, recognized by strict physical disability and wheelchair-bounding conditions [5].

In addition to the stages of the disease, some of the patients experience digestive struggles [7], reduced bone density [8], osteoporosis [9], scoliosis [10], urological dysfunction [11], and sleep troubles [12]. Moreover, RTT patients have an enhanced frequency of sudden mortality and usually die because of breathing and cardiac problems [13-15].

Using gene screening methods, mutations of the methyl-CpG-binding protein 2 (*MECP2*) gene were recognized as the reason for some RTT cases [3]. Then, *de novo* mutations in the *MECP2* gene were recognized as the main cause of over 95% of typical RTT cases [16]. Even though approximately 600 recognized mutations leading to RTT have been detected in *MECP2*, just 8 missense and nonsense mutations including T158M, R133C, R255X, R106W, R306C, R294X, R168X, and R270X comprise about 70% of all mutations in RTT [17] and a further 15% of mutations happen due to large deletions in *MECP2* gene. In addition, *MECP2*-related mutations have been linked to both intellectual disability [18] and autism [19].

Table 1.1. Clinical Presentations of RTT Patients. The clinical symptoms of RTT patients have been classified into 4 stages including stagnation, rapid regression, plateau/pseudo-stationary, and late motor deterioration. Each stage of the disease happens at a specific age and includes different symptoms. The start of the symptoms is at 6-18 months of age and ended up at 10 years of age. The information has been adapted from Vashi et al., 2019, and Kyle et al., 2018 [4, 5].

	Stage and age of onset	Symptoms
1	Stagnation (6-18 months)	• Developmental delays • Decreased eye contact • Possibility of stereotypic hand movements • Possibility of reduced brain size (microcephaly)
2	Rapid regression (1-4 years)	• Loss of purposeful hand skills • Loss of speech • Possibility of movement problems • Possibility of breathing abnormalities • Autistic-like characteristics • Development of microcephaly • Possibility of seizures
3	Plateau/pseudo-stationary (2 years)	• Hand apraxia/dyspraxia • Loss of movement ability • Loss of motor coordination problems • Improvement of communication abilities • Seizures
4	Late motor deterioration (10 years)	• Severe physical disability • Muscle faintness and stiffness • Possibility of wheelchair-binding

1.2. The Structure and Function of the *MECP2* Gene and MeCP2 Protein

The *MECP2* gene (**Figure 1.1**) is located on the X-chromosome and is around 76 kb [20], including transcription start site (TSS), the 4 exons, and 3 introns, along with multiple polyadenylation (Poly A) signals, which generates 2 isoforms (MeCP2E1 and MeCP2E2) through alternative splicing [21-25]. The exons 1, 3, and 4 encode MeCP2E1 which is the dominant isoform in the brain [23-25]. On the other site, exons 2, 3, and 4 encode MeCP2E2 which is expressed at higher levels than MeCP2E1 in the placenta and liver [24, 25]. The TSS at exon 1 and exon 2 leads to the formation of 2 proteins that differ just at their N-terminal region with 21 unique amino acids in MeCP2E1, whereas 9 amino acids in MeCP2E2 [25]. The *MECP2* gene codes the MeCP2 protein, which is a methyl-binding protein with various levels of expression in different human tissues and is abundantly expressed within neurons [26]. MeCP2 is an epigenetic regulator of gene transcription which mediates its role *via* binding exclusively to methylated DNA and cooperating with required proteins and complexes [27-29]. Initially, MeCP2 was defined as a suppressor of methylated DNA transcription *via* association with a co-repressor complex including mSin3A, a transcriptional repressor, and histone deacetylases, which can lead to chromatin compaction and gene silencing [30, 31]. Contrary to the initial discovery, the latest findings have exhibited that MeCP2 can be an activator of gene expression *via* connection with CREB (cAMP response element-binding protein), which is an activating factor [32]. The expression of *MECP2* is associated with the postnatal maturation of the Central Nervous System (CNS), and the differentiation of neurons [33]. The calculated MeCP2 protein molecular weight is around 53 kDa, but it has been detected at around 75 kDa and has 5 main domains including the N-terminal Domain (NTD), Methyl Binding Domain (MBD), Intervening Domain (ID), Transcription Repression Domain (TRD), and C-terminal Domain (CTD). Three AT-hook domains, which are located inside ID, TRD, and CTD facilitate the AT-rich DNA binding ability of MeCP2. The MBD plays a role in the binding ability of MeCP2 to methylated DNA, whereas the ID assists in the stabilization of the structure and binding capability of MBD. The TRD facilitates transcriptional repression through cooperation with the corepressor components, and the CTD enables MeCP2-chromatin binding [34, 35]. A study from our lab has shown that MeCP2E1 is equivalently expressed across diverse brain regions, while the MeCP2E2 isoform has different levels of expression in mouse brain regions [36].

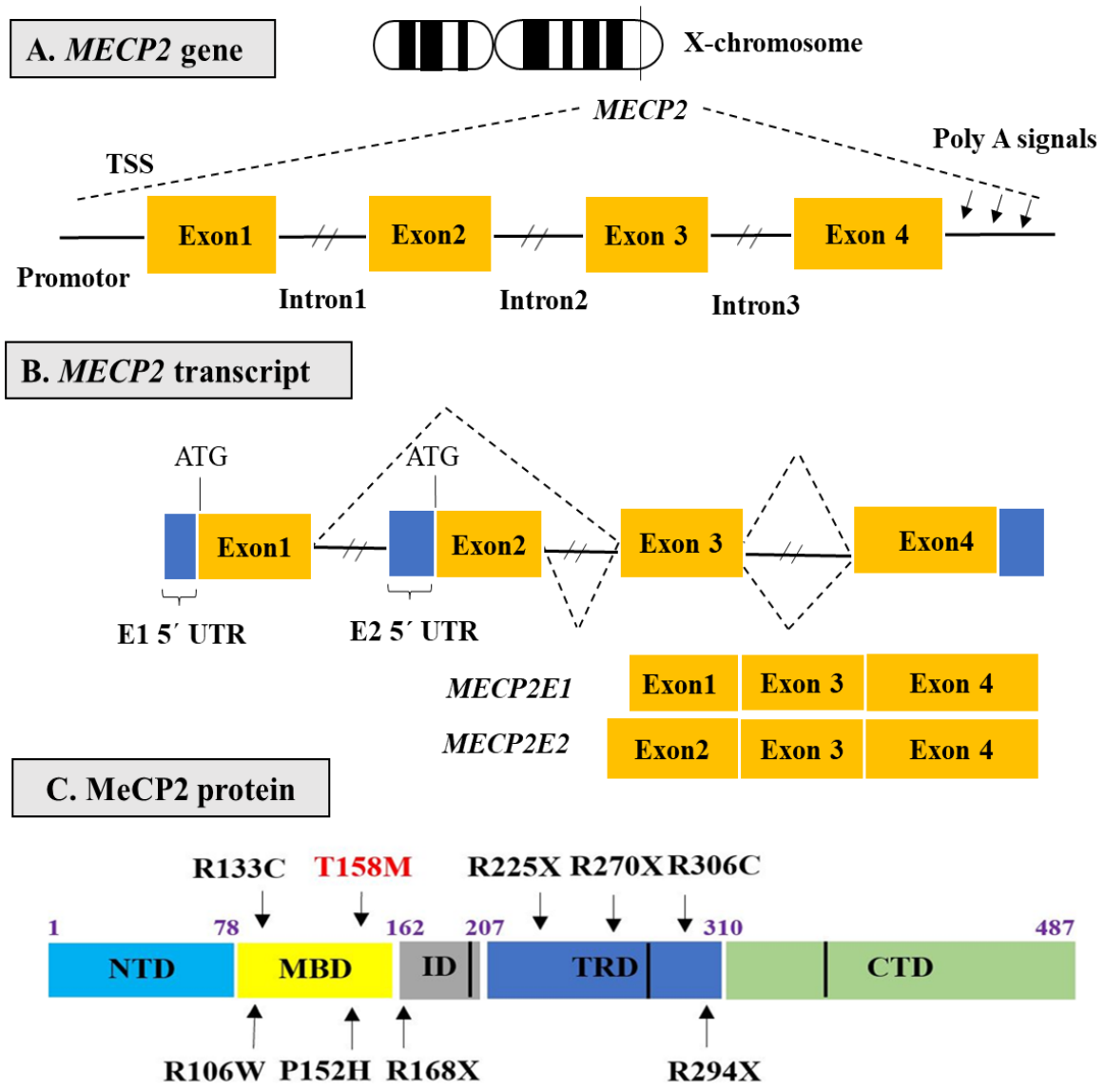

Figure 1.1. Schematic of the *MECP2* Gene and MeCP2 Protein Structures. A) The *MECP2* gene is located on the X-chromosome. **B**) Alternative splicing of the *MECP2* transcript generates the 2 isoform transcripts. The ATG is the translation start site which is indicated for each isoform. **C)** The MeCP2 protein contains 5 domains with specific functions. The **black** color shows the most common mutations, and the **red** color indicates the particular mutation (T158M) that we have studied. The number of amino acids at the start and the end of each domain are presented in **purple**. The figure has been adapted from Kyle et al., 2018; Liyanage and Rastegar 2014; Pejhan, and Rastegar, 2021 [5, 25, 35]. **A)** ***MECP2*:** Methyl-CpG Binding Protein 2 gene, **Poly A**: Polyadenylation signals. **B)** **Coding sequences**, **non-coding sequences**, **TSS**: Transcriptional Start Site, and **UTR**: Untranslated Region. **C**) **CTD**: C-Terminal Domain, **ID**: Intervening Domain, **MBD**: Methyl-CpG-Binding Domain**, NTD:** N-terminal Domain, **TRD**: Transcriptional Repression Domain.

1.3. Biological Systems to Study RTT

Since RTT is a monogenic disease and the result of *MECP2* gene mutations, numerous RTT animals [37, 38], and cellular models [39, 40] have been used for its study. The diverse phenotypes and various lifespans of these models have been explained as a limitation in different studies [4]. Contrary to humans, mice models display earlier and clearer symptoms of MeCP2-deficiency during development. Interestingly, the mice models contribute to our comprehension of the various brain region's roles in *Mecp2*-deficiency. Also, they are beneficial to examine probable curative methods as they show most symptoms detected in RTT patients [5]. Additionally, RTT-related models can be derived from MeCP2-mutant cell lines including neurons from human embryonic stem cells or mouse embryonic stem cells [41].

1.3.1. RTT-Mouse Models

1.3.1.1. *Mecp2* Null Mouse Models

Due to the lack of the *Mecp2* gene in non-vertebrates [42], RTT mouse models are required for the study of disease mechanisms. After the discovery of *MECP2* as the RTT-causing gene, two *Mecp2*-null mouse models (*Mecp2tm1.1Bird* and *Mecp2tm1.1Jae)* were generated, which lack MeCP2 protein products [37] or expresses minor MeCP2 protein pieces [43]. Consequently, both models show RTT-associated symptoms and have been widely used to study the disease mechanism. Although RTT mainly affects females, they demonstrate phenotypic variation because of skewed X-chromosome inactivation (XCI) or non-random XCI [44]. Consequently, most RTT mice studies happen in hemizygous *Mecp2*-mutant male mice owing to their stable phenotype and complete absence of MeCP2 protein, which is beneficial for mechanistic study [41]. Hemizygous male *Mecp2*-null mice show RTT-like symptoms including tremors, breathing abnormalities, hind limb clasping, hypoactivity, and deficiency of muscle tone [37, 43]. A decreased brain and body weight, a quick and severe regression of phenotypes, and death between 6-12 weeks of age are other symptoms of *Mecp2*-null male mice. Like males, heterozygous female mice show similar, but milder symptoms at a later age of development (4-6 months) and usually have a normal lifespan [4, 45].

1.3.1.2. *Mecp2*-Mutant Mouse Models

The knock-in or *Mecp2*-mutant mice models are different from knock-out or null mice due to the expression of mutant/truncated MeCP2 protein [43]. The exon 3 deletion of the *Mecp2* gene resulted in the formation of the Jaenisch strain (*Mecp*2tm1.1jae), expressing an MBD-deficient MeCP2 protein, showing similar behavioral symptoms to the *Mecp2* null mice with somewhat milder symptoms and longer lifespan [46]. Furthermore, establishing a premature STOP codon in the mouse *Mecp2* gene generated a mouse model with truncated proteins at amino acid 308 (*Mecp*2308). The *Mecp*2308 mouse model seems normal till about 6 weeks of age and then develops similar but milder neurological symptoms as *Mecp2* null mice [47]. *Mecp2*-mutant mouse models show an expansive scale of phenotypes observed in human RTT patients [4]. In both *Mecp2*-mutant mice and patients, motor defects are the extreme clinical presentation comprising diminished mobility, compromised motor coordination, gait, ataxic, and tremors [48]. Although patients lose purposeful hand movement leading to stereotypic hand wringing, mouse models show hind limbs clasping [37, 43]. At the phenotypical level, both *Mecp2* mouse models and patients display decreased brain volume and neuronal hypotrophy [49]. At the behavioral level, loss of speech abilities and neurological defects, are two characteristics specific to human patients, immeasurable in mouse models, but learning problems are common in both models [50, 51]. Interestingly, human patients showed higher anxiety and less sociability compared with *Mecp2*-mutant mice [45, 52, 53]. Metabolic disturbances in both models involve neurometabolic abnormalities [54], including enhanced cholesterol and triglycerides of serum [5, 55, 58], the irregular structure of mitochondria [57], and increased oxidative damage [58]. Eventually, both RTT patients and mouse models suffer from breathing and cardiac abnormalities [14, 59], seizures, and a reduced lifespan [37]. In general, *Mecp2*-mutant mice demonstrate a wide scope of phenotypes that phenocopy human RTT patients' symptoms, which makes them an outstanding model to study this disorder [37]. Since RTT patients mostly carry missense mutations leading to a less competent or unstable MeCP2 protein instead of a total loss of it, so *Mecp2*-null mouse models do not permanently represent human patients' circumstances at the molecular level. To avoid this limitation, numerous mouse models carrying *MECP2* point mutations have been generated to recapitulate clinically related mutations observed in human patients [4].

In RTT patients, 6 out of 8 most common missense mutations have established mouse models recapitulating disease symptoms. These mice have been helpful in the comprehension of RTT-causing mutation's contribution to the disease progression and severity of symptoms [4]. For instance, the MeCP2 T158M mutation shows severe symptoms in patients, whereas the R133C mutation leads to the maintenance of speech and motor [60]. Studies showed that whereas both mutations (T158M and R133C) produce MeCP2 proteins with decreased DNA-binding capability, the T158M mutation moreover results in unstable protein, and consequently more severe RTT-like phenotypes [61]. Although the *MECP2* gene is expressed as 2 isoforms, the levels of their expression differ among different tissues, and MeCP2E1 compared with MeCP2E2 is abundant in the brain [36, 62]. Studies that removed either one of MeCP2E1 or MeCP2E2 through the body noticed that only the removal of *MECP2E1* results in RTT-like symptoms and reduced life duration. In contrast, loss of *MECP2E2* was needed for the development of the placenta [63, 64]. Moreover, the MeCP2 protein undergoes various posttranslational modifications, involving phosphorylation at 421 (S421) and serine 80 (S80), significant for MeCP2-chromatin binding and its performance in the control of gene expression in neurons. As a result, mutation of either of these serine residues in mice stopped this site-dependent phosphorylation [65, 66].

The generation of mouse models including RTT-related mutations has been similarly completed. For instance, the insertion of a premature STOP codon in position 168 of the *Mecp2* gene resulted in the generation of a shortened MeCP2 protein including an integral MBD without the CTD, TRD, and nuclear localization signal (NLS) in the R168X mice model (*Mecp2*R168X). These mice show neurological symptoms including breathing abnormalities and hindlimb clasping like other mouse models [67]. The A140V MeCP2 mutant mice (*Mecp2*A140V) is another knock-in mouse model, which generates a mutant MeCP2 protein without the binding capability leading to Alpha thalassemia/mental retardation syndrome X-linked protein [68]. These *Mecp2*A140V mice have a seemingly normal lifespan without seizures, and breathing abnormalities detected in other mouse models, but they indicated decreased branching of dendrites as shown in RTT patients' brain autopsies [69]. Other models of *Mecp2* mouse carrying phosphorylation mutations include *Mecp2*S421A; S424A (increased spatial memory and synaptogenesis), *Mecp2*S80A (decreased mobility), and *Mecp2*S421A (increased dendrite branching) [65, 67, 70].

Most of the RTT-associated missense mutations recognized in patients occur in the MBD and TRD of MeCP2 in *Mecp2*^{T158M}, with one of the most common mutations happening at residue T158, changing it to a methionine (MeCP2 T158M) or alanine (T158A) in rare cases. To reveal the role of MeCP2 T158M mutation in RTT pathology, a *Mecp2*^{T158M} mouse model has been developed and showed many RTT-like symptoms. For instance, *Mecp2*$^{T158/y}$ male mice weighed significantly less compared with sex- and age-matched *Mecp2*$^{+/y}$ littermates at 4 weeks and afterward [71]. In the case of brain weights, in *Mecp2*$^{T158/y}$ male mice, it significantly decreased at the postnatal age of 42 days (P42) and P100 compared with *Mecp2*$^{+/y}$ littermates, and they showed early death compared with *Mecp2*$^{+/y}$ littermates. In contrast, *Mecp2*$^{T158/+}$ female mice weighed significantly more compared to *Mecp2*$^{+/+}$ littermates at P250 and P300, but they showed significantly reduced brain weight compared with *Mecp2*$^{+/+}$ littermates at P300. So, both sexes of the *Mecp2*^{T158M} mouse model showed RTT-like phenotypes in an age-dependent manner. Additionally, the *Mecp2*$^{T158/y}$ male mice showed significantly decreased survival compared with *Mecp2*$^{+/y}$ littermates. As a result, increasing MeCP2 T158M protein stability or expression level could improve RTT-like symptoms, which has been confirmed through an *in vivo* study in a Tg mouse model expressing MeCP2 T158M throughout the CNS. Another finding of this study showed that pharmacological elevation of MeCP2 T158M level rescues RTT-like phenotypes, which has been the focus of my thesis. In general, these discoveries reveal that decreased levels of MeCP2 T158M trigger RTT pathology and offer evidence that pharmacological elevation of MeCP2 protein stability or expression shows an efficient therapeutic method for the reversal of the RTT-associated abnormalities [71].

1.3.2. *Mecp2*-Deficient Cellular Models

Mecp2-deficient cultivated neuronal cells derived from postnatal or embryonic *Mecp2*-deficient mice showed biological and structural defects like *Mecp2* knockout mice [72-74]. *Mecp2*-deficient microglia and astrocytes have been proven to make irregular levels of solvable factors that prevent neuronal dendrite branching *in vitro*. Moreover, *Mecp2*-deficient astrocytes have also been indicated to affect the function of gap junction in astrocytes, leading to their failure to sufficiently sustain the dendrite's development [75-77].

Proof of cellular and mouse models show the complexity of MeCP2's role in the brain and its various function in various regions of the brain. Furthermore, the precise expression levels of MeCP2 in all brain-cell types are important for the normal function of the brain [41].

1.4. Mammalian Brain Development and Function

Mice studies have shown that MeCP2 protein expression is in close relation with the maturation of neurons and the greatest levels happen after the complete maturation of neurons [78, 79]. Consequently, it is significant to present a summary of the path of brain development in mammals to acquire vision into the potential time intervals of brain vulnerabilities to *Mecp2* dysfunction. Many stages have been involved in the complex process of mammalian brain development which is strictly controlled [80]. In mice, prenatal development of neurons happens, and then the rest of the process including proliferation, migration, and maturation happens at their destination. Numerous growth factors affect neurons in this process at various developmental steps [80, 81]. Contrary to the postnatal development of the brain in humans, in mice, it is completely prenatal [82]. Major events throughout the development of the brain involve the removal of neurons, and the formation, and elimination of synapses [81]. In the first week after birth, in the cortex of a rat, the formation of synapses reaches the highest level [82], whereas, in the hippocampus, the maximum rate of synaptogenesis is accomplished by P25 [83]. Similarly, in the cerebellum, synaptogenesis matches diverse cerebellar cell type's maturation with Purkinje cells producing the first synapses soon postnatally, however, granule cells start to generate synapses at P15 and endure till P30 [84, 85]. Also, the detected phenotypes in the case of MeCP2 abnormalities in both RTT models highlight the significance of MeCP2 functions in several brain regions [86] as shown in **Table 1.2**.

Table 1.2. Brain Regions' Function and Dysfunction in RTT.

Brain region	Function	Dysfunction
Olfactory bulb	Transmission of olfactory signals to the cortex	Unusual morphology of synapsis [87]
Cerebral cortex	Cognition, thinking, and ocular managing	Compromised motor coordination, unusual social activities [86]
Thalamus	Mobility and sensory perception	Seizures and disturbed sleep pattern [12, 87]
Hypothalamus	Regulation of homeostasis	Abnormal stress response [72, 86]
Hippocampus	Linkage of feelings to memories and spatial arrangement	Compromised intellectual capabilities [86]
Amygdala	Managing of memory communication related to feelings	Enhanced anxiety [72, 86]
Brainstem	Regulation of autonomic roles including digestion	Compromised movement and breathing irregularities [90]
Cerebellum	Regulation of coordination skills, intellectual acts, and muscle tone	Gait, lack of purposeful activities, and deterioration [12, 87]

Due to the association between RTT abnormalities with brain regions, a schematic of the adult murine brain has been provided in **Figure 1.2.** Consequently, understanding the function of each brain region and the correlated MeCP2 dysfunction phenotype is important in RTT therapeutic approaches. For instance, due to the involvement of the cerebellum in the control of coordination activities, muscle tone, consciousness, and language, MeCP2 dysfunction leads to abnormal gait, ataxia, and atrophy [87, 91]. Cerebral cortex-derived MeCP2 dysfunction leads to compromised motor coordination, and irregular social behavior since it plays a role in elevated intellectual functions such as visual processing and reasoning [86]. The hippocampus as a component of the limbic system participates in spatial organization and linking of emotions to memories. Thus, a deficiency of MeCP2 leads to impaired cognitive abilities (memory and learning) [86]. Furthermore, disturbed sleep patterns and seizures are attributed to the MeCP2 dysfunction in the thalamus involved in movement and sensory perception [12, 87].

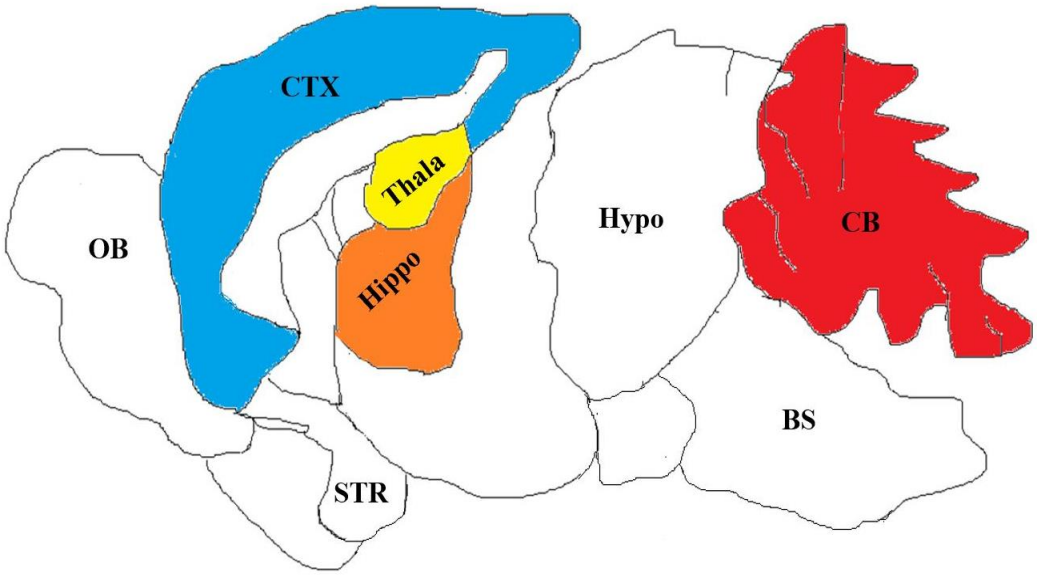

Figure 1.2. Schematic of the Adult Murine Brain. In this figure, 8 brain regions have been shown including the Brain stem (BS), Cerebellum (CB), Cortex (CTX), Hippocampus (Hippo), Hypothalamus (Hypo), Olfactory Bulb (OB), Striatum (STR), and Thalamus (Thala). However, we have studied the effect of metformin in 4 particular brain regions including CB, CTX, Hippo, and Thala due to their contribution to the RTT-like symptoms at the phenotypical and behavioral levels, which are shown in color [86, 87, 12, 92].

1.5. RTT-associated Therapeutic Approaches

Studies have identified *MECP2* downstream pathways with the possibility of target therapy *via* drug treatments to improve different signaling pathways including growth factor and neurotransmitter signaling along with metabolism. Significantly, numerous of these therapies improved RTT-like symptoms in *Mecp2*-mutant mice and have initiated clinical trials in patients. Conversely, these approaches showed various restrictions [93]. Initially, due to the unknown role of *MECP2*, recognizing it's regulating pathways, particularly those sensitive to *MECP2* loss, is challenging. Also, the recruitment of *MECP2* to DNA methylation is greatly cell-type-specific, which is another obstacle [94-96]. So, the genes under the control of *MECP2* will probably change depending on the status of methylation in different cell types at the given stage of development [97]. Lastly, it is hard to understand which pathways are mainly impacted due to *MECP2* mutation and which are less affected distant downstream that will probably have less significance as therapeutic targets [93, 98]. However, improvements in the techniques of molecular biology have facilitated resolving these problems. Here, we emphasize therapeutic approaches for RTT into 2 groups including direct targeting therapy of *MECP2* mutations (gene therapy, readthrough components, and reactivation of silent X) or targeting *MECP2* downstream pathways (neurotransmitter signaling, growth factor signaling, and metabolic defects in RTT) [4].

1.5.1. Direct Targeting of *MECP2/Mecp2* Gene

Directly targeting *MECP2/Mecp2* gene, leading to *MECP2/Mecp2* and its downstream pathways restoration is a fascinating therapeutic approach [4]. Nonetheless, dosage control is the biggest concern of this method, since both under-expression and overexpression of *MECP2* lead to human disorders [99]. Therefore, adequate *MECP2* levels per cell are required to be considered to fulfill its therapeutic advantage whereas decreasing the risk of overexpressed *MECP2* [4].

One approach includes targeting the mutations of *MECP2* with tiny molecules recognized as translational readthrough-inducing drugs (TRIDs) [4], which is an interesting method for 35-40% of RTT patients, carrying *MECP2* nonsense mutations [17]. TRIDs facilitate the read-through of premature stop codons by their ribosome binding ability and weakening codon/anticodon identification, permitting the introduction of another amino acid instead of the stop codon [100].

Since this method only enhances *MECP2* in cells including the nonsense mutation, without any effect on normal *MECP2* levels, concern does not exist regarding elevated dosages of *MECP2*. Nevertheless, since TRIDs produce a mutated *MECP2* instead of an entirely functional protein, it only marginally improves the RTT symptoms of patients. In general, this approach can be a valuable path to follow for RTT because even a minor increase in *MECP2* levels is connected to recovered symptoms. However, attempts are ongoing to increase the efficiency of TRIDs to help RTT patients. Another method of directly targeting *MECP2* is the reactivation of the silent X chromosome leading to the restoration of endogenic *MECP2*. In mammalian cells, the XCI suppresses one X chromosome in each cell for its dosage compensation [101]. Accordingly, because of the *MECP2* localization on the X chromosome, one copy of it has been silenced and in RTT patients' cells a normal copy of *MECP2* is inactive. So, RTT patients' cells can use their own regulatory functions for the regulation of *MECP2* expression [4].

Since RTT patients are heterozygous mosaics for *MECP2* mutation, a normal copy of *MECP2* is expressed in around half of their cells. Therefore, reactivation of inactivated X chromosome will cause 2x of *MECP2* normal levels in these cells. Consequently, this process requires to be modified to only target *MECP2* or its nearby areas and can only be a potential moderate therapeutic method for patients with *MECP2* loss-of-function mutations [4]. Prominently, the exclusive mice designed for the study of this method offer a tremendous path to examine Xi-reactivating drugs exactly for the RTT treatment [102].

Besides readthrough components and reactivation of silent X, gene therapy has been proposed as an ultimate probable therapeutic strategy for RTT by insertion of a normal copy of *MECP2* into cells [4, 95]. Gene therapy is an encouraging therapeutic method for numerous disorders and has been effective in the restoration of symptoms in different mouse models including obesity, diabetes, and ALS. In the case of RTT, gene therapy methods should use a suitable vector with the ability to cross the BBB and transduce several cells in the CNS and be capable of preserving the stable longstanding expression of the exogenous *MECP2*. Like the reactivation of Xi, gene therapy targets all cells despite the condition of *MECP2* mutation. Accordingly, cells including the normal *MECP2* will have double the normal level of the protein resulting in probable toxic effects of *MECP2* overexpression [4].

In addition to dosage concerns, high viral titers are other disadvantages in the case of gene therapy. In general, high viral titers are required to infect a great percentage of cells, however, cells that accidentally receive more than one viral fragment, and consequently more than one copy of *MECP2*, would be overloaded [4]. Approaches to avoid these problems can provide a factor like a small interfering RNA (siRNA) or silencing RNA, which are of double-stranded and non-coding RNA molecules, usually 20-24 base pairs length, to block endogenous *MECP2* leading to the exclusive expression of transgenic *MECP2* [103]. On the other hand, the advantages of recombinant adeno-associated virus (AAV) vectors including their capability to cross the BBB, infect neurons, and long-lasting and safe expression of transgene have made them beneficial for the preclinical studies of gene therapy, but upcoming studies should enhance the AAV9 therapy's specificity before transferring to the clinic [104, 105]. A further barrier to gene therapy includes the control of dosage in humans. Because of the small size of the mice, they cannot directly inform regarding the applicable doses for clinical purposes [4]. Also, due to recently reported harsh neuronal and hepatocyte poisonousness following high-dose AAV9 administration, attempts in the optimization of dosage will be necessary [106].

1.5.2. Indirect Targeting of Me*CP2* Downstream Pathways

In addition to directly targeting the mutated *MECP2/Mecp2* gene, other therapeutic approaches which target downstream signaling pathways including neurotransmitter and growth factor signaling along with the metabolic defects could be beneficial for the RTT treatment [4].

The decrease in dendrite size and number is an obvious attribute of RTT, and *Mecp2*-mutant mouse models. Dendrites sense neurotransmitters and electrical signals from neurons and a neurotransmitter signaling deficiency was suggested in RTT [107]. Target therapy of these pathways has proven diverse effects in mice, and some have been investigated in clinical trials [4]. For instance, in *Mecp2*-mutant mice, a norepinephrine reuptake suppressor improved breathing abnormalities [108], without any effect on RTT patients [109].

A sphingosine-1 phosphate analog called fingolimod (FTY720) has been demonstrated to enhance BDNF levels and improve mobility in *Mecp2*-mutant mice [110]. Like BDNF, the binding of Insulin-like growth factor-1(IGF) to its receptor (IGF-1R), triggers a signaling pathway, and IGF-1 levels are controlled by MeCP2 at the transcriptional level [111].

At the transcriptional level, BDNF was recognized as a *MECP2* target gene [112]. It is a member of the neurotrophin family of growth factors, binding to its receptor namely tropomyosin-related kinase B (TrkB) to induce downstream signaling related to neurite development, synaptic function, and differentiation of neurons [113]. In rodent brains, MeCP2 controls the production of mature BDNF (mBDNF, a neurotransmitter modulator) [114], derived from a precursor-BDNF (pro-BDNF), which is cleaved by extracellular proteases to convert into mBDNF. Pro-BDNF and mBDNF apply reciprocal impacts by binding to the p75 neurotrophic receptor (p75NTR) and TrkB receptors, respectively. The discrepancy in the ratio of mBDNF/pro-BDNF is connected to neuropsychiatric disorders [115]. In both RTT patients and *Mecp2*-mutant mice, the expression of brain *BDNF/Bdnf* is significantly decreased, but due to BDNF's incapability to pass through BBB, its administration is not a practical therapy [116, 117]. In fact, *BDNF* is a significant and possibly the most studied MeCP2 target gene. The association of BDNF with MeCP2 has been examined largely in animal models, but also in the context of human RTT patients [116, 118, 114]. The multi-promoter feature of the *BDNF* gene is important for further flexibility of BDNF expression in response to various scales of stimuli. Initially, BDNF was extracted from the brain of the pig with isoelectric points around 9-10, which is the reason for BDNF stability during biochemical purification [119]. BDNF protein is derived from a precursor polypeptide including 270 amino acids (pre-proBDNF) in the endoplasmic reticulum [120]. The deletion of the "pre" section of the synthesized protein, leads to the production of proBDNF, after transfer to the Golgi apparatus. The molecular weight of proBDNF is 32kDa, comprising the pro-domain and the mature BDNF, containing 129 and 118 amino acids, respectively [119]. Then, the cleavages of the proBDNF to a shortened form of BDNF (~28kDa molecular weight) by the subtilisin/kexin-isoenzyme-1 (SK-1) protease resulted in the generation of the final product. In fact, 3 distinct proteases including the matrix metalloprotease-7 (MMP-7), furin, and plasmin are involved in the production of the mature BDNF (mBDNF) (~14kDa) [120-122]. ProBDNF and mBDNF are localized in the secretory granules on mice hippocampal neurons [123] and segments of adult mice hippocampus [124]. The final processing of the mBDNF could similarly occur after secretion in the extracellular space [126]. The mechanism of regulation of BDNF by MeCP2 is controversial. Prior findings were more supporting a repression model as membrane depolarization can relieve MeCP2 from its binding site at the *Bdnf* promoter IV, leading to the transcriptional activation of *Bdnf* [126].

The phosphorylation of MeCP2 at Ser421 and decreased CpG sites methylation within the *Bdnf* promoter IV provoked by neuronal depolarization were imagined to trigger the separation of MeCP2 and its corepressors (HDAC1 and Sin3a) from the *Bdnf* promoter IV [127].

In the *Mecp2*-null mice, studies exhibited reduced *Bdnf* mRNA and protein, proposing an activator role for MeCP2 in *Bdnf* transcription [117, 128]. The dual role of MeCP2 in the regulation of BDNF describes these divergences [129]. A study in neuroblastoma cells showed that MeCP2 attaches to promoters of its target genes and can activate or repress these target genes' expression [130]. Besides phosphorylation, other epigenetic modifications contribute to the MeCP2 double-performing model. For example, MeCP2 regulates the transcription of microRNAs targeting the 3'UTR of *Bdnf* transcripts [131]. Likewise, MeCP2 alterations might affect the transcriptional expression of *BDNF/Bdnf* besides the BDNF protein stability or synthesis. That could describe some of the divergences between the various models that have studied BDNF at the transcript or protein level [132]. Noteworthy, MeCP2 regulation is *via* the regulatory connection of BDNF-MeCP2 which includes phosphorylation of MeCP2 at serine residues that help in reaction to specific drugs [133, 134].

In addition to neurotransmitter and growth factor signaling, RTT-associated metabolic deficits can be pharmaceutically targeted [4]. It is shown that in *Mecp2*-mutant mice, before the initiation of symptoms, a significant increase of cholesterol in the brain, and triglycerides were detected in the liver and serum [55]. In addition to mice, some RTT patients showed elevated levels of lipids, indicating that treatment with statin drugs may benefit them [58, 135]. Defects in cholesterol homeostasis are correlated with numerous neurological disorders including RTT [136, 137]. Besides cholesterol synthesis defects, both RTT patients and *Mecp2*-mutant mouse models show irregular structure and function of the mitochondria [138-140]. Notably, impaired mitochondrial function can seriously affect the generation of cellular energy. Although mitochondria are essential in all body cells, their role is particularly significant in tissues requiring high energy. RTT has shown common symptoms with mitochondrial disorders, containing early symptomatic initiation, developmental and neurological regression, digestive problems, and seizures [141]. Regularly, both RTT patients and *Mecp2*-mutant mice are characterized by enhanced oxidative stress and reduced mitochondrial enzyme levels [139, 142]. In general, these studies indicate deficiencies in the generation of energy by mitochondria in RTT, which is associated with the synthesis of cholesterol.

Fascinatingly, anaplerotic substances can reload intermediate mixtures in the energy creation pathway, increasing mitochondrial-mediate energy production. For instance, triheptanoin reversed some symptoms of metabolic diseases by modifying the generation of energy [143, 144].
In addition to cholesterol impairment, the compromised glucose metabolism could be targeted as an RTT-associate therapy [145], which will be elaborated in the case of brain metabolism and the role of MeCP2.

1.6. MeCP2 and Brain Metabolism

RTT patients' reformed neural activity has been connected to impairments of glucose metabolism [5]. An enhanced level of cerebral glucose metabolism in the frontal brain region of RTT patients was detected [146]. Lately, a study in a hyperglycemic mouse has suggested notably enhanced expression of HDAC1 and MeCP2, advocating a robust relationship between MeCP2 and glucose metabolism. Thus, irregular metabolism of glucose might present in a brain-region and cell- type-specific dependent manner and could result in the more severe clinical presentation of RTT patients [147]. Likewise, the patterns of insulin intolerance were additionally mentioned. In an RTT mice model, an enhanced blood glucose level, enhanced insulin resistance, and a lower glucose absorption rate were detected in contrast to control mice [148]. Studying other factors associated with MeCP2 is significant besides irregular glucose metabolism and insulin resistance to influence RTT glucose metabolism [149]. Consequently, the association between MeCP2 function with the glucose metabolism of the brain and the related pathways is essential for detecting RTT-related glucose metabolic deficits and additional MeCP2-related neurological conditions. The MeCP2-mediated regulation of insulin expression happens *via* the binding of MeCP2 to the Insulin-2 gene promoter and preventing the cAMP-responsive element (CRE) binding. Accordingly, this results in the prevention of insulin expression, and insulin overexpression in the lack of MeCP2 [150]. Ultimately, dysregulated insulin exposure will cause insulin resistance. Future studies should emphasize realizing the accurate procedure since it could provide complete insight into the development of metabolic syndrome [151]. Additionally, disruption of MeCP2 function similarly affects downstream signaling including mTOR and AKT signaling which are reduced in cells lacking MeCP2 [152].

The impaired metabolism due to altered expression/mutations of the *MECP2* gene is a sign in mutated MeCP2-associated diseases including various human neurodevelopmental and neurodegenerative diseases such as RTT, MSD, severe neonatal encephalopathy, Autism Spectrum Disorders (ASD), X-linked mental retardation, Hirschsprung's disease, Huntington disease, early onset schizophrenia, and Angelman syndrome [3, 40, 78, 153-162]. For instance, in RTT, irregular systemic and brain glucose consumption, insulin resistance, compromised cholesterol metabolism, and unusual mitochondrial function are common metabolic abnormalities [55, 156-158]. Because of the putative link between MeCP2-connected disorders and metabolism, defining an association between MeCP2 function and brain metabolism is beneficial through cellular pathways including the mechanistic target of rapamycin (mTOR) complex and adenosine-monophosphate activated protein kinase (AMPK) is important [157].

1.6.1. Role of mTOR in Glucose Metabolism and Protein Translation

In eukaryotic cells, mTOR signaling is a cellular pathway that is a fundamental regulator of proliferation, growth, metabolism, and survival, which is located downstream of MeCP2 and is negatively affected by *MECP2* mutations [159]. The phosphorylation of principal targets of mTOR *via* its serine/threonine protein kinase activity controls several cellular processes. The mTOR includes 2 complexes gathered in cells, mTORC1, and mTORC2. The shared proteins of both complexes of mTOR complexes include mTOR and GβL, but the distinct proteins are Raptor and Rictor related to mTORC1 and mTORC2, in order. The mTORC1 complex is responsible for receiving environmental stimuli, controlling anabolism-catabolism equilibrium in cells, regulating lipids, proteins, and nucleotide synthesis, and repressing catabolic pathways like autophagy. On the other side, the proliferation and survival of cells are attributed to the mTORC2 [160]. Mostly, the effect of *MECP2* mutations on the regulation of mTORC1-dependent protein synthesis has been studied. The p70S6 Kinase 1 (S6K1) and eIF4E (eukaryotic Initiation Factor 4E) binding protein (4EBP), as the direct downstream mTORC1 targets are associated with the initiation of translation [160, 161]. The 4EBP phosphorylation results in its liberation from the eIF4E permitting the initiation of translation. S6K1 phosphorylates and activates the ribosomal protein S6 (rPS6 or eS6) which is a component of the 40S ribosomal subunit participating in protein synthesis [160].

The S6Ks proteins are the mTOR substrate involved in the regulation of cell growth. S6K1 and S6K2 have been discovered as the fundamental *in vivo* kinases involved in succeeding rpS6 phosphorylation on five serine residues in the C-terminal tail of the protein. The S6K1 and S6K2 themselves are activated by the mTOR, a leading regulator of growth through sensing environmental signals [162]. Because rpS6 is a fundamental element of the 40S little ribosomal subunit and as rpS6 phosphorylation is triggered with anabolic signals, the current model is that the activity of S6K controls growth *via* influencing protein translation [163]. The discoveries of more substrates like eukaryotic elongation factor 2 kinase (eEF2K) and eukaryotic initiation factor 4B (eIF4B) have strengthened the theory of S6Ks' relation to the translational machinery [164]. Furthermore, a study in the 8 weeks of *Mecp2*-null male mouse brain demonstrated decreased levels of phosphorylated rPS6 showing diminished protein synthesis. Also, the same reduction in phosphorylated rPS6 levels has been reported in the hippocampus and cortex of heterozygous 10 months of age *Mecp2+/-* female mice [152].

The human ESCs-derived *MECP2*-deficient neurons have substantially decreased amount of stimulated level of Protein Kinase B (PKB) or AKT (a positive upstream controller of mTOR and activator of the cells proliferation, survival, and growth), reduced nascent protein generation, and decreased size of soma [165]. Owing to decreased *BDNF* levels in RTT patients, the activation of mTOR by *BDNF* is compromised [166, 168]. Also, in the cerebellum of human post-mortem RTT, hyperactivated mTOR components were detected [159]. The influences of *MECP2/Mecp2* mutations on the mTOR pathway in the human background contrary to mice at diverse steps of disease development with distinctive mutations is not recognized [152, 159].

1.6.2. AMPK and Energy Metabolism

The AMPK pathway is another regulator of glucose metabolism in addition to the mTOR pathway [169]. An *in vitro* study has shown AMPK/HDAC5/GLUT4 pathway as a probable target in the therapy of diabetes and insulin resistance [169]. Likewise, another study has proposed nitric oxide as the stimulator of AMPK activity, resulting in enhanced expression of GLUT4 [170]. Lately, increased AMP and ADP levels were detected in *Mecp2* null mice linked with MeCP2 diseases, which may result in increased AMPK-dependent activation of glycolysis [171].

Consequently, the compromised MeCP2 function can disrupt the AMPK signaling pathway and lead to numerous RTT-associated symptoms in patients, involving high blood glucose and insulin resistance [172].

1.7. Metformin Targets AMPK and mTOR Pathways

Due to various benefits of metformin, including safety, high efficacy of blood glucose regulation, and low cost, it has been used for more than 60 years. The modification in cellular energy metabolism is the fundamental mechanism of its action [173]. The common hypoglycemic effects of metformin are attained by several mechanisms [174].

Finding novel applications for this old drug is a current hot spot, and it has been described in clinical and animal research to apply neuroprotective influences in numerous neurological disorders [175-177].

The clinical, pre-clinical, and cellular studies of metformin in abundant neurological diseases have been shown in **Table 1.3**. Although it has been revealed that metformin has a widespread neuroprotective effect, further validation in animal models and the detection of its basic mechanisms are lacking. Since metformin passes throughout the BBB and has neurophysiological effects, we have focused on the probable metformin's roles in neuron and neurological disorders, mainly RTT [178, 179].

Table 1.3. The *In vitro* and *In vivo* Studies of Metformin in Neurological Disorders.

Fragile X Syndrome (FXS)		
Disease Model	**Effect**	**References**
• FXS patients	• Improvement of hyperactivity • Improvement of social responsiveness • Improvement of irritability • Improvement of social avoidance	[180]
▪ *Fmr1*-KO mouse	▪ Reversal of social behavior deficiencies ▪ Rescue of enduring depression	[178]
➢ Mechanism	➢ Normalization of ERK signaling ➢ Regulation of MMP-9 expression	
Major Depressive disorder (MDD)		
• MDD patients	• Improvement of depressive-like behaviors • Improvement of aggressive-like behaviors	[176, 181]
▪ HFD-induced insulin-resistant mice	▪ Improvement of synaptic defects ▪ Improvement of anxiety-like behaviors	[182]
➢ Mechanism	➢ Stimulation of 5-HT neurotransmission	
Huntington's disease (HD)		
• HD patients with T2DM ▪ Hdh150 knock-in mouse model of HD	• Improvement of cognition ▪ Decrease of the abnormal huntingtin load ▪ Complete restoration of the irregular behavior	[183] [177]
➢ Mechanism	➢ Activation of the mTOR/PP2A pathway	

Parkinson's disease (PD)		
• MPTP-induced PD mice ➢ Mechanism ▪ Bcat-1 knockdown worm model of PD ➢ Mechanism ❖ LPS-induced rat model of PD	• Improvement motor of damage induced • Improvement of oxidative stress ➢ Increasing levels of BDNF ▪ Unusual mitochondrial respiration's correction ➢ AMPK stimulation ➢ Induction of BDNF ❖ Suppression of reactive astrocytes ❖ Inhibition of microglia activation ❖ Reduction of mitochondrial respiration ❖ mTOR-independent mechanism	[184] [185] [186]
Alzheimer's disease (AD)		
• Non-diabetic and AD patients ▪ SAMP8 mice ➢ Mechanism	• Improvement of learning/memory and attention • Decreased risk of AD development in T2DM patients ▪ Improvement of memory ➢ Reduction of APPc99 and p-tau ➢ Reduction of tau phosphorylation ➢ Control of GSK3β and protein kinase C	[187, 188] [189]

Autism (ASD)		
▪ BTBR T+ Itpr3tf/J (BTBR) mouse mode ➢ Mechanism	• Considerable reversible of: Social deficits Decreased repetitive grooming Decreased marble burying ➢ Reduction of mTOR gene and protein expression ➢ Reduction trend in S6K expression	[190]
Rett Syndrome (RTT)		
• MeCP2-308 heterozygous female mice ➢ Mechanism ▪ Human brain cell line	• Normalization of the diminished mitochondrial ATP generation and ATP levels in the brain ➢ Reduction of oxidative damage in the brain ➢ Decrease of the enhanced generation of reactive oxidizing species in blood ➢ Increase of the mitochondrial biogenesis and antioxidant defense pathways in the brain ▪ Post-transcriptional regulation Stimulation of *MECP2E1* and *BDNF* ▪ Transcriptional regulation Inhibition of *MECP2E2*	[191] [152]

Neurons are a key CNS cell type without a regeneration ability and have distinctive roles [192]. In some neurological disorders, loss, or damage of a distinct group of neurons leads to protein accumulation in neurons, like amyloid plaques in AD and dopaminergic neuron loss in PD [193]. The detection of pathological protein aggregation in these diseases supplies a crucial speculative foundation for the development of correlated drugs. As cited above, metformin has various impacts on numerous neurological diseases, including AD, PD, HD, MDD, and FXS [176-191]. The lysosomal degradation process to improve old cellular elements and remove injured organelles and protein accumulation is called autophagy. Metformin regulates the aberrant protein's expression in the brain by autophagy [194]. Neurons are further susceptible to autophagy-associated gene mutations due to being non-mitotic [195]. With no efficient autophagy, neurons accumulate ubiquitinated proteins and ultimately deteriorate [196, 197]. In the autophagy regulatory pathways, mTOR and AMPK signaling pathways act as principal nodes, integrating the metabolic signals and energy states of cells [198]. Phosphorylation on acetyl coenzyme A carboxylase (ACC) on Ser79 and Thr172 of the AMPK catalytic subunit alpha are two conventional markers of AMPK activity [160, 192]. mTORC1 inhibits autophagy mostly *via* inhibiting phosphorylation of unc-51-like autophagy-activating kinase 1/2 (ULK1/2) and class III phosphatidylinositol 3-kinase (class III PtdIns3K complexes). A widespread indicator of the mTORC1 activity is the phosphorylation of its substrate RPS6KB1/S6K at Thr389 [200]. Additionally, AMPK prevents mTORC1 activity [201]. These findings indicate that metformin has a possibly intricate controlling mechanism that impacts the generation of irregular proteins [205]. In a tauopathy mouse model, the induction of the PP2A expression through the AMPK/mTOR signaling pathway following chronic administration of metformin, decreased Tau phosphorylation in the hippocampus and cortex of TAU-P301S mice [203]; nevertheless, metformin also boosted the number of insoluble tau species and the number of inclusions with β-sheet structure in the cortex of P301S mice and promoted the buildup of recombinant tau protein *in vitro* [204]. In a diabetes mouse model (db/db), metformin restrained the enhancement of total and phosphorylated tau, induced a tau kinase, and diminished the reduction of the hippocampal synaptophysin [205]. The molecular and behavioral studies in ischemic rats 2 weeks pre-treated with metformin (200 mg/kg/day) showed the improvement of short-term memory, neuronal plasticity, and memory formation, as well as the protective effects in the hippocampus [192].

These results are attributed to the subsequent activation of AMPK, induction of BDNF, and induction of P70S6K, suggesting the AMPK/BDNF/P70S6K pathway in an experimental model of global cerebral ischemia [199]. In the FXS mouse model (Fmr1-KO), metformin (200 mg/kg/day) rescues the social deficits, lasting depression, and compromised spine morphology observed in this model by normalizing ERK signaling, and the expression of MMP-9 [178]. In an Alzheimer's mouse model (APP/PS1), IP injections of metformin (200 mg/kg/day) for 10 days repaired memory, by impeding cyclin-dependent kinase 5 hyperactivation *via* constraining Calpain, subsequently resulting in inhibition of Tau hyperphosphorylation [207]. In terms of MDD, oral metformin administration of metformin (200 mg/kg/day) for 2 weeks in the CSDS mouse model alleviated depression-like behaviors and improved synaptic deficiencies by upregulation of BDNF expression *via* stimulation of AMPK/CREB signaling [208]. Besides the approved efficiency of the 200 mg/kg/day metformin dosage for the treatment of mouse models of neurological disorders, the improved cardiac function and lack of hypoglycemia in 10 weeks of age male C57BL/6 mice after 6 weeks of treatment approved its safety [209]. In an AD mouse model, metformin reduces the level of Tau hyperphosphorylation possibly by blocking protein kinase R-like endoplasmic reticulum (ER) kinase (PERK) pathway, and the activities of the GSK3β, calpain 1, and cyclin-dependent kinase 5 (Cdk5) [210]. In the Aβ-induced model of mitochondrial dysfunction in transgenic C. elegans, metformin modifies metabolic abnormalities linked with mitochondrial dysfunction and decreases protein accumulation [211]. In a High-Fat Diet (HFD) mouse model promoted by insulin resistance, metformin enhanced insulin activity for the generation of ATP and oxidative stress in an AMPK-independent manner. Deletion of Ndufs3 in a neuron-specific Ndufs3 conditional KO (cKO) mouse model's forebrain neurons led to decreased complex I activity, modified brain energy metabolism, and movement impairment. However, metformin treatment prolonged the neurological symptom's presentation [212]. In another study, metformin reversed chemotherapeutic resistance by somewhat hindering mitochondrial respiration [213] and was connected to tumor necrosis factor type 1 receptor-associated protein (TRAP1)-related pathways [213]. Metformin rescues TRAP1 lost-mediated mitochondrial phenotypic changes, containing recovery of mitochondrial membrane potential, mitochondrial nuclear protein inconsistency, and mitochondrial unfolded protein response (mtUPR) upregulation [200]. Mitochondrial nuclear protein discrepancy can initiate stress signals *via* mtUPR and consequently affect mitochondrial activity and monitor stability [214, 215].

Metformin improves mitochondrial function through an increase of chaperone protein and decreases carbonylation and oxidation of whole-brain proteins, which are indicators of neuronal oxidative stress. Consequently, the neuroprotective role of metformin is through modifying mitochondrial respiration and rising oxidative stress *via* a variety of complex methods [216].

1.8. History of Metformin

Metformin has been approved and used in therapeutic purposes for more than 60 years due to its safety profile, low cost, penetrability to BBB, efficiency of blood glucose management, and obvious cardioprotective effect [173]. It is the first treatment for type 2 diabetes mellitus (T2DM) with an extended history. As a biguanide product, it was separated from the plant French lilac (Galega officinalis) extracts in the 1920s. Later, metformin was accepted for therapeutic purposes of T2DM in Europe and Canada in 1957 and in the USA in 1995 [244].

1.9. Mechanism of Metformin Action

The main metformin's mechanism of action is the change of cellular energy [181]. Metformin exerts its hypoglycemic effects through multiple mechanisms such as inhibition of hepatic gluconeogenesis and uptake of intestinal glucose, enhancement of glucose uptake in peripheral tissues, and advancement of marginal insulin sensitivity [173]. The hypoglycemic effect of metformin could be dependent or independent of AMPK activation. Metformin-mediated activation of AMPK occurs *via* lysosomal or mitochondrial processes. Initially, metformin-mediated inhibition of complex I of mitochondria leads to the reduction of ATP level, an increase of AMP/ATP ratio, inhibition of glucagon-induced cyclic AMP (cAMP) production, and activation of AMPK [174, 217]. Metformin-mediated activation of AMPK results in the inhibition or activation of different downstream targets and pathways [218], such as acetyl CoA carboxylase (ACC) activity and fatty acid oxidation [219], in order. Second, stimulation of small heterodimer partner (SHP) protein generation and improvement of hepatic insulin resistance by controlling gluconeogenesis and insulin sensitivity [220]. Third, the promotion of CREB binding protein following inhibition of gluconeogenic gene's expression [221]. Fourth, inhibition of the mTORC1 signaling through direct inhibition of Raptor or indirect activation of the tuberous sclerosis complex (TSC) to suppress cellular anabolic activity [222]. In a rat model of obesity and diabetics, metformin stimulates the gastric AMPK-dependent pathway to decrease hepatic gluconeogenesis and blood glucose levels [223, 224].

Though, in genetic loss-of-function experiments, such as in hepatic AMPK-deficient mice, metformin reduces blood glucose levels, proposing an AMPK-independent effect of metformin on gluconeogenesis [225]. In the AMPK-independent pathway, metformin impedes cAMP generation to decrease the generation of glucose [226], prevents mitochondrial glycerophosphate dehydrogenase, and results in the modified hepatocellular redox state (preventing AMP: ATP and NADH: NAD+ ratio) and decreased hepatic gluconeogenesis or by directly targeting Fructose1,6-bisphosphatase (FBP) [227]. In this mechanism, metformin-mediated inhibition of mTORC1 is through inhibition of the Rag family of GTPase [227] or upregulating DNA damage response 1 (REDD1), a negative regulator of mTORC1 [228].

1.10. Metformin Transportation and Distribution

BBB is a complicated, vital boundary, and attaining appropriate BBB penetration is a big hurdle for the treatment of CNS disorders. Orally administered metformin can rapidly pass the BBB and accumulate in the CNS [229]. Thirty minutes after the IP injection of metformin (200 mg/kg) in C57BL6 mice, the metformin concentration in the cerebrospinal fluid arrives peaks at 29 μM [230]. According to the pre-clinical studies, metformin can cross the BBB [231, 232] and it was able to re-establish the activity of AMPK in the brain [232, 233]. Conversely, owing to conflicts of AMPK activity in inflammatory CNS settings, it is significant to reveal the drug's peculiar pharmacological targets inside the brain. It is obvious that research is necessary to verify the brain region-specific actions of metformin and translate the drug's action at the molecular level [234]. At biological pH, metformin is a hydrophilic and cationic drug, which is unattached to plasma proteins and is released unaffected in the urine [235]. The solute carrier transporters are a family of above than 300 membrane-bound proteins in charge of the absorption, distribution, metabolism, and renal secretion of metformin. Amongst metformin transporters, Organic Cationic Transporter (OCTs) appear in the hepatocyte, enterocyte, and renal tubule cells [236]. Besides OCT, plasma membrane monoamine transporter (PMAT), thiamine transporter 2 (THTR-2) multidrug and toxin compound extrusion-1 and -2 (MATE-1 and -2) are other transporters of metformin [237]. The OCT1, OCT2, and OCT3 have been separated from various organs such as the human brain. In the brain, OCT2 and OCT3 are mostly placed in central neurons, and OCT3 is more extensively dispersed and presents in astrocytes [238, 239].

The conducted research in the models of rats, mice, or humans demonstrated that there was no active OCTs vector in BBB. Consequently, metformin does not appear to depend on OCTs to attain BBB penetration [240].

1.11. Side Effects of Metformin

Side effects include comprised gastrointestinal complaints, vitamin B12 deficit, progeny damage, lactic acidosis, and neurodegenerative disorders. Consequently, monitoring of the patients under metformin treatment is critical to avoid side effects, particularly lethal and permanent injury. Normally, the most common adverse effect is gastrointestinal problems, which happen in 2–63% of T2DM patients, including vomiting, diarrhea stomach discomfort, turgidity, and dysgeusia [241].

1.12. Rationales, Hypothesis, and Aims

Multiple reports from our lab indicate RTT-associated abnormalities in the mTOR pathway [152, 161] and the *MECP2-BDNF-miR132* regulatory network [114]. Also, another study has shown that metformin could induce the transcript levels of *MECP2E1* and *BDNF in vitro* [138]. These findings along with other literature have provided us a with solid foundation for our rationale, and the derived hypothesis and specific aims of research which will be elaborated accordingly.

1.12.1. Rationales

1.12.1.1. Rationale 1

The analysis of 4 patients, including one T158M cerebellar tissue post-mortem was used to examine the effect of *MECP2* mutations on downstream pathways. In the human RTT brain, the active mTORC1 or mTORC2 complexes' higher phosphorylation contrary to controls was an indicator of the elevated and compromised mTOR–P70S6K signaling pathway. The overactivation of the mTOR pathway could lead to the depletion of essential cellular resources required for other functions which results in compromised function in the RTT brain and neurons, and other subsequent functions including protein synthesis, neuronal plasticity, and synapse formation. The AMPK and mTORC1 are vital controllers of cellular metabolism that are individually stimulated and repressed in rapid response to cellular energy reduction [152].

A pre-clinical study on C57BL6 mice has shown metformin as a strong inhibitor of hepatic mTORC1 following the reduction of cellular energy levels due to inhibition of mitochondrial complex I and consequent reduction of cellular ATP levels [242].

1.12.1.2. Rationale 2

Our lab has studied the transcript and protein levels of the *MECP2-BDNF-miR132* regulatory network in the brain of RTT humans in comparison with their controls [118, 114]. The results reported a compromised *MECP2-BDNF-miR132* regulatory network which has been shown by a significant reduction of the transcript level of the *MECP2-BDNF-miR132* regulatory network components in a brain-region-dependent manner. However, *MeCP2E1/E2*-BDNF protein levels are not correlated with changes in their transcripts [114]. Another study in MeCP2 T158M knock-in mice reported a reduced methylated DNA binding ability of MeCP2 and unstable MeCP2 protein levels in an age-dependent manner, resulting in the RTT-like phenotype. On the other hand, it is shown that the genetic increase of the MeCP2 T158M expression rescued numerous RTT-associated phenotypes in mice. Additionally, proteasome inhibition enhanced MeCP2 T158M levels. So, genetic, or pharmacological elevating MeCP2 T158M protein expression is sufficient to improve RTT-like phenotypes and advocate the targeting of the expression or stability of MeCP2 T158M mice as a therapeutic method [71]. In another study from our lab, the analysis of nascent RNA synthesis in a human brain cell line showed the regulatory effect of metformin on the *MECP2E1/E2-BDNF* at the transcriptional (*MECP2E2* inhibition) and/or post-transcriptional (*MECP2E1* and/or *BDNF* stimulation) level. Additionally, similar pre-clinical and clinical studies of the possible effect of metformin in RTT-like symptoms have been included in **Chart 1.1** of this thesis with details. For instance, the study of chronic metformin effect on (a 4-month-old adult male C57BL/6J, drinking water, 2 mg/ml) showed improved locomotor and balance function, while encouraging anxiolytic impact and compromised perceptive function [243].

1.12.2. Hypothesis

1.12.2.1. Hypothesis 1

We hypothesize that inhibition of the overactivated mTOR pathway could be a possible therapeutic approach for RTT and that despite the well-known effect of metformin *in vitro*, further investigation for its effectiveness *in vivo* is required [36]. Also, metformin could exert its effect through direct/indirect mechanisms on the brain S6 and p-S6 (235/236) as the readout of the mTOR pathway *in vivo.*

1.12.2.2. Hypothesis 2

Due to the stimulatory effect of metformin on reduced *MECP2-BDNF* transcripts *in vitro*, we hypothesize that metformin treatment could rescue the reduced *MECP2-BDNF* transcripts and improve RTT-like symptoms of a transgenic mice model at the phenotypical and behavioral levels.

1.12.3. Aims

1.12.3.1. Aim 1. To study the effect of metformin on the MeCP2-BDNF and mTOR pathway *in vivo* at the molecular level.

1.12.3.2. Aim 2. To study the effect of metformin on the improvement of RTT-like symptoms *in vivo* at the phenotypical and behavioral levels.

Chapter 2. Material and Methods

2.1. Ethical Approval

The establishment of mice colonies as well as metformin treatments and IP injections used in this thesis were reviewed and approved by the University of Manitoba Animal Research Ethics Board and under the animal protocol 18-053 for the Rastegar lab.

2.2. Mouse Models

Mice were maintained with ambient room temperatures of 19-22°C, with access to food (P500 rodent diet from the lab) and drinking tap water, managed by the University of Manitoba Animal Facility staff.

For Aim 1 of my thesis, C57BL/6 mice were purchased from the University of Manitoba Animal Facility. C57BL/6 is an inbred strain of lab mice commonly used as a "genetic background" for models of human diseases due to the accessibility of congenic strains, and simple breeding [244].

For Aim 2 of my thesis, mice were directly purchased from the Jacksons' lab prior to the start of my thesis. According to the website of Jacksons' lab (https://www.jax.org/), the B6.129P2(Cg)-*Mecp2*tm4.1Bird/J (Strain #:026762, RRID: IMSR_JAX:026762) mouse colony, referred to as MeCP2-GFP-T158M or *Mecp2*T158M, but according to the literature [69], it is referred as the MeCP2 T158M–knock-in ($Mecp2^{T158M}$) mice that develop a RTT-like phenotype. To be consistent with other studies, we have used the same name ($Mecp2^{T158M}$) throughout this thesis.

The development of $Mecp2^{T158M}$ mice has been shown with reference to the website of Jackson Lab (https://www.jax.org/strain/026762) and literature in **Figure 2.1**. An EGFP open reading frame (ORF) was attached to the terminal of the *Mecp2* coding sequence of exon 4. Also, a *loxP* site flanked NEO cassette was used for the insertion of the T158M point mutation into exon 4 of the *Mecp2* gene [245].

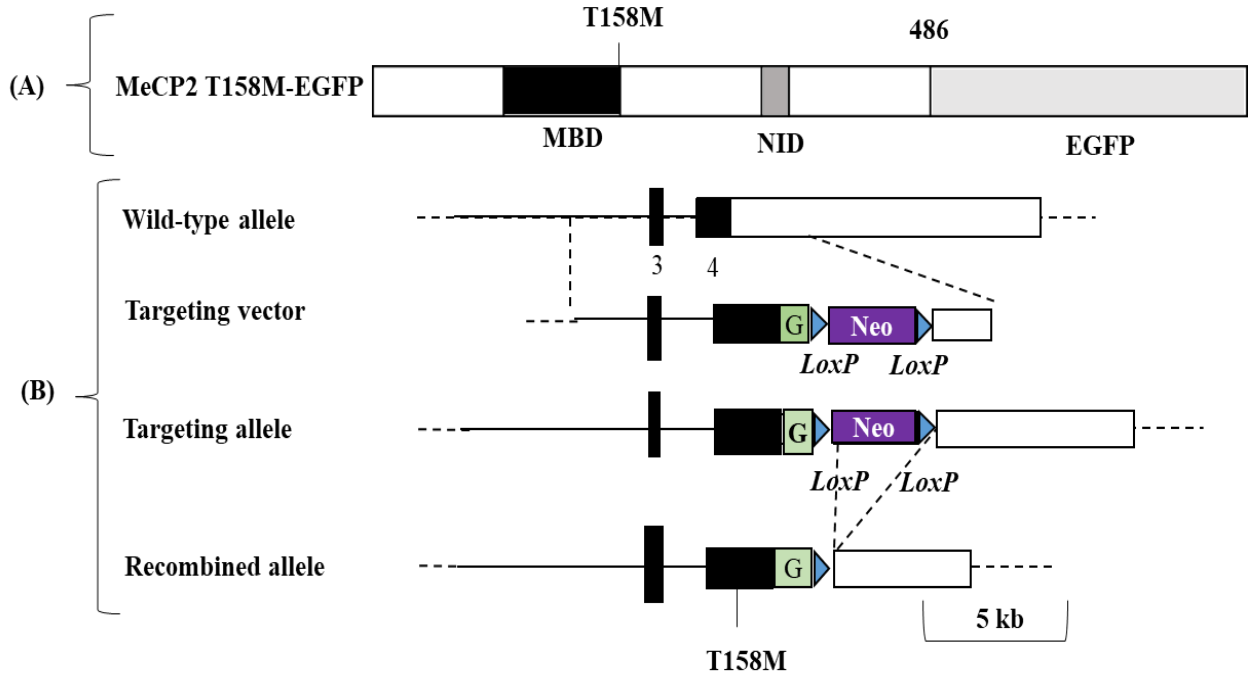

Figure 2.1 Schematic of MeCP2 T158M-EGFP Mouse Generation. A) The relation of the Methyl-Binding Domain (MBD) to the T158M missense mutations has been shown [59]. **B**) The approach for the generation of embryonic stem cells expressing wild-type or mutant MeCP2-EGFP fusion protein from the endogenous *Mecp2* gene locus has been shown. Top: Exons 3 and 4 of the endogenous loci (numbered black boxes) including the 3' untranslated region (UTR) of the mRNA (open box) are indicated. The construction of the targeting vector was similar in each case excluding the existence of the T158M mutations (red lines). The EGFP open reading frame (G in the green box) was merged to the C-terminus of MeCP2, and a neomycin-resistance cassette (Neo) (purple box) was located downstream Ranked by *loxP* sites (blue arrowheads). Effectively targeted clones were treated with Cre-recombinase to delete the neomycin cassette [38].

2.3. Drug Preparation and Treatments

For all *in vivo* treatment studies, the male and female C57BL/6 mice, as well as the WT and *Mecp2*^{T158M} mice received daily IP injections of 1X Phosphate Buffer Saline (1X PBS) as vehicle and metformin (EMD Millipore Crop, USA, Affiliate to Merck KGaA, Darmstadt, Germany, 317240-5GM, Lot: 3218213, Batch M.W. 165.6 g/mol) for 3 consecutive weeks. Two different concentrations of metformin including 200 mg/kg (Aim 1) and 250 mg/kg (Aim 2) were used for *in vivo* studies. The rationale of dose selection for Aim 1 *versus* Aim 2 has been explained based on our pilot study and literature. It is shown that with a dose of 200 mg/kg body weight, metformin passes the BBB [178] and has been reported to increase neurogenesis and spatial learning in female C57/129J mice [246]. Another study has shown that IP injection of metformin (200 mg/kg/day) in adult WT and *Fmr1*−/y mice (*Fmr1*-deficient male mice) rescued core phenotypes in *Fmr1*−/y male mice and selectively normalized impaired extracellular-signal-regulated kinase (ERK) signaling [33], eIF4E phosphorylation, and expression of matrix metalloproteinase 9 (MMP-9), suggesting metformin as a possible therapeutic drug for FXS [171]. Furthermore, IP injection of metformin in the concentration of 200 mg/kg in BTBR T+ Itpr3tf/J (BTBR) mouse model of ASD, inverted social deficits, and diminished repetitive grooming in BTBR mic, and increased the possibility of metformin having a positive influence on reducing behavioral impairments in ASD [249]. Therefore, to be in line with similar studies, we selected the concentration of 200 mg/kg body weight per day in our pilot study in Aim 1. In addition to the literature, the preliminary result of our pilot study confirmed the safety and tolerability of metformin at 200 mg/kg body weight without observing any adverse effect on mice body weight and/or blood glucose levels.

These results in C57BL/6 mice provided a solid foundation for the rest of our experiments with a higher dosage of metformin (250 mg/kg body weight) in *Mecp2*^{T158M} which agrees with relevant studies. Metformin at both 200 and 250 mg/kg doses inhibits hepatic mTORC1 signaling measured by phosphorylation of the ribosomal S6K1 (specific substrate of mTORC1 and its downstream target S6 through dose-dependent mechanisms including AMPK [222]. For instance, IP injection of metformin at 250 mg/kg/day for 5 days in the male rat model of Temporal lobe epilepsy (TLE) showed the anti-seizure effects of metformin [250], which is ascribed to the inhibition of BDNF over-expression and its receptor and the activation of the AMPK signaling pathway following the reduction of the mTOR activation [250].

Furthermore, the restoration of implicated neurogenesis has been reported following metformin treatment (250 mg/kg/day, by gavage) in the dentate gyrus, and the consequent improvement of the intellectual ability of obese mice [251]. All these findings lead to considering the possible beneficial effects of metformin in 250 mg/kg body weight in *Mecp2*^{T158M} mice.

The calculation of drug dosage, preparation of the drug, and vehicle solutions were completed on a weekly basis in accordance with the body weight changes as well as the water and food consumption of mice over time, and all steps were performed under the biological cabinet (1300 Series A2, Thermo 1375, Serial 115970-757). Drug calculation and preparation for Aim 1 was completed in collaboration with Marjorie Buist. Also, for Aim 2, the calculation of drug dosage for the first set of experiments was completed in collaboration with our lab associate (Dr. Arsalan Alizadeh). For both Aims, metformin was dissolved in the proper volume of vehicle and all the solutions were stored at 4°C until usage and warmed at room temperature for 20 min prior to *in vivo* injections. Furthermore, all the IP injections were completed with 1 ml Syringes (REF 309659, Lot 9270311) and 26G sterile needles (lot 9350601, 26G* 1.2, 0.45 mm*13).

For the preparation of the drug and vehicle solution, the measurement of the mice's body weights was completed in each set of experiments for the calculation of metformin dosage. In terms of vehicle, 10X PBS was diluted into 1X PBS with high pure water (Invitrogen, Lot: 1668494, REF: 10977-015). Next, the calculated amount of the drug was dissolved in the calculated volume of the vehicle, mixed well until complete homogenization of the solution, and was filtered (Thermo Scientific Nalgene Syringes Filter 0.2 µm, cat. No. 194-2520) prior to *in vivo* injections.

2.4. Experimental Design

2.4.1. Experimental Design of Aim 1

According to the experimental design in Aim 1 (**Figure 2. 2**), a total number of 24 mice from both sexes including 12 males and 12 females were randomly categorized into 2 groups called the vehicle (control) and experimental groups (metformin). Half of the male mice and half of the female mice were treated with metformin (200 mg/kg) through daily IP injections, a dose formerly utilized in animal studies [238, 246, 171, 264, 252, 253]. The other half of the males and females received vehicle (10µl/g of sterile 1X PBS) from P28 to P49 once per day (approximately the same time of the day) for 21 days.

For the pilot study, IP injections were completed by other members of our lab or Central Animal Care Services (CACS) staff, alternatively on the right and left side of mice. The weekly blood glucose test was completed through collaborative work between me and another lab member using collected blood from the tail vein. Ultimately, after 21 days of treatment, mice from all experimental groups were euthanized at P49, and different tissues including the liver and 4 brain regions (cortex, cerebellum, thalamus, and hippocampus) were dissected by our lab technician (Carl Olson) for molecular analysis. The rationale behind the selection of brain regions is the contribution of the cortex, cerebellum [254-256], thalamus, and hippocampus [257, 258] to the RTT symptoms and the effect of metformin on the impaired pathways in these regions.

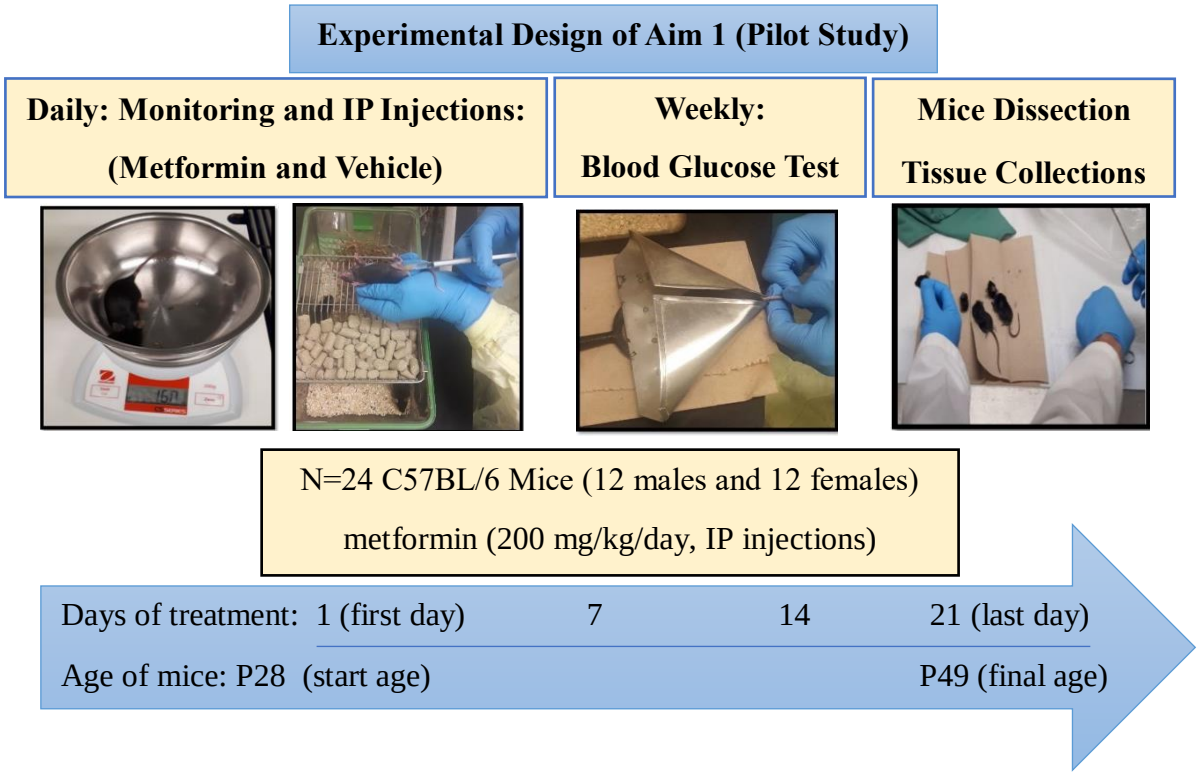

Figure 2.2 Experimental Design of Aim 1. In a pilot study, a total of 24 C57BL/6 mice (12 males and 12 females) were purchased from the University of Manitoba Animal Center at 4 weeks of age (28 days) from both sexes. Mice were randomly categorized into 4 groups including male C57BL/6+ vehicle, female C57BL/6 + vehicle, male C57BL/6 + metformin, and female C57BL/6+ metformin. All groups underwent daily monitoring and weekly blood glucose tests (in collaboration with other lab members or CACS). At the end of the treatments, dissections and collecting of tissues were completed by Carl Olson for molecular analysis.

During the period of 3 weeks of the experiment, I completed the daily monitoring of mice according to the endpoints, monitoring, and record-keeping policies including 3 main criteria as such; physical signs (Normal, Ruffled, Hunched, Porphyrin, Closed eyes, Sunken eyes, Slow Resp, Fast Resp, Bloody Fences, Skin Wounds), body condition (Emaciated, Under-conditioned, Well-conditioned, Over-conditioned, Obese), and behavior (Normal, Not moving, Depressed, Isolated, Hyperactive). Also, the measurement of daily body weight was completed and recorded as shown in Endpoint Monitoring Checklist (**Table 2.1**).

Table 2.1 Endpoint Monitoring Checklist.

Endpoint Monitoring Checklist

Species | Protocol
Room | PI
Animal I.D.#
Experimental Treatment

Start Wt.	Date														
_____g	Time	AM	PM	AM	PM	AM	PM	AM	PM	AM	PM	AM	PM	AM	PM
	Physical Signs														
	Body Condition														
Calc Endpoint wt(___%)	Behaviour														
_____gm	Weight (gms)														
	Treatment Given (drug/dose)														
	Comments														
	Humane Endpoint Reached (Y/N)														
	Initials														

Significant Indicators

Physical Signs				Body Condition		Behaviour	
N	Normal	SR	Slow Resp	1	Emaciated	N	Normal
R	Ruffled	FR	Fast Resp	2	Under-conditioned	NM	Not moving
H	Hunched	D		3	Well-conditioned	D	Depressed
PS	Porphyrin	BF	Bloody Feces	4	Over-conditioned	I	Isolated
CE	Closed eyes	SW	Skin Wounds	5	Obese	H	Hyperactive
SE	Sunken eyes						

2.4.2. Experimental Design of Aim 2

In Aim 2 (**Figure 2.3**), 4 groups of age, sex, and genotype-matched mice including *Mecp2*$^{T158M/y}$ male mice, *Mecp2*$^{+/y}$ male, *Mecp2*$^{T158M/+}$ female mice, *Mecp2*$^{+/+}$ female mice underwent metformin treatment. Mice from both sexes were categorized into 3 groups including the sham, vehicle, and an experimental group (metformin, 250 mg/kg/day). The selection of the metformin concentration in this study agreed with similar dosages in literature in males or females [259, 260].

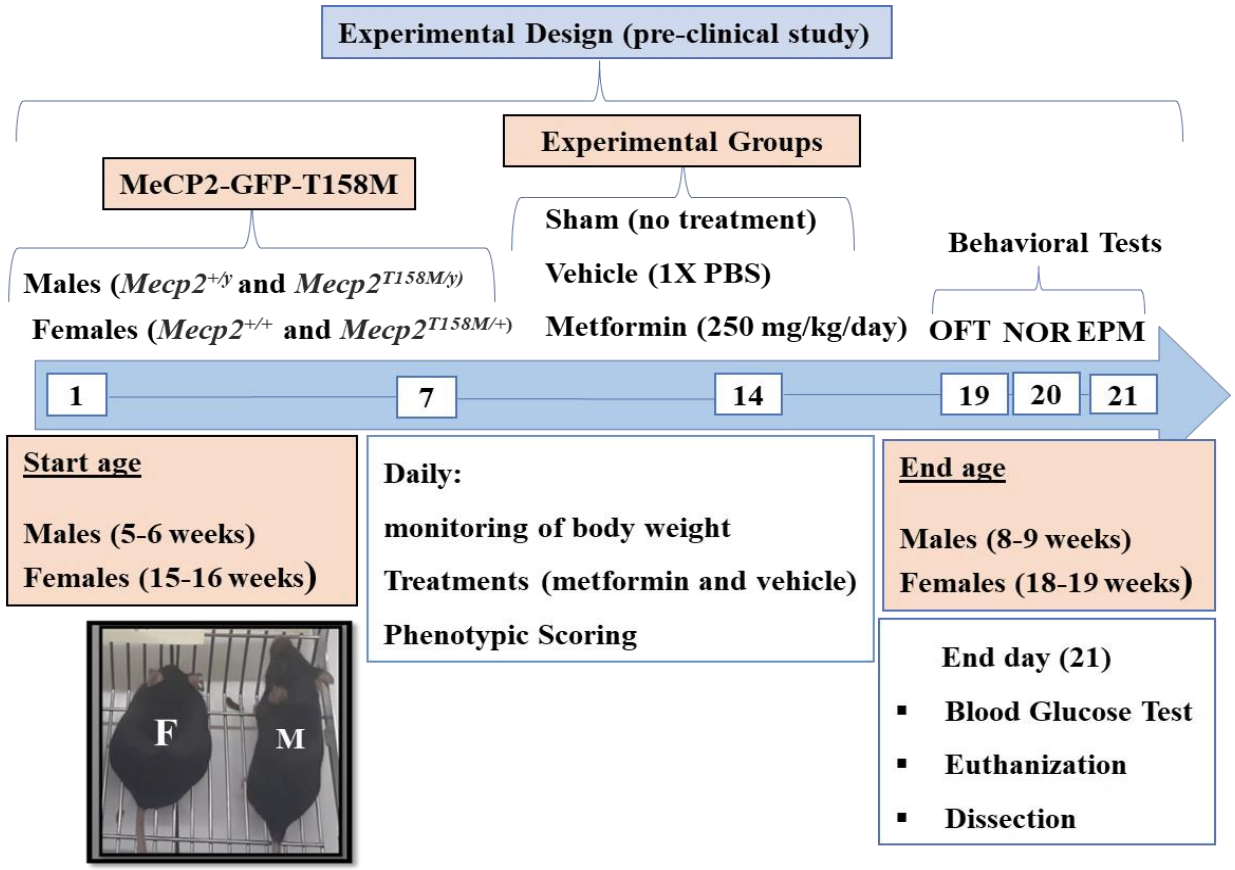

Figure 2.3. Experimental design of Aim 2. Four groups of age-, sex-, and genotype-matched mice including *Mecp2*$^{T158M/y}$ male, *Mecp2*$^{+/y}$ male, *Mecp2*$^{T158M/+}$ female, *Mecp2*$^{+/+}$ female were categorized into 3 groups including the sham, vehicle, and metformin-treated mice. I completed IP injections for 21 days, but daily monitoring and scoring were completed in collaboration with CACS. At the end of 21 days, I completed a series of behavioral tests in the BMSB and CHRIM behavioral test rooms. Then, the euthanization of mice, dissection of tissues, and measurement of blood glucose level were completed by our lab technician, and tissues were stored in a -80 °C freezer for future molecular analysis.

Evaluation of phenotypic scoring was completed to measure RTT-like phenotypes in 6 categories including activity, gait, hind limb clasping, tremor, breathing, and general condition. Mice were given a score of 0, 1, or 2 for each category, corresponding to the sign being absent, present, or severe, respectively [38]. I oversaw daily IP injections, body weight measurement, and daily scoring, but to avoid bias, blind scoring was completed by CACS for some of the mice during the week. After 18 days of IP injections, mice were transferred to behavioral rooms in BMSB (in collaboration with Dr. Tabrez Siddiqui) or the Children's Hospital Research Institute of Manitoba (CHRIM) behavioral room to conduct behavioral tests. For my project, I performed Open Field Test (OFT), New Objective Recognition Test (NOR), and Elevated Plus Maze (EPM). In both behavioral rooms in BMSB and CHRIM, after proper training with our lab research associates (Dr. Arsalan Alizadeh and Mr. Abbas Rezaian), behavioral tests were mostly completed independently. At the end of 21 days of treatment and after 4-5 hours of the last injection, mice were euthanized with CO2 by our lab technician, and tissues including liver and 4 brain regions (cortex, cerebellum, thalamus, and hippocampus) were collected and stored in a -80C° freezer for future analysis.

2.5. Molecular Analysis: Western Blotting

2.5.1. Total Protein Extraction

We completed the total protein extraction and quantification of metformin-treated and control C57BL/6 mice tissues including the liver and 4 brain regions as previously described [36, 261]. First, an average of 15 mg mice tissue was rinsed with 1000 µl of 1X PBS and placed in a sterile microtube (VWR, Cat No. 87003-294) and span inside a cold centrifuge (5430R) for 3 min at 2000 rpm. Then, the homogenization of tissues was completed in an ice-cold NP40 lysis buffer [5M NaCl, 10% NP40, 1 M Tris, pH: 8.00] and Roche Cocktail protease inhibitor (PI) (1:50) (Cat No. 11 836 153 001). After sonication with an Ultrasonic processor (130 watts, 20 kHz, Time 0:00:10, Pulse: 01: 01, AMP1, 60%), tissue lysate was centrifuged for 3 min at 2000 rpm at 4 °C and the supernatant including the proteins was transferred into a new microtube, aliquoted in 50 µl volume, and kept at -80°C for later usage.

2.5.2. Total Protein Quantification (Bradford Assay) and Sample Preparation

The total extracted proteins were quantified by Bradford assay with Bio-Rad Protein Assay Dye Reagents (#5000006) as previously reported [161, 262]. One of the protein aliquots was used for the determination of protein concentration to avoid repeated freezing and thawing of the stocks. After dilution (1:10) of samples with autoclaved water (18µl water + 2µl sample), 5µl of each dilution was added into each well of 96 well plates in triplicates. Also, 5µl of each component of Pre-Diluted Protein Assay Standards of Bovine Serum Albumin dilution (BSA) Set (Thermo Scientific, Prod #23208, Lot # P1204898) were added into the wells in triplicate. In the next step, 200 µl of previously diluted (1:5) Bio-Rad Protein Assay Dye Reagents (#5000006) was added to each well-containing standard and samples. The absorbance value of the mixture of samples and dye was evaluated in comparison to BSA set by use of a spectrophotometer (Spectra Max M3, Molecular Devices), and then the protein concentrations from the machine were used for the calculations required volumes of components of Western blot samples. A total of 10-30 µg from the total extracts was used for the preparation of Western blot samples by diluting those in 3 components including NP40 lysis buffer, β-Mercaptoethanol (BME), and 4x dye in a microtube. Then, after dilution, samples were boiled for 5 min, desaturated, and quickly centrifuged before loading on a gel.

2.5.3. SDS-PAGE Electrophoresis

Separation of extracted proteins was completed on polyacrylamide gels based on their molecular size with Western blot (80V, 0.1A, 10W) as previously described [263, 264]. After electrophoresis, the separated proteins were transferred with Bio-Rad semi-dry transfer apparatus (25V, 25A, 10 min+4 min) or wet-transfer (100V, 0.13A, 33W, 70 min) into Nitrocellulose (BIO-RAD, Cat.#162-0094) or polyvinylidene difluoride (PVDF) membrane (BIO-RAD, Cat.#1620177). A transfer sandwich was assembled in the following order: in the semi-dry transfer from bottom to the top [spouge, 3MM paper (Whatman, Cat No: 10547922), membrane, gel, 3MM paper, fume), and in the wet transfer from black to red (2-layer sponges, 2 layers-3MM paper, gel, membrane, 2 layers-3MM paper, 2-layers fume).

Except for the PVDF membrane which requires activation with 100% methanol for 5 seconds prior to putting into the transfer buffer, the rest of the components of the transfer sandwich were immersed in semi-dry transfer buffer (Trans-Blot Turbo TM, 5X Transfer Buffer, Cat# 10026938) or Towbin buffer (14.4 g Glycine, 3.03 g Tris base, 0.5 g SDS, 200 ml methanol, 800 ml H2O) in advance of assembly.

After the transfer step, to block nonspecific protein-binding sites on membranes were blocked with 5% fat-free milk or 5% BSA (Sigma-Aldrich, PCode: 1002934080, A7284-1L, Lot#SLBZ9467) for 2 hours at room temperature. Then, incubation of the membrane was completed with 3% fat-free milk or 3% BSA overnight in a cold room in a shaker.

A list of primary antibodies, their concentration, and their condition have been shown in **Table 2.2**. Following primary antibody incubation and to remove the unbound proteins, the membranes were washed with 1X TBST [450 ml autoclaved H2O, 50 ml 1X TBS, 250 µl Tween 0.2% Tween 20 (Lot # SLCC9501)]. Then, membranes were incubated with the 3% milk or 3% BSA of secondary antibody (HPR-linked Antibody, Anti-Rabbit IgG, 7074P2, lot 26) for 1 hour at room temperature. To eliminate any unbound secondary antibodies, membranes were washed with 1X TBST (3x, 10 min, 30 rpm) at room temperature.

In the last step, an equal volume of ECL components (Thermo scientific, Super signal TM west pico plus, Lot UA288176) was used for the detection of signals on the membrane. Then, using a chemiluminescence method based on an enzymatic reaction by horseradish peroxidase (HRP) produced a light signal, which could be captured by Fusion FX (VILBER LOURMAT). The detected bands were quantified by Image J software (https://en.softonic.com/windows). GAPDH (Glyceraldehyde 3-phosphate dehydrogenase) was detected on all membranes as a loading control, and results for each antibody were normalized to GAPDH.

Table 2.2 List of Primary Antibodies.

Primary Antibody	Dilution	Company and Catalogue Number	Source	Molecular Weight (KDa)	Incubation solution
MeCP2	1:1000	Sigma-Aldrich abn1728	Rabbit Polyclonal	75	3% milk Overnight 4 °C
BDNF	1:1000	Abcam ab108319	Rabbit monoclonal	Pro-BDNF (35 & 45) mBDNF (15)	3% milk Overnight 4 °C
S6	1:1000	Cell signaling 5G10	Rabbit IgG	32	3% milk Overnight 4 °C
PS6 (235/236)	1:1000	Cell signaling	Rabbit	32	3% BSA Overnight 4 °C
AMPK	1:1000	Sigma SAB 4502329	Rabbit	62	3% milk Overnight 4 °C
p-AMPK alpha (p-Thr172)	1:1000	Cell signaling # 2531S Sigma-SAB 4502329,	Rabbit	62	3% BSA Overnight 4 °C
GAPDH	1:5000	Sigma G9545	Rabbit	37	3% milk Overnight 4 °C

2.6. PCR-Based Genotyping of *Mecp2*^{T158M} Mice

The maintenance and breeding of our *Mecp2*^{T158M} mice were completed by Genetic Model Center (GMC) by crossing *Mecp2*$^{T158M/+}$ with (Dam) with *Mecp2*$^{+/y}$ (Sire). Then, I completed the genotyping of mice by extraction of DNA from a small ear punch biopsy at P21-P25, as previously described [59]. Furthermore, WT and mutant primer sets resulted in 2 distinct bands (547 and 321 bp) in the T158M female in PCR, 1 band (321 bp) in the T158M male, and 1 band (547 bp) in WT mice, an indicator of the *Mecp2* alleles.

2.6.1. DNA Extraction and Quantification

The DNA extraction of mice tissue was completed using a DNA extraction kit (Qiagen cat. No. 96506 and pure link TM Genomic DNA kit, Cat. no. K1820-01, K1820-02, k1821-04) according to the protocol [34, 265, 266]. First, 180 µl Pure Link Genomic Digestion Buffer and 20 µl of proteinase K were added to the tissue in each tube. Then, samples were incubated at a heat block (55 °C) with infrequent mixing until complete dissolving and then, the lysate was centrifuged at max speed (14 000 RCF for 3 min), and the supernatant was transferred to a new, sterile, microcentrifuge tube. After the addition of 20 µl of RNase A to the lysate, mixing, vertexing, and incubation was completed at room temperature for 2 minutes. Then, 200 µl Pure link Genomic lysis/Binding buffer and 200 µl of 96-100% ethanol were added to the lysate and mixed well. A total of 640 µl lysate was added to the Pure link Spin Column and was centrifuged the column at 10000 RCF for 1 minute at room temperature. The collection tube was discarded and replaced with a clean Pure Link Collection Tube. To wash the genomic DNA, 500µl wash buffer 1 was added to the column and was centrifuged at room temperature at 10000 RCF for 1 min. Then, the collection tube was discarded and replaced with a clean Pure Link collection tube. Then, 500 µl Wash Buffer 2 was added to the column and was centrifuged at maximum speed for 3 minutes at room temperature. Afterward, the collection tube was discarded. The spin column was placed in a sterile, 1.5 ml microcentrifuge tube and for the elution of DNA, incubated with 50 µl high pure water (Invitrogen, Ultrapure Distilled Water, Cat Number 10977015). After incubation at room temperature for 5 min, the column was centrifuged at maximum speed for 5 min, and purified genomic DNA was collected in the tube. Quantification of the extracted DNA was completed using a Nanodrop which was blanked with H20 and loaded with 1 µl DNA. The quantified DNA was stored at - 20 C° for genotyping.

2.6.2. PCR

First, all the required reagents including primers, Platinum II Green Hot Start 2X Master Mix (Invitrogen, Thermo Fisher Scientific, Cat Number 14001012), and high-purity water were placed on ice to be thawed. Then, a short and rapid mixing and spinning of each component of the PCR reaction were completed. For multiple reactions, a PCR Master Mix (MM) was prepared and 13 µl was distributed into each PCR tube and 30-150 ng of template DNA was added to the same PCR tube including MM (final volume: 15 µl), and reactions were incubated in a thermal cycler. The condition will be different according to the used primers (**Table 2.4)** and the recommended condition for our primers has been shown in **Table 2.3**. Also, the number of cycles (35-50) depended on the results, and the annealing temperature was set based on the primers.

Table 2.3 PCR Conditions.

Step	Temperature	Time
Initial denaturation	95C°	1 min
Denature	95C°	30 S
Annealing	60 C°	30 S
Extension	72 C°	45 S
Hold	4 C°	---

Table 2.4 List of Genotyping Primers [59].

Mutant primer	**Sequence 5′-3′**	**Amplicon Size**
Mutant Reverse	CTG AACTTG TGG CCG TTTAC	547 bp
Forward (common)	CAGCAGCAT CTGCAAAGAAG	
WT primer		
Wild Type Reverse	CTG GTCAACAGCTTGTCTGG	321 bp
Forward (common)	CAGCAGCAT CTGCAAAGAAG	

2.6.3 Agarose Gel Electrophoresis

To prepare 1.5 % gel, 0.6 g of Agarose (Lot# 091M0170V) was dissolved in 40 ml of 1X TBE (270 ml autoclaved H2O + 30 ml of 10X TBE (Sigma, T4415-1L, PCode: 1003141592, USA, Lot# SLCH3251) and was put in microwave until completely dissolved. Then, it was left at room temperature, and 4 µl SYBR-safe DNA gel stain (Invitrogen by Thermo Fisher Scientific, Lot#2162808, Ref: S333102) was added. Afterward, it was poured into the tray and left to solidify for 1 h at room temperature. In the next step, the rest of the 1X TBE buffer was added to the cassette and after removing the comb, the DNA ladder and samples were loaded and the gel was connected to the current to run (80 -100V, 0.43 A, 34W). The results of the genotyping have been shown in **Figure 2. 4**.

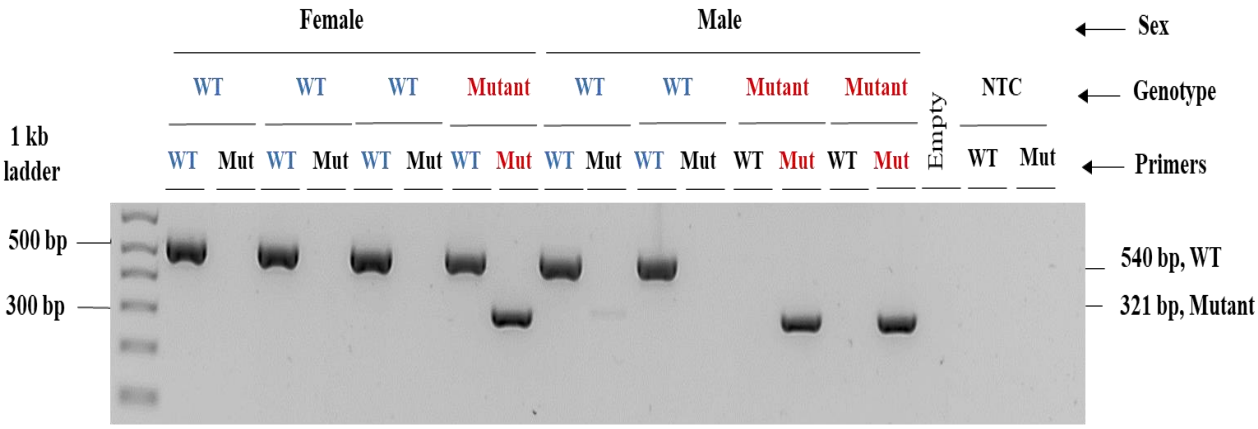

Figure 2.4. PCR-based Genotyping and Agarose Gel Electrophoresis. The result of genotyping using T158M WT and mutant primers gave rise to 2 bands (547bp and 321bp) in *Mecp2*$^{T158M/+}$ female mice, 1 band (321 bp) in *Mecp2*$^{T158M/y}$ male mice, and 1 band (547 bp) in *Mecp2*$^{+/y}$ male and *Mecp2*$^{+/+}$ female WT mice. For each sample, 2 sets of primers (WT and Mutant) were used, and the PCR products were loaded into the gel. As a positive control, Non-Template Control (NTC) was used which lacks a DNA template and only includes primes and water.

2.7. Phenotypical Analysis

2.7.1. Evaluation of Phenotypic Scoring

After a normal period of development (4 weeks in males and 15 weeks in females), RTT-like symptoms appear in both sexes of mice containing hypoactivity, mobility problems (gait and hind limb clasping), tremors, and breathing abnormalities. Furthermore, reduced body weight in *Mecp2*^{T158M} mice, increased body weight in *Mecp2*$^{T158M/+}$ female mice, and reduced brain weight in both *Mecp2*^{T158M} mice, and *Mecp2*$^{T158M/+}$ mice have been reported like null mice [71].

To study the progress of RTT-like phenotypes and the possible effect of metformin on their improvement, the evaluation of phenotypic scoring was completed in *Mecp2*$^{T158M/y}$ male mice, *Mecp2*$^{+/y}$ male, *Mecp2*$^{T158M/+}$ female mice, and *Mecp2*$^{+/+}$ female mice in 6 categories as shown in **Table 2.9**.

The start of scoring was 5-6 weeks for male mice and 15-16 weeks of age for female mice. The scoring reference chart and endpoint monitoring checklist were provided prior to the start of my thesis (Marjorie Buist) and Dr. Rastegar reviewed and already approved our animal protocol. Then, I completed daily monitoring of body weight, tooth condition, food-water consumption, evaluation of phenotypic scoring, and daily injections.

The monitoring steps were completed in a metal laminar flow hood at the same location (BMSB and CHRIM) and around the same time of day (either in the morning or the afternoon) for each set of experiments. The endpoint was determined to be the time when mice lose a minimum of 20% of their highest weight, at which point they were euthanized by CACS staff using carbon dioxide.

Table 2.5 Scoring Reference Chart.

1) Mobility/Activity Mouse is observed when placed on bench, then when handled gently.	
0	WT
1	reduced movement compared with WT, with extended freezing periods or extended delay to movement when first placed on the surface
2	complete loss of movement when placed on the surface; mouse can move in response to a gentle prod or a food pellet placed nearby (note: mice may become more active when in their own cage environment)
2) Gait	
0	WT
1	hindlimbs spread wider than WT when walking or running and/or lowered pelvis when walking or running resulting in "waddling" gait
2	tremor when feet are lifted, walks backwards or 'bunny hops' by lifting both rear feet at once; lack of full strides by hindlimbs resulting in dragging of hindquarters
3) Hindlimb clasping Mouse observed when suspended by holding base of the tail	
0	WT; hindlimbs splay outward
1	one hindlimb is pulled into the body or forelimbs are stiff and splayed outward without motion; hindlimbs may be drawn towards each other (without touching)
2	one hindlimb is pulled into the body and forelimbs are stiff and splayed outward without motion and might form a widened bowl shape; or both hindlimbs are pulled tightly into the body, either touching each other or touching the body, with or without abnormal forelimb posture
4) Tremor Mouse observed while standing on the flat palm of the hand	
0	no tremor
1	intermittent mild tremor
2*	continuous tremor or intermittent violent tremor
5) General condition Mouse observed for indicators of general well-being such as coat condition, eyes, body stance	
0	clean shiny coat, clear and opened eyes, normal body stance
1	dull or squinty eyes, dull or ungroomed coat, somewhat hunched stance
2*	piloerection, hunched stance, eyes crusted or narrowed
6) Breathing Movement of flanks observed while animal is standing still	
0	normal breathing
1	periods of regular breathing interspersed with short periods of more rapid breathing or with pauses in breathing
2*	very irregular breathing; gasping or panting

Table 2.6 Scoring Chart and End Point Monitoring Checklist.

Animal ID#		Species		Protocol	
		Room		PI	

Experimental Treatment						
Start Weight (gms)						
Date						
Weight (gms)						
% of peak weight						
Experimental Treatment given (ip.)						
1) Activity/mobility						
2) Gait						
3) Hind-limb clasping						
4) Tremor						
5) General condition						
6) Breathing						
Tooth condition						
Food/Water consumption						
Treatment given? (remedial)						
Comments						
Humane endpoint reached (Y/N)						
Initials						

For scoring 1)-6), write a 0, 1 or 2 based on observations.

2.7.2. Characterization of RTT-like Phenotypes

To evaluate the phenotypic characterization of *Mecp2*^{T158M} mice, daily monitoring of body weight was completed by myself and/or CACS staff. Also, according to **Figure 2.5**, the final measurements of dissection criteria (brain measurements and blood glucose level) were completed by our lab technician in sham mice at the basal level. Also, to investigate the effect of metformin as a drug intervention at the phenotypical level, the same procedure was conducted in the vehicle and metformin-treated mice. The brain measurements included whole brain weight, volume, and length well as the weight of the cortex, cerebellum, thalamus, and hippocampus.

Figure 2.5. Characterization of RTT-like Phenotypes in WT and *Mecp2*^{T158M} Mice. At the end of the experiments, mice were euthanized, and the brain tissues were dissected by our lab technician. At the same time, blood glucose level and brain criteria were measured including brain weight (digital scale), brain length (as shown in the picture), and brain volume (Graduated cylinder). (Photo is courtesy of Carl Olson from our lab).

2.8. Behavioral Tests Analysis

To evaluate the effect of metformin on the behavioral impairment in RTT mice, I conducted the behavioral tests of *Mecp2*^{T158M} mice and that of the control WT mice at the basal level (sham) and after the end of the treatments. The males were tested at 8 weeks and female mice were 18 weeks of age during the daytime of the circadian cycle at the end of experiments (days 19, 20, and 21). The mice were exposed to an inclusive set of behavioral tests according to the timeline in **Figure 2. 2** and were adapted to the behavior laboratory for at least 30 min before each test.

2.8.1. Open Field Test

The OFT is a behavioral test to measure the general locomotor activity, exploratory propensity, and anxiety in rodents. The mice were in the center of the apparatus (50×50×40 cm) and permitted to move around freely for 10 min. The movements of the mice were recorded for 10 min using a video camera (Free 2X webcam Recorder) and analyzed using any maze software and Ethovision 7. Different criteria including total distance traveled (cm), velocity, time in the center, and time in corners were recorded. The test chamber was cleaned with 10% ethanol between testing each mouse.

2.8.2. New Objective Recognition Test

The NOR is used to measure memory function and recognition [267, 268]. It is a 2-days test with 3 sessions including habituation, familiarization/training, and testing (**Figure 2.6**).

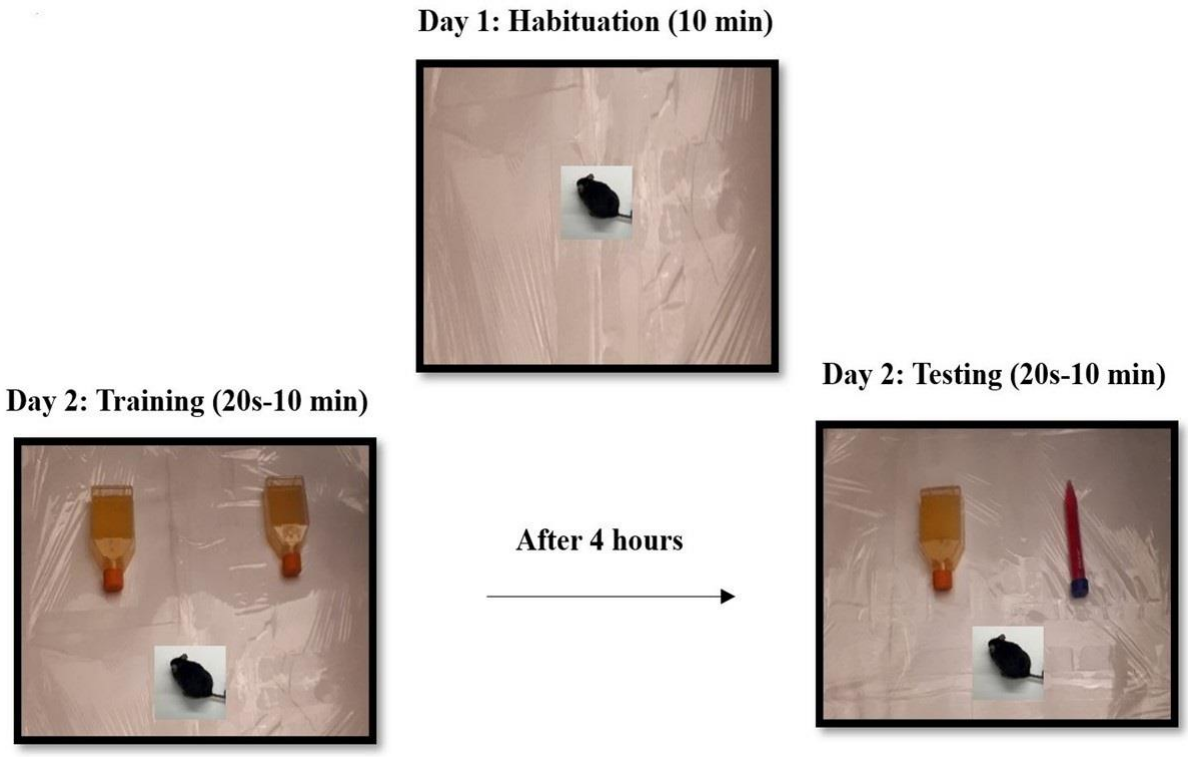

Figure 2.6. Novel Object Recognition Test. The NOR test is a two-day behavioral test that includes three steps; 1. Habituation, 2. Familiarization/training, and 3. Testing. On the first day and at the same time with OFT, mice were habituated for 10 min in the open field. The next day, during the familiarization/training session (the 20 second), mice were exposed to two alike objects to familiarize themselves with them. After 4 h of the training session, during the testing session, mice have exposed to one of the familiar objects and a new object with dissimilar shape, size, quality, and denseness. The spent time with each object was analyzed by the Ethovision 7 software [267].

The experiment was conducted in a 50x50x40 cm open field box. On the first day and along with OFT, a short habituation session was completed. Each mouse was placed in the empty open field box facing the wall closet to the experimenter and allowed to explore the open field for 10 minutes, then returned to the home cage. In a familiarization/training session and 24 hours later, 2 randomly selected alike objects were in the box, 5 cm away from the same wall. The object pair was randomly assigned to each mouse and each group was tested. Mice were allowed to behave freely until both 20-seconds exploration of both objects and when a 10 min period was over (the maximum session time). After the familiarization session, the objects and the open field were cleaned with 10 % ethanol and dried before the next use. In the testing session, 4 hours after the familiarization session, mice were returned to the box, and one of the familiar objects was substituted with a novel object. Again, mice were allowed to move freely until 20 s of total object exploration time had been reached and stopped when a 10 min period was over [268]. The apparatus and objects were cleaned with 10 % ethanol after every session to minimize olfactory signals. The time spent exploring each object was measured using Any Maze software or Ethovision 7.

2.8.3. Elevated Plus Maze

The EPM test measures anxiety-like behavior *via* a plus-shaped maze device including 2 open arms and 2 enclosed arms. The mice were in the center of the maze and their activity was recorded for 10 min with a video tracking system (BMSB camera, CHRIM camera). To evaluate the anxiety-like behavior of mice, time spent in arms (open and closed) and the number of entries into each arm were calculated by means of tracking software. The maze was carefully cleaned with 10 % ethanol after each test [269].

2.9. Statistics

Statistical analyzes were performed using GraphPad Prism 9 software and the data were presented as the mean ± SEM [270]. The analysis of data was completed using a 2-tailed t-test with Bonferroni's correction for the comparisons between WT and *Mecp2*^{T158M} mice, but between groups were analyzed using t-test and Two-way ANOVA followed by Tukey's post hoc test.

Chapter 3. Results of Aim 1

3.1. The Effect of Metformin on the MeCP2-BDNF and mTOR Pathway in Murine Brain

As previously discussed in Chapter 1, metformin is the inhibitor of the mouse hepatic mTOR pathway and a regulator of the *MECP2E1/E2-BDNF* homeostasis network *in vitro* [120, 153, 159, 222]. However, to test the efficacy of metformin *in vivo* in mice brain tissues, we conducted a pilot study in both sexes of the C57BL/6 mice strain, which has been used as a background for several transgenic mouse models [271]. It is shown that 200 mg/kg/day is higher than that used in diabetes patients (10-40 mg/kg). Prior metformin studies in the mouse model used a higher amount of metformin (250–350 mg/kg) because of the difference in drug sensitivity between humans and rodents [272-273]. In agreement with other studies, we used 200 mg/kg of metformin in our pilot study in both sexes of C57BL/6 mice, which is a safe and tolerable metformin dosage [232-236]. In this regard, 24 C57BL/6 mice (12 males and 12 females) underwent treatment with metformin (200 mg/kg/day) or vehicle *via* IP injections for 3 consecutive weeks. At the end of 21 days, the liver, as the main target tissue of metformin and 4 RTT-related brain reigns (cerebellum, cerebral cortex, hippocampus, and thalamus) were collected for molecular analysis.

3.2. The Effect of Metformin on the Mice's Average Body Weight and Blood Glucose Level

To assess the effects of 3 weeks of treatment with metformin (200 mg/kg/day), the mice's body weight was monitored daily (**Figure 3.1**), and blood glucose level (**Figure 3.2**) was measured weekly in the metformin-treated mice and their age and sex-matched controls. The sex-differences analysis showed a significantly higher (**$p < 0.01$,****$p < 0.0001$, ****$p < 0.0001$) average body weight (**Figure 3.1**) of C57BL/6 male mice in comparison with the age-matched C57BL/6 female mice in an age-dependent manner. However, no sex differences were detected in terms of blood glucose level (**Figure 3.2**). Like body weight, the level of blood glucose was not affected by metformin treatment in either sex of C57BL/6 mice. In conclusion, our pilot study confirmed the safety and tolerability of metformin 200 mg/kg/day dosage treatment compared with their age- and sex-matched control on a regular chow diet. This agrees with other studies as it is shown that in overweight and HFD-induced diabetic C57BL/6 mice, acute metformin treatment prevents the increase of body weight and rescues glucose intolerance [258].

Nonetheless, another study in a mouse model of non-insulin-dependent diabetes mellitus called the *db/db* mouse did not show any effect of metformin on body weight and blood glucose level [198].

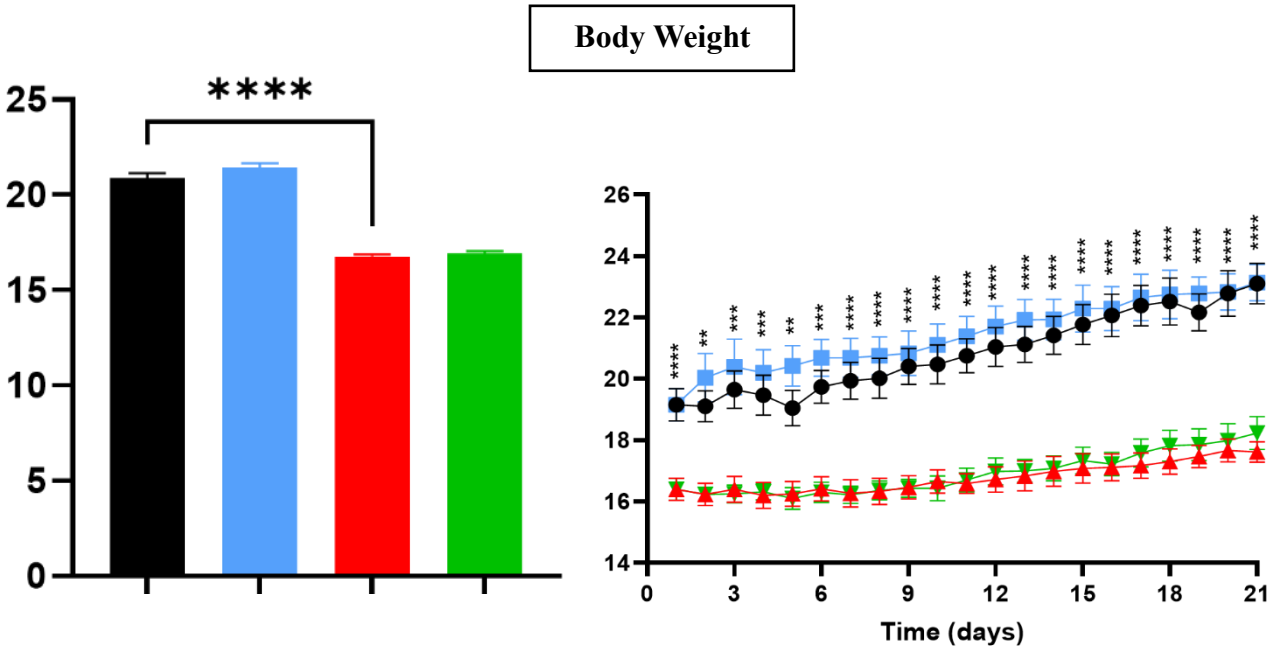

C57BL/6				
Male			Female	
Treatments	Vehicle	Metformin	Vehicle	Metformin
Number	6	6	6	6
*/**/***/**** Sex-differences: control male (vehicle) and control female (vehicle)				

Figure 3.1. The Effect of Metformin on the Average Body Weight of C57BL/6 Mice. Sex-differences analysis showed a higher average body weight of C57BL/6 male mice as compared with C57BL/6 female mice in an age-dependent manner; however, metformin did not change the average body weight of either sex of C57BL/6 mice. The analysis was completed by two-way ANOVA followed by Tukey's multiple comparisons tests and unpaired t-test. The levels of significance are shown by $^{**}p < 0.01$, $^{****}p < 0.0001$, and $^{****}p < 0.0001$, and data are reported as mean ± SEM with N=6.

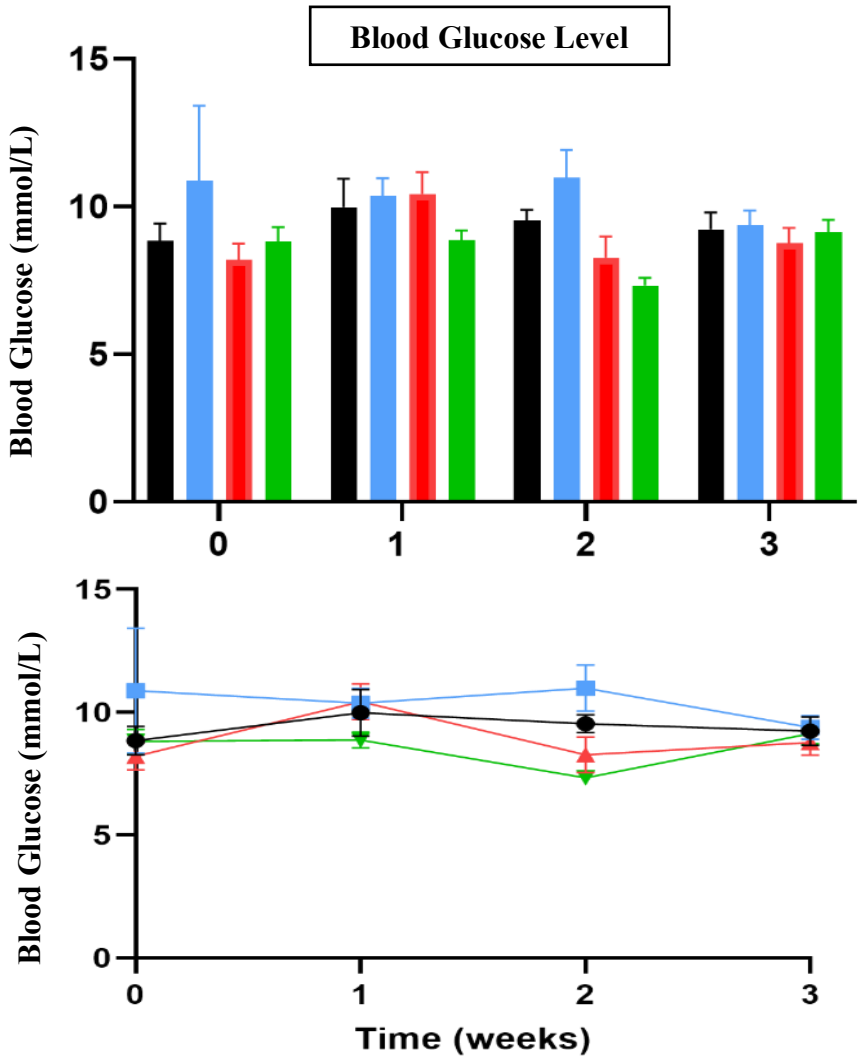

C57BL/6				
Male			Female	
Treatments	Vehicle	Metformin	Vehicle	Metformin
Number	6	6	6	6

Figure 3.2. The Effect of Metformin on the Blood Glucose Level of C57BL/6 Mice. Metformin did not change the blood glucose level of either sex of C57BL/6 mice. The analysis was completed by two-way ANOVA followed by Tukey's multiple comparisons tests and unpaired t-test. The data are reported as mean ± SEM with N=6.

3.3. The Effect of Metformin on AMPK and p-AMPK in Murine Brain

As previously discussed in Chapter 1, Mitochondrial complex I is a well-known inhibitory direct target of metformin leading to diminishing cellular respiration and increasing the ratio of AMP: ATP levels in the liver [274]. As a result, this metformin-mediated energy exhaustion leads to the activation of AMPK indicated by the increased level of p-AMPK which is the activated form of AMPK [275].

Accordingly, we studied the protein level of AMPK, p-AMPK, and the ratio of p-AMPK/AMPK in 4 brain regions (cerebellum, cortex, hippocampus, and thalamus) in alphabetical order (**Figure 3.3. A-E**). The detection of AMPK proteins in 4 brain regions (**Figure 3.3**) with antibodies from Sigma was completed. Results showed that 3 weeks of metformin treatment did not change the protein level of AMPK in the cerebellum (**Figure 3.3.B**), cortex (**Figure 3.3.C**), and hippocampus (**Figure 3.3.D**), but it induced ($^{**}p < 0.01$) AMPK at the protein level in the thalamus of C57BL/6 females (**Figure 3.3.E**). Despite the detection of AMPK, the detection of p-AMPK was unsuccessful regardless of repeated Western blot attempts.

To achieve this, we tested two antibodies from Sigma and Cell signaling according to the company's instructions. Although the detection of p-AMPK (Cell signaling) in positive control extract was successful, no signal was detected for p-AMPK in actual samples which could be due to the degradation of protein because of multiple freezing and thawing of the sample, regardless of using phosphatase inhibitors. As a result, p-AMPK detection could be further addressed by using fresh aliquots of samples in future studies.

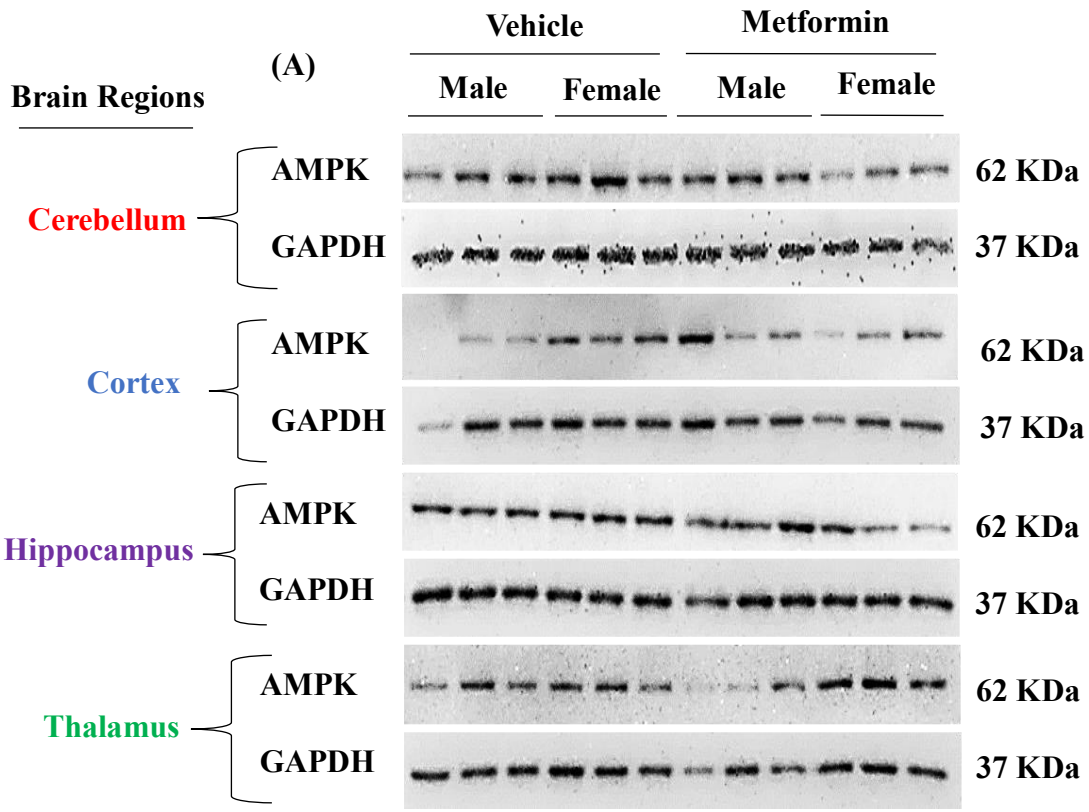

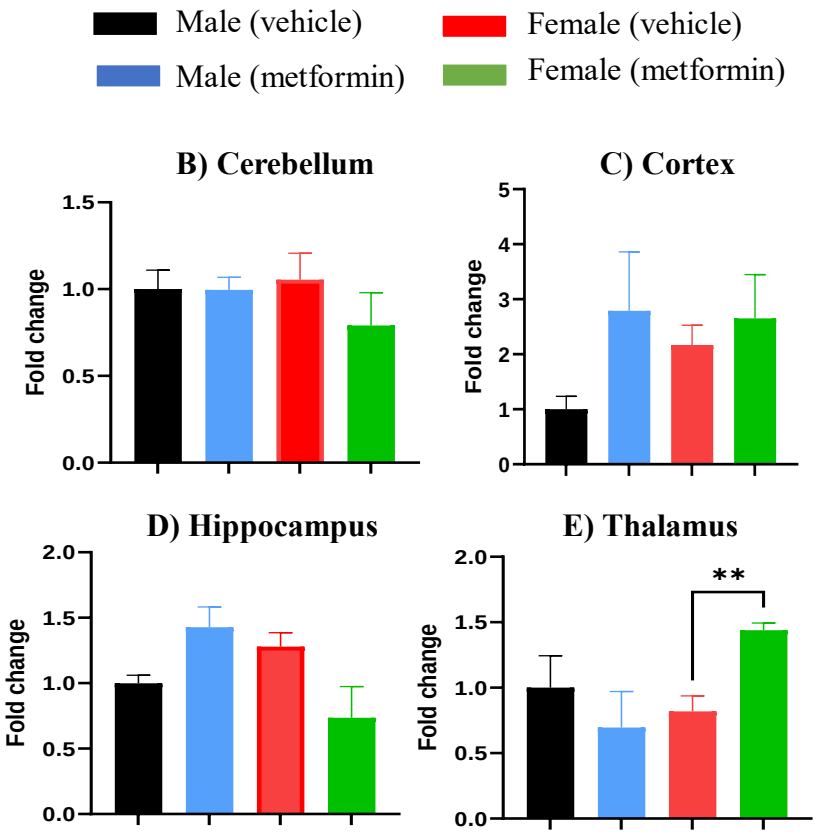

Figure 3.3. The Effect of Metformin on the AMPK in the Murine Brain. A) Representative and **B-E)** quantification of AMPK protein level after 3 weeks of metformin treatment in the C57BL/6 mice compared with their age and sex-matched controls showed increased (**$p < 0.01$) level of AMPK in the **E**) thalamus tissues of C57BL/6 female mice. Data were analyzed by unpaired t-test and values are indicated as the mean ± SEM with N=3.

3.4. The Effect of Metformin on Murine Hepatic S6 and p-S6 (235/236)

A study on C57BL/6J mice showed that metformin (200 mg/kg), is a strong inhibitor of hepatic mTORC1 activity, which is quantified by phosphorylation of the mTORC1-specific substrate (S6K1) and its downstream target S6 [222]. So, we studied the possible effect of metformin on hepatic p-S6 (235/236)/S6, as a readout of the effect of metformin treatment on the mTOR pathway (**Figure 3.4**).

The sex-differences analysis detected a higher (**$p < 0.01$) level of hepatic p-S6 (235/236) in the control C57BL/6 female mice compared with their age-matched control C57BL/6 male mice (**Figure 3.4.C**). Three weeks of metformin treatment significantly (*$p < 0.05$) increased the level of p-S6 (235/236) in C57BL/6 males and decreased (*$p < 0.05$) its level in C57BL/6 females (**Figure 3.4.C**). Furthermore, sex-differences analysis detected a higher (*$p < 0.05$) level of p-S6 (235/236)/S6 ratio in C57BL/6 female mice compared with C57BL/6 male mice, which was increased (*$p < 0.05$) in C57BL/6 male mice after metformin treatment compared with age and sex-matched control (**Figure 3.4.D**).

In conclusion, metformin's effect on hepatic p-S6 (235/236) is sex-dependent and it is attributed to the elevated level of p-S6 (235/236) and p-S6 (235/236)/S6 ratio in C57BL/6 female mice [216].

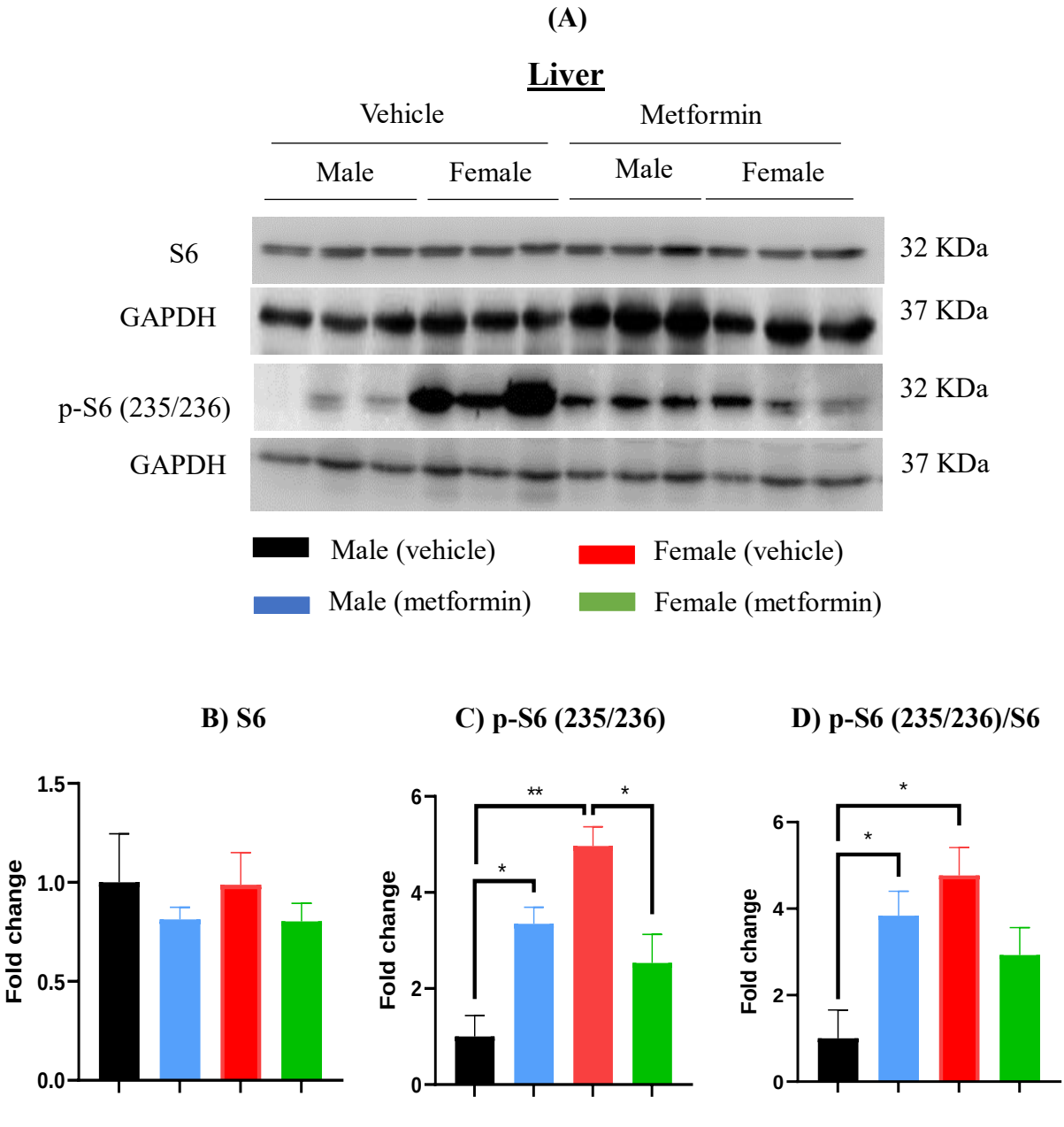

Figure 3.4. The Effect of Metformin on Murine Hepatic S6 and p-S6 (235/236). A) Representative immunoblots and **B-D**) quantification of data by normalization of relative band intensities with respect to GAPDH. **C**) The sex-differences analysis detected a significantly higher level of p-S6 (235/236) (**$p < 0.01$) in C57BL6 females compared with males. Metformin significantly induced (*$p < 0.05$) the level of p-S6 (235/236) in males and inhibited (*$p < 0.05$) it in females. **D**) Although the ratio of p-S6 (235/236)/S6 was higher (*$p < 0.05$) in females, metformin was significantly induced (*$p < 0.05$) its level in males without any effect on females. The analysis of data was completed with an Unpaired t-test and is presented by mean ± SEM with N=3. Also, the levels of significance are shown by *$p < 0.05$ and **$p < 0.01$.

3.5. The Effect of Metformin on MeCP2-BDNF and p-S6 (235/236)/S6 in the Murine Brain

Previous studies from our lab have reported RTT-associated molecular abnormalities in the brain including (a compromised *MECP2-BDNF-miR132* regulatory network and an impaired mTOR signaling pathway) in the human RTT brain [120, 159]. On the other hand, metformin has been reported as a beneficial drug *via* the induction of the *MECP2E1-BDNF* and inhibition of the mTOR pathways leading to the improvement of RTT-like phenotypes [152, 222, 171]. Therefore, we studied the feasibility of the similar effects of metformin on MeCP2-BDNF, and its downstream target including p-S6 (235/236) and S6 in C57BL6 mice brain tissues.

To examine the possible effect of metformin, we studied the protein level of MeCP2-BDNF, AKT/p-AKT, and p-S6 (235/236)/S6 in 4 brain regions of C57BL6 mice including the cerebellum (**Figure 3.5**), cortex (**Figure 3.6**), hippocampus (**Figure 3.7**), and thalamus (**Figure 3.8**) by Western blot.

Cerebellum is a particular brain region that is important in locomotion activities [162, 276]. Also, due to the regulatory effect (inhibition/stimulation) of metformin on the *MECP2*/BDNF in human cells [152], the effect of metformin in the cerebellum of C57BL/6 mice was studied to examine whether the same effect can be detected *in vivo.* Consequently, we tested the cerebellum tissues treated with metformin for 3 weeks compared with the age and sex-matched controls. Total extracts were analyzed by Western blot with MeCP2, BDNF, S6, and p-S6 (235/236) specific antibodies (**Figure 3.5**). Regardless of repeating the experiments, no signal was detected for mBDNF (15 KDa) in the cerebellar samples. In C57BL/6 female mice, metformin significantly ($*p < 0.05$) reduced the level of pro-BDNFs (45 KDa) (**Figure 3.5.C**).

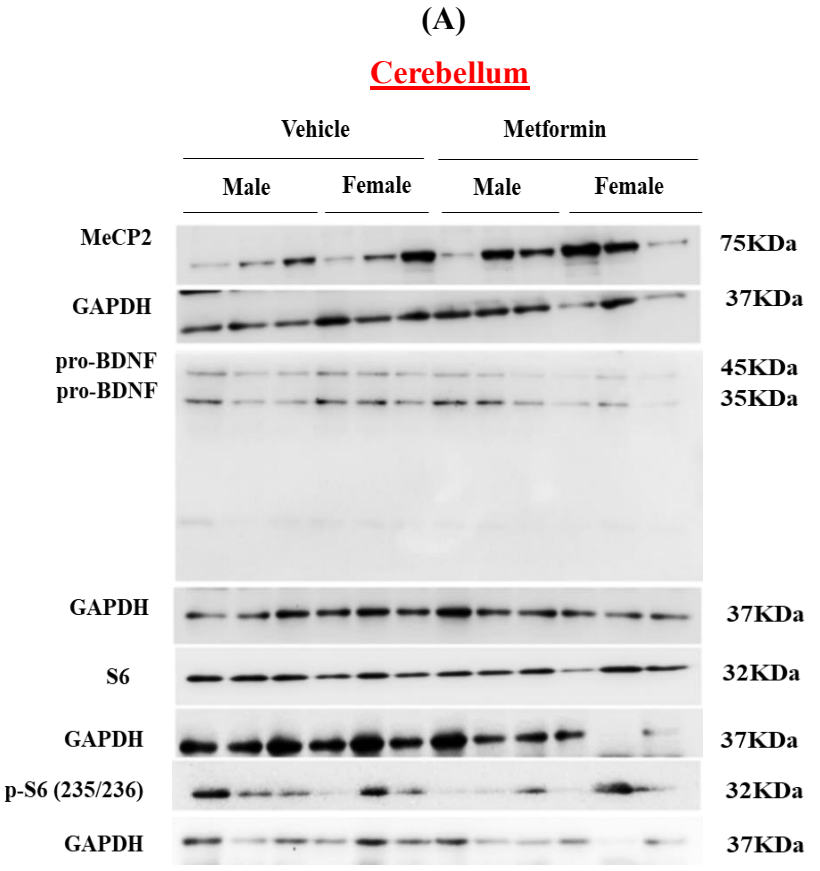

Figure 3. 5. The Effect of Metformin on MeCP2-BDNF and p-S6 (235/236)/S6 in the Murine Cerebellum. A) Representative immunoblots and **B-D**) quantification of data by normalization of relative band intensities with respect to GAPDH. Metformin reduced the level of **C**) pro-BDNF (45 kDa) (*$p < 0.05$) in females. Also, mBDNF was not detected in the cerebellum of C57BL6 mice. The analysis was completed with an unpaired t-test and Two-way ANOVA following Tukey's multiple tests. The differences were indicated by *$p < 0.05$ and data were presented as mean ± SEM for the N=3.

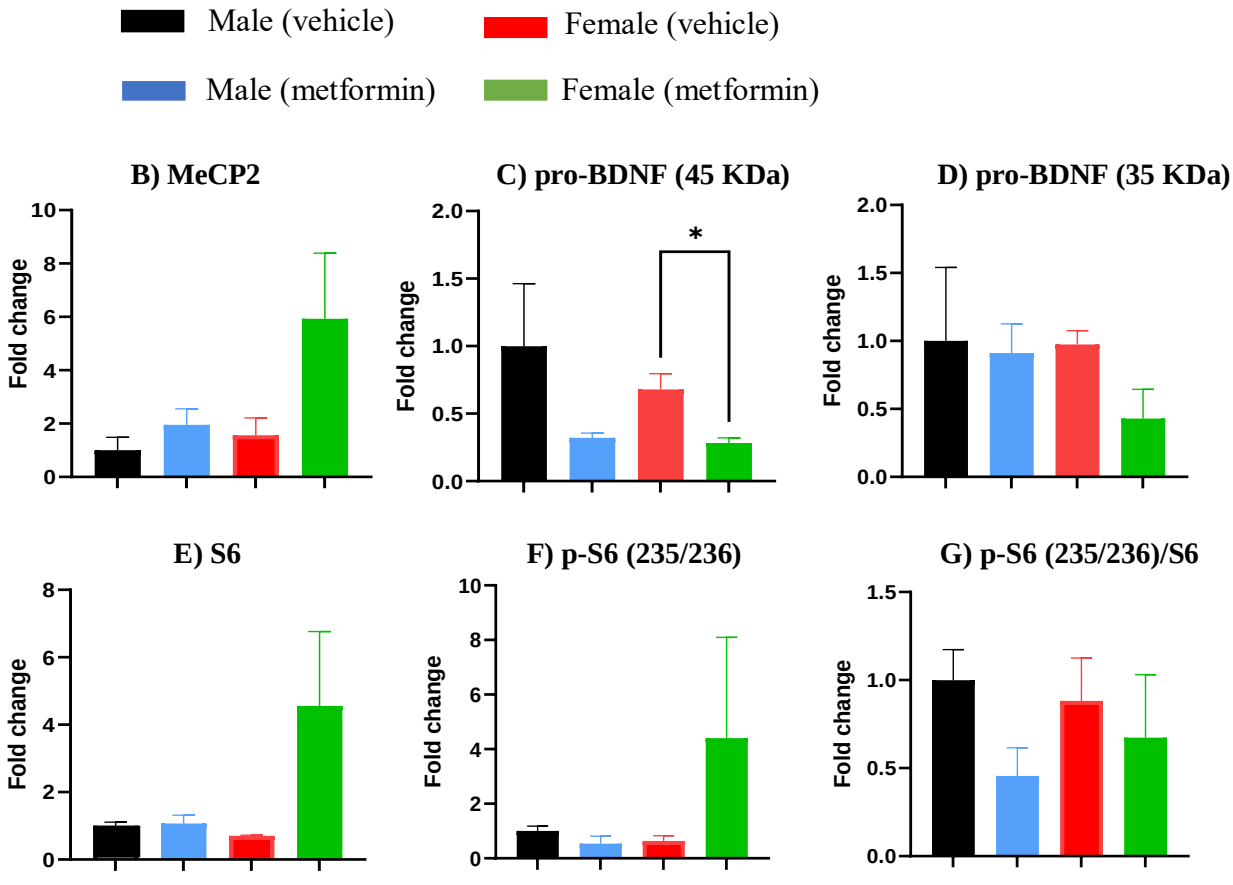

The results of the Western blot in the cortex (**Figure 3.6**) showed that metformin treatment did not affect the cortical protein level of MeCP2, pro-BDNF, BDNF, S6, and p-S6 (235/236) in either sex of mice.

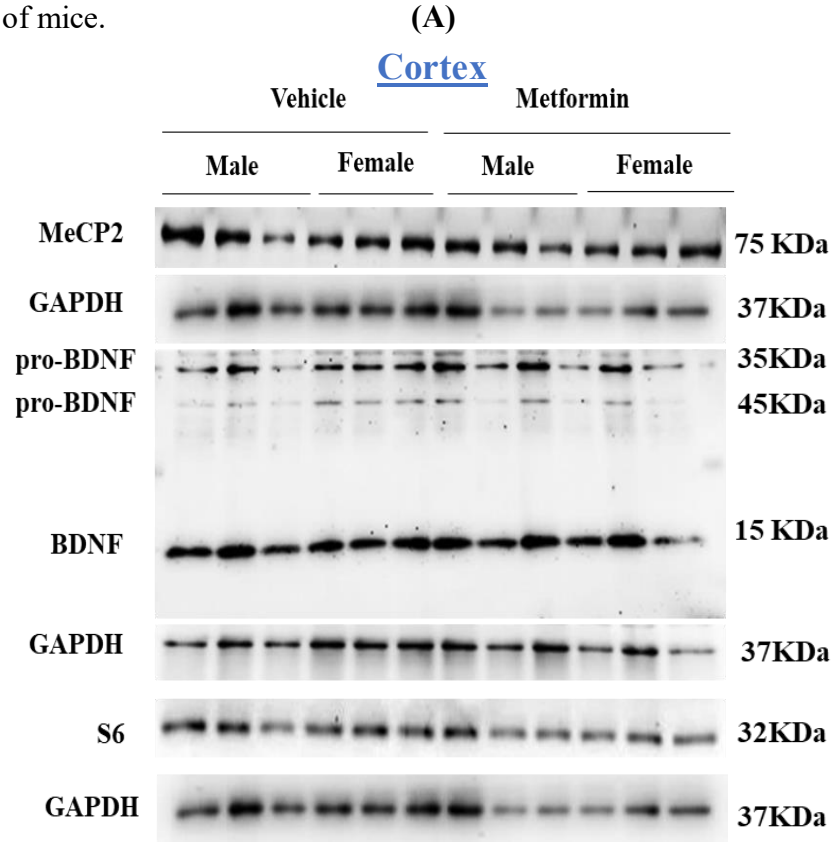

Figure 3. 6. The Effect of Metformin on MeCP2-BDNF, and p-S6/S6 in the Murine Cortex. A) Representative immunoblots has shown. After 3 weeks of treatment, according to the Unpaired t-test analysis, metformin did not affect the cortical protein levels. The analysis of data was completed with an Unpaired t-test and 2-way ANOVA followed by Tukey's test. All the data are reported as mean ± SEM with N=3.

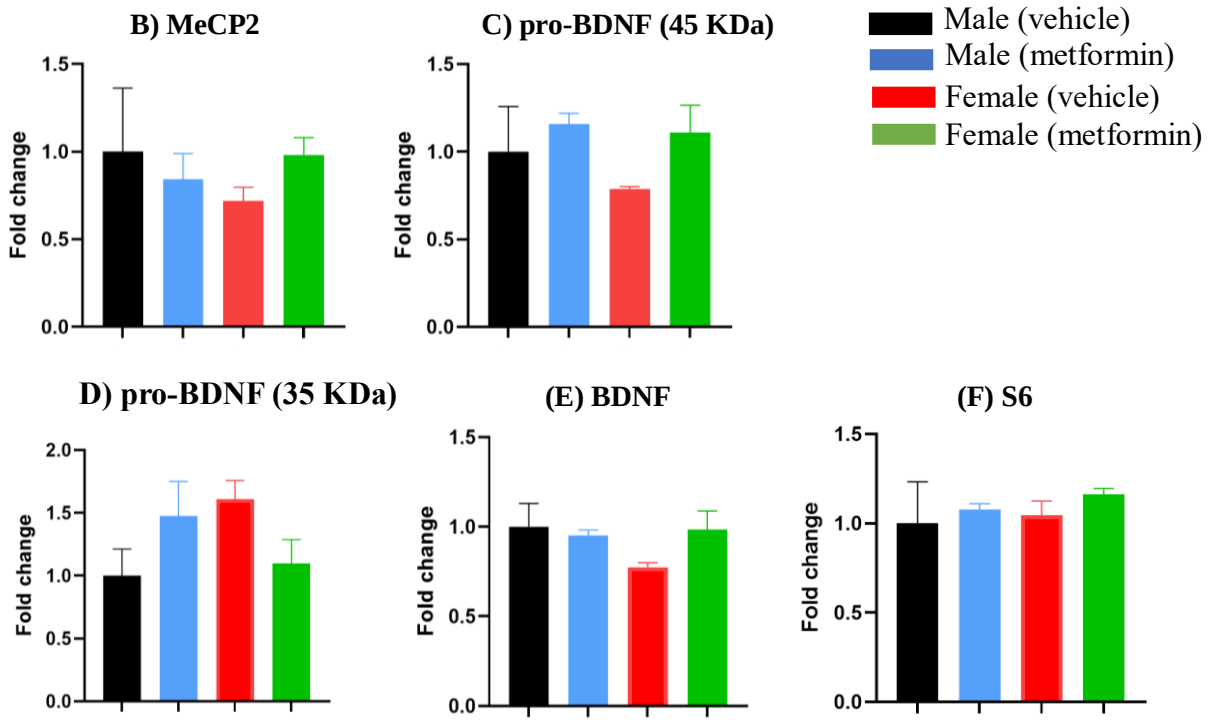

In the hippocampus (**Figure 3.7**) metformin-treated C57BL/6 male mice showed significant induction of MeCP2 (**Figure 3.7.B**), pro-BDNF (45 KDa) (**Figure 3.7.C**), and mBDNF (**Figure 3.7.E**) compared with age- and sex-matched control.

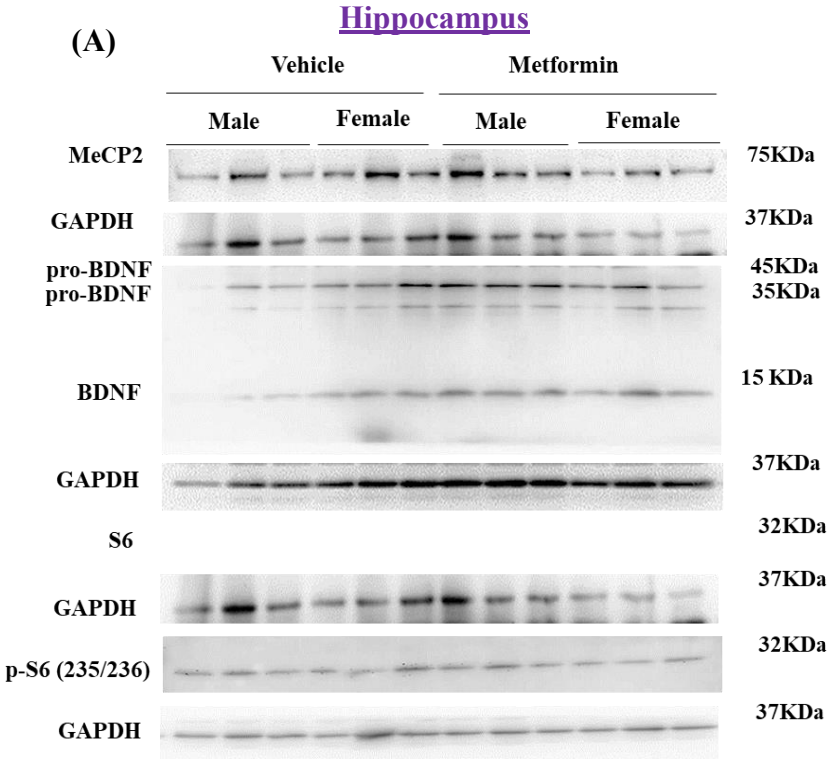

Figure 3.7. The Effect of Metformin on MeCP2-BDNF, p-S6/S6 in the Murine Hippocampus. A significant induction of **B**) MeCP2, **C**) pro-BDNF (45 KDa), and **E**) BDNF compared with age- and sex-matched control was detected. **E**) Also, the sex-differences analysis showed a higher level of mBDNF in females compared with males. The analysis of data was completed with Unpaired t-test and 2-way ANOVA followed by Tukey's test. All the data are reported as mean ± SEM with N=3.

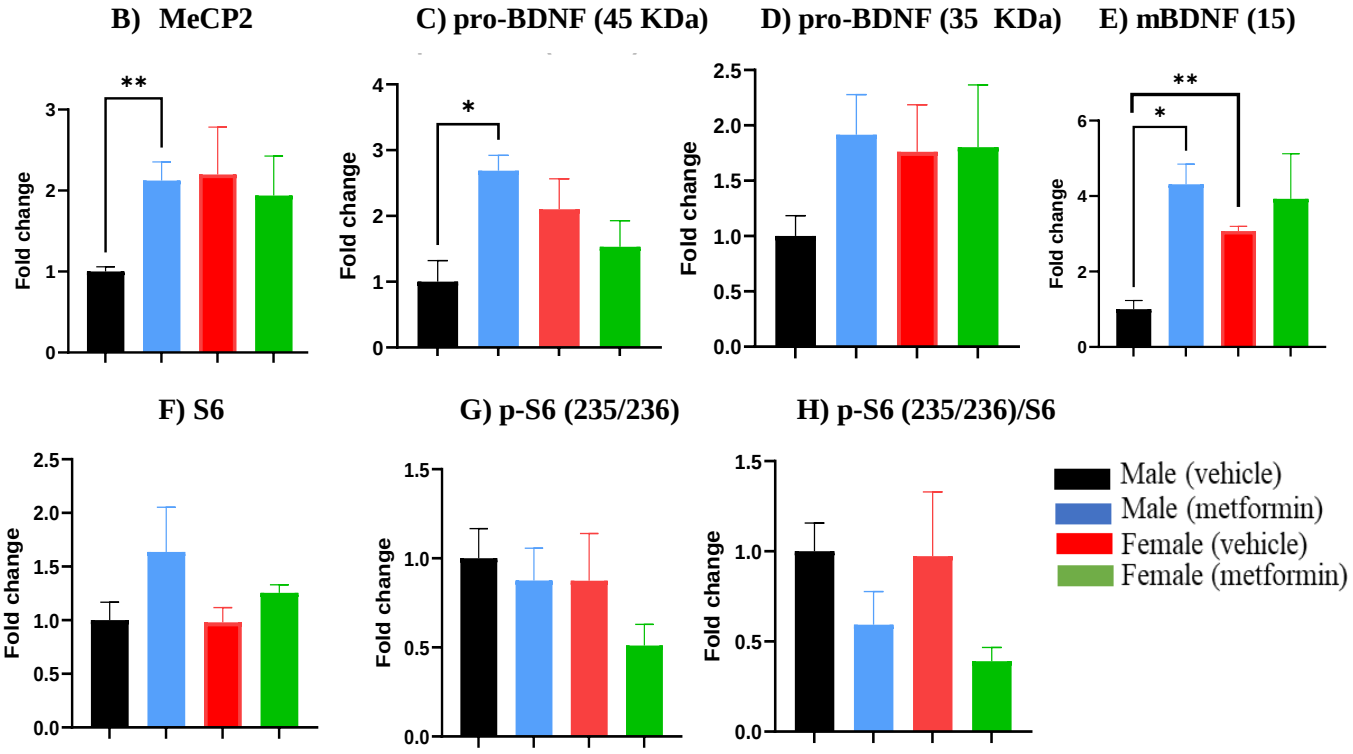

In the thalamus extracts **(Figure 3.8)**, protein analysis showed significantly lower level of mBDNF (15 KDa) in control C57BL/6 female mice compared with their age-matched control males (**Figure 3.8. E**). Metformin significantly induced the level of pro-BDNF (35 kDa) (**Figure 3.8. D**) in female mice and inhibited mBDNF protein level in male mice compared with their age-and sex-matched control (**Figure 3.8.E**).

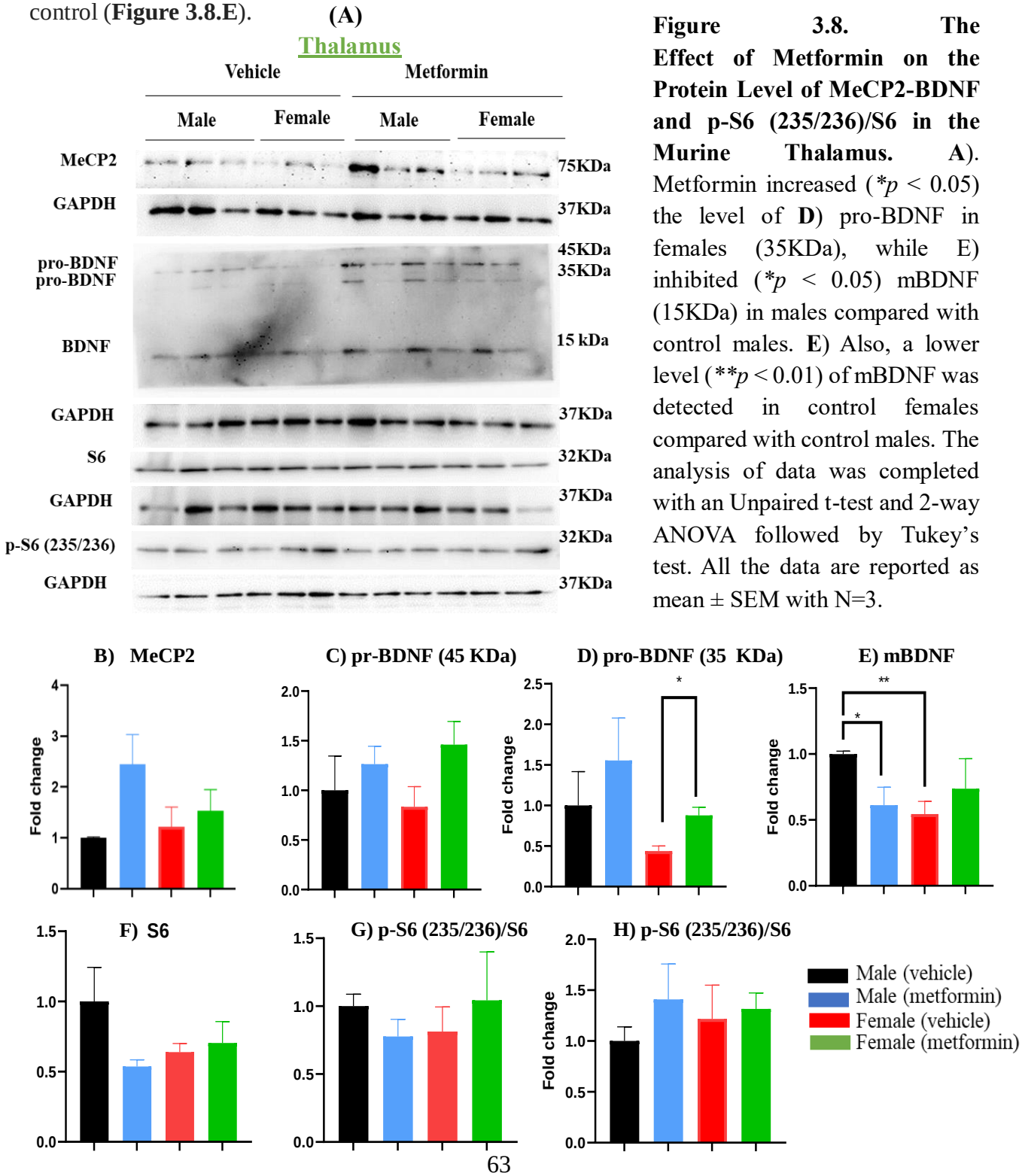

Figure 3.8. The Effect of Metformin on the Protein Level of MeCP2-BDNF and p-S6 (235/236)/S6 in the Murine Thalamus. A). Metformin increased (*$p < 0.05$) the level of **D**) pro-BDNF in females (35KDa), while E) inhibited (*$p < 0.05$) mBDNF (15KDa) in males compared with control males. **E**) Also, a lower level (**$p < 0.01$) of mBDNF was detected in control females compared with control males. The analysis of data was completed with an Unpaired t-test and 2-way ANOVA followed by Tukey's test. All the data are reported as mean ± SEM with N=3.

3.6. Summary of Metformin Effect on Murine Tissues at the Protein Level

According to protein studies in the liver and brain tissues of metformin-treated C57BL/6 male and female mice compared with their age- and sex-matched controls, a summary of metformin effects at the protein level has been proposed, which in case of p-S6 (235/236) is sex- and region-dependent and in the case of BDNF is brain-region dependent (**Figure 3.9).**

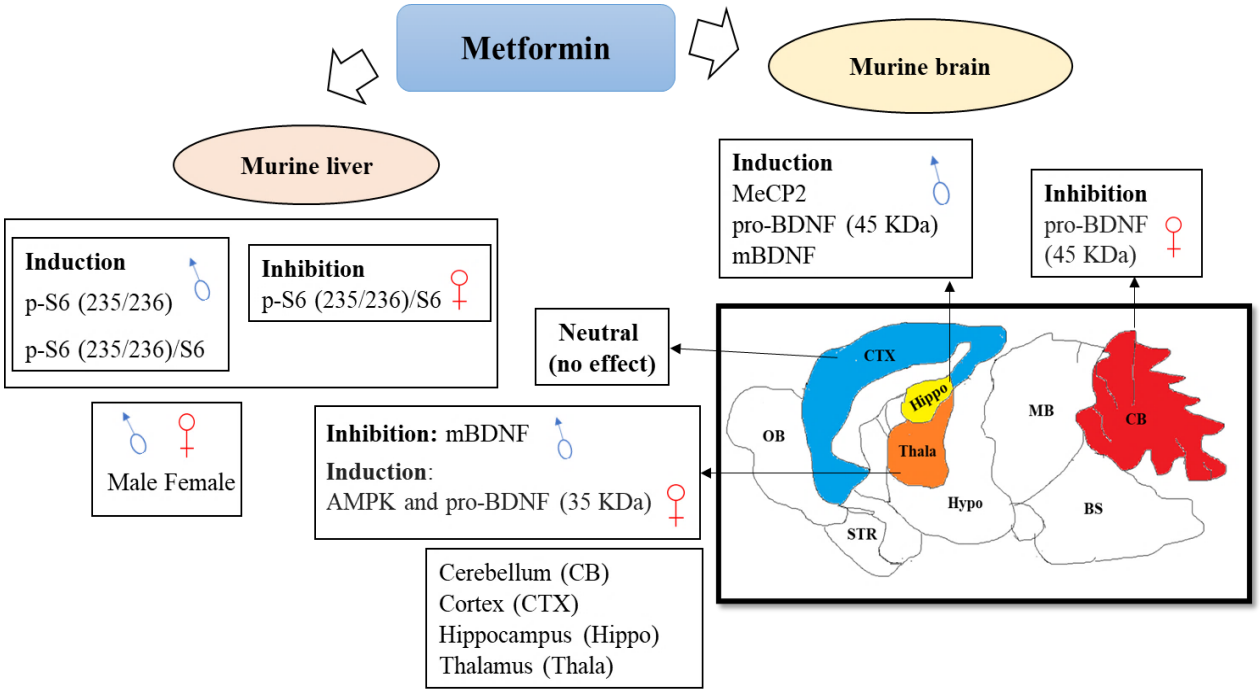

Figure 3.9 Metformin Indicated Sex-and Region-specific Effects in Murine Tissues [92]. In the C57BL/6 male murine liver extracts, metformin induced the level of p-S6 (235/236) and the ratio of p-S6 (235/236)/S6 in males but decreased the level of p-S6 (235/236) in the female hepatic extracts. In mice brain tissues, metformin increased the level of MeCP2 and mBDNF in the hippocampus extracts of C57BL/6 male mice but reduced the level of mBDNF in the thalamus. Also, metformin-induced the level of AMPK in the thalamus extracts of C57BL/6 mice females. Ultimately, it could be concluded that the metformin effect in the murine liver and brain of C57BL6 mice is sex- and region-dependent at the protein level of p-S6 (235/236), and brain-region dependent in the case of BDNF.

Summary of Aim 1 Results: Pilot study

To study the regulatory effect of metformin at the protein level in murine tissues

---

1. A pilot study approved the safety of metformin treatments (200 mg/kg/day, IP injections for 21 days) *in vivo.*
2. A metformin-mediated and sex-dependent increase of male murine hepatic p-S6 (235/236) and reduction of female hepatic p-S6 (235/236) is proof of the principle on the possible change of hepatic mTORC1 activity.
3. Unlike murine hepatic tissues, metformin-mediated change of brain mTORC1 activity was not detected.
4. A wide spectrum of metformin-mediated regulatory effects was detected on the murine brain tissues in a sex and brain-region-specific manner at the protein level.
5. At the basal level, murine female mBDNF in the thalamus is lower than in control females and in the hippocampus is higher than in control male

Chapter 3. Results of Aim 2

In Aim 1 of my thesis, the effects of 3 weeks of metformin treatment (200 mg/kg/day, IP injections) were presented at the molecular level on the MeCP2-BDNF and S6 in C57BL/6 in murine tissues. In Aim 2 of my thesis, I will focus on the results of 3 weeks of metformin treatment (250 mg/kg/day, IP injection) on the improvement of RTT-like symptoms in *Mecp2*^{T158M} mice at the phenotypical and behavioral level.

Although no present cure is available for RTT, numerous therapeutic methods for RTT treatment have been studied [57, 277, 278], including AAV-mediated gene therapy [278] and reactivation of the WT copy of *Mecp2* on the inactive X chromosome (Xi). Recently, a study [255] has reported the effect of MeCP2 T158M mutation in RTT etiology through the generation of a knock-in *Mecp2*^{T158M} mouse model, indicating compromised DNA binding affinity and disrupted MeCP2 protein level, results in the development of RTT-like phenotypes. Following this study, targeting MeCP2 protein expression or stability was suggested as a probable treatment procedure for the treatment of RTT [69, 279]. In accordance with similar studies [255], to screen RTT-like symptoms before and after metformin treatment, 3 approaches had been used including phenotypic characterization (average body weight, brain measurements, and blood glucose level), evaluation of phenotypic scoring (activity, gait, hind limb clasping, tremor, general condition, and breathing) and a series of behavioral tests (OFT, NOR, and EPM Tests).

3.7. The Evaluation of Phenotypic Characterization of *Mecp2*^{T158M} Mice

In classical RTT, the MeCP2 T158M is the most common missense mutation [71]. To study the function of this mutation in RTT etiology, we used a *Mecp2*^{T158M} knock-in mice model representing this mutation at the basal level (sham). For the sake of this, *Mecp2*^{T158M} male and female mice including *Mecp2*$^{+/y}$, *Mecp2*$^{T158M/y}$, *Mecp2*$^{+/+}$, and *Mecp2*$^{T158M/+}$ mice were categorized into 12 groups based on their sex, genotype, and treatments given to mice and the details of mice numbers are explained in each related figure and section of the results. For some of the mice, incomplete scoring records or lack of behavioral test data and dissection criteria are attributed to sudden death or humane endpoints being reached.

3.7.1. The Effect of Metformin on the Phenotypic Characterization of *Mecp2*$^{T158M/y}$ Male Mice

Prior to the therapeutic intervention with metformin, the phenotypic characterization of *Mecp2*$^{+/y}$ and *Mecp2*$^{T158M/y}$ male mice was evaluated at the basal level (sham) (**Figure 3.10**). The results showed a lower body weight (**Figure 3.10. A**), lower brain weight, and smaller brain volume (**Figure 3.10. C**) in *Mecp2*$^{T158M/y}$ mice as compared with age- and sex-matched *Mecp2*$^{+/y}$ male mice which are along with prior discoveries in *Mecp2*-null mice (microcephaly); However, no difference was detected in case of blood glucose level, and brain regions weight of *Mecp2*$^{T158M/y}$ male compared with *Mecp2*$^{+/y}$ male mice (**Figure 3.10. B and D**).

To study the effect of metformin on the phenotypic characterization of *Mecp2*$^{+/y}$ and *Mecp2*$^{T158M/y}$ mice, at the end of the experiment, the measurement of brain criteria (weight, length, and volume) and blood glucose level were completed by Mr. Carl Olson, and I performed the related analysis as represented in **Figure 3.11**. In sex-differences analysis, *Mecp2*$^{T158M/y}$ male mice indicated a lower level of body weight compared with that of *Mecp2*$^{+/y}$ male mice. Three weeks of metformin treatment showed a reduction in the body weight of *Mecp2*$^{T158M/y}$ male mice as compared with the body weight of age- and sex-matched *Mecp2*$^{+/y}$ mice (**Figure 3.11.A**).

Although the brain phenotype was not affected, metformin significantly reduced the level of blood glucose in *Mecp2*$^{T158M/y}$ male mice in comparison to the age-matched *Mecp2*$^{+/y}$ male mice (**Figure 3.11.B**). In the case of whole brain measurements, *Mecp2*$^{T158M/y}$ male mice showed significantly lower brain weight and smaller brain length contrary to age-matched *Mecp2*$^{+/y}$ male mice as control (**Figure 3.11.C**).

In conclusion, the evaluation of phenotypic scoring of *Mecp2*^{T158M} knock-in mice with the purpose of RTT-like phenotype development screening agreed with earlier discoveries in *Mecp2*-null mice which *Mecp2*$^{T158M/y}$ male mice weighed considerably less and had substantially decreased brain weights compared with their age- and sex-matched *Mecp2*$^{+/y}$ male mice [37, 296].

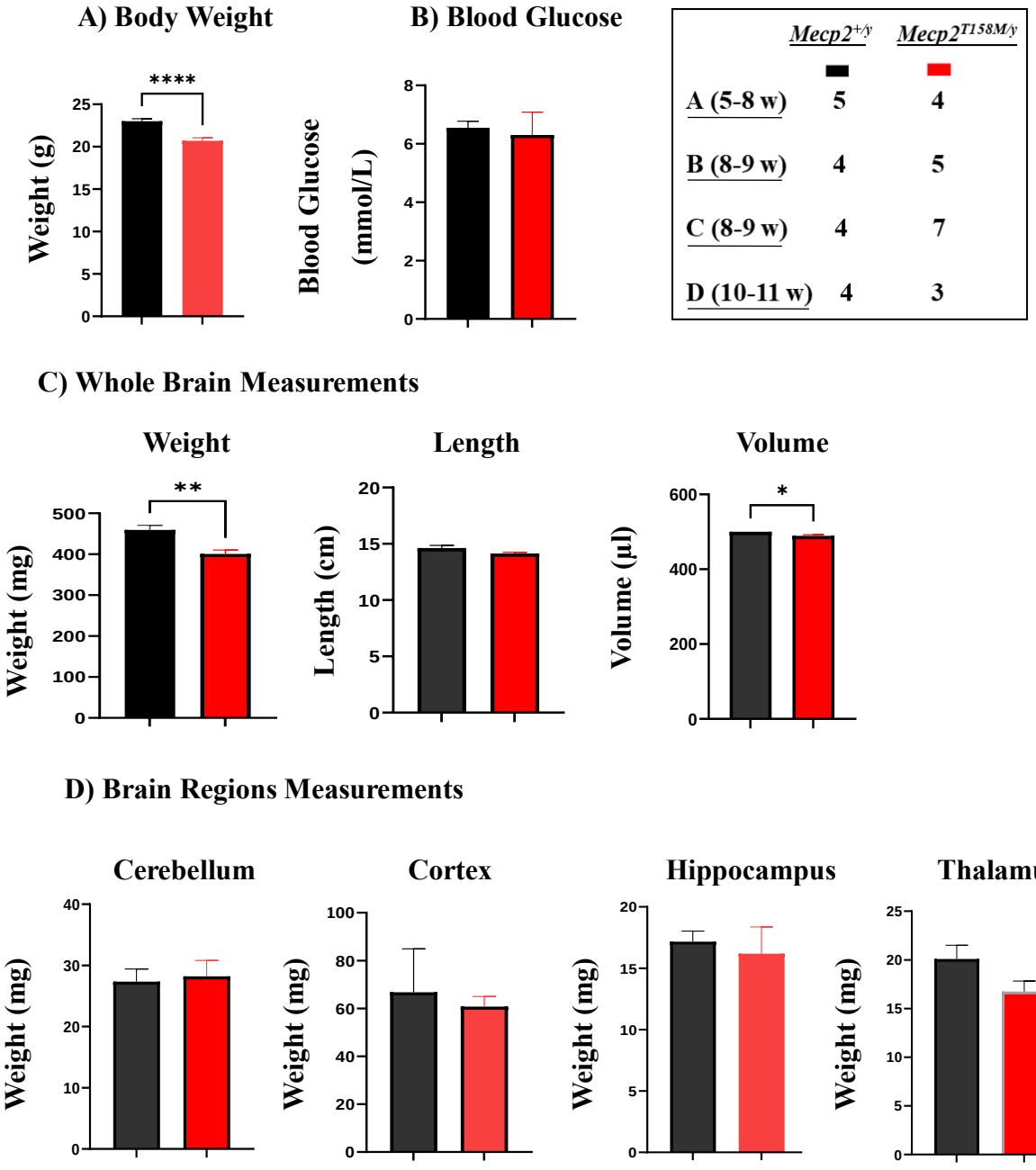

Figure 3.10. The Evaluation of Phenotypic Characterization in *Mecp2*$^{+/y}$ and *Mecp2*$^{T158M/y}$ Male Mice at the Basal Level. A lower level of **A**) body weight, **C**) brain weight, and **B**) smaller size of brain volume of *Mecp2*$^{T158M/y}$ mice were detected compared with age- and sex-matched *Mecp2*$^{+/y}$ male mice (microcephaly); **B**) however, the blood glucose level of *Mecp2*$^{T158M/y}$ male in comparison with *Mecp2*$^{+/y}$ mice did not change. All the statistical analysis was completed by unpaired t-test, and the level of differences are $*p < 0.05$ $**p < 0.01$ and $****p < 0.0001$. All the values are shown as mean ± SEM.

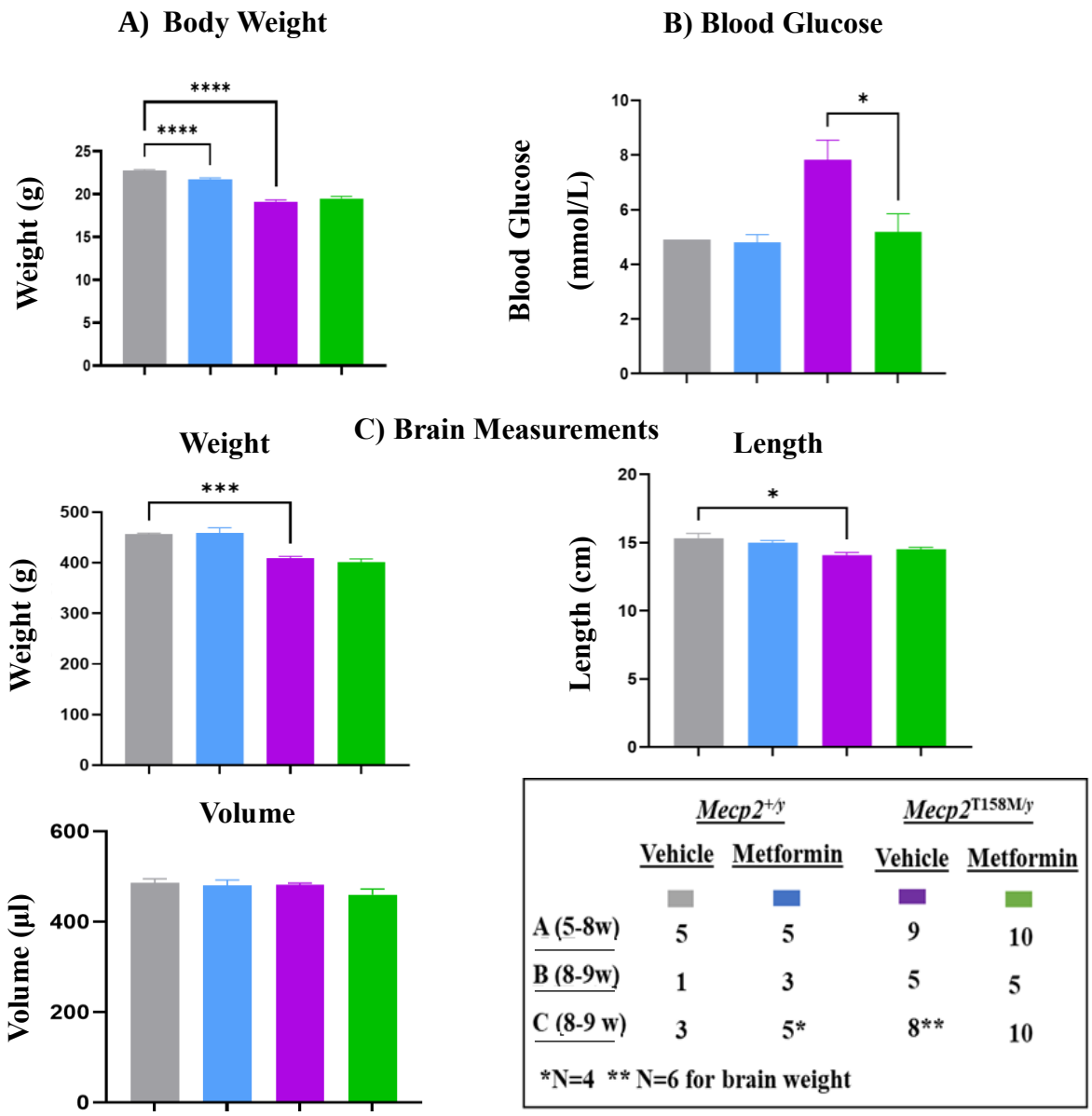

Figure 3.11. The Effect of Metformin on the Phenotypic Characterization of *Mecp2*$^{+/y}$ and *Mecp2*$^{T158M/y}$ Male Mice. A) A lower level of body weight was detected in control *Mecp2*$^{T158M/y}$ male mice compared with control *Mecp2*$^{+/y}$ male mice in an age-dependent manner. Furthermore, a metformin-mediated body weight loss was detected in control *Mecp2*$^{+/y}$ male mice compared with control *Mecp2*$^{+/y}$ male mice. **B**) Metformin significantly reduced the level of blood glucose in *Mecp2*$^{T158M/y}$ male mice in comparison with the *Mecp2*$^{+/y}$ male mice. **C**) A lower level of brain weight and smaller brain length was detected in control *Mecp2*$^{+/y}$ male mice compared with control *Mecp2*$^{+/y}$ male mice. All the statistical analysis was completed with unpaired t-test and two-way ANOVA followed by Tukey's Multiple comparisons test and the level of differences are $*p < 0.05$, $***p < 0.001$, and $****p < 0.000$. All the values are shown as mean ± SEM.

3.7.2. The Effect of Metformin on the Phenotypic Characterization of *Mecp2*$^{T158M/+}$ and *Mecp2*$^{+/+}$ Female Mice

In addition to *Mecp2*^{T158M} male mice, we investigated the phenotypic characterization of *Mecp2*$^{+/+}$ and *Mecp2*$^{T158M/+}$ female mice as the most relevant mice model to the RTT, at the basal level. At the end of 21 days of experiments, measurement of dissection criteria (body weight, brain weight, and blood glucose level) in 18-19 weeks old female mice were completed by our lab technician, Mr. Carl Olson, and subsequently, I completed the analysis as shown in **Figure 3.12**. A higher level of average body weight was detected in *Mecp2*$^{T158M/+}$ female mice compared with *Mecp2*$^{+/+}$ female mice (**Figure 3.12.A**).

Regarding the brain measurements (**Figure 3.12.C**), *Mecp2*$^{T158M/+}$ female mice showed lower brain and cortex weight, and smaller brain volume compared with *Mecp2*$^{+/+}$ female mice (microcephaly).

Contrary to higher body weight and lower level of brain measurements detected in *Mecp2*$^{T158M/+}$ female mice, no differences were found in the blood glucose level of either of the mice groups (**Figure 3.12**). In the case of control groups, *Mecp2*$^{T158M/+}$ female mice showed a significantly higher level of average body weight compared with control *Mecp2*$^{+/+}$ female mice; However, 3 weeks of metformin treatment did not affect the average body weight, blood glucose level, and brain measurements of either of *Mecp2*$^{+/+}$ and *Mecp2*$^{T158M/+}$ female mice (**Figure 3.12**).

In conclusion, our results agree with other studies since *Mecp2*$^{T158M/+}$ heterozygous female mice showed increased body weight compared with age-and sex-matched *Mecp2*$^{+/+}$ female mice, but they were microcephalic [71].

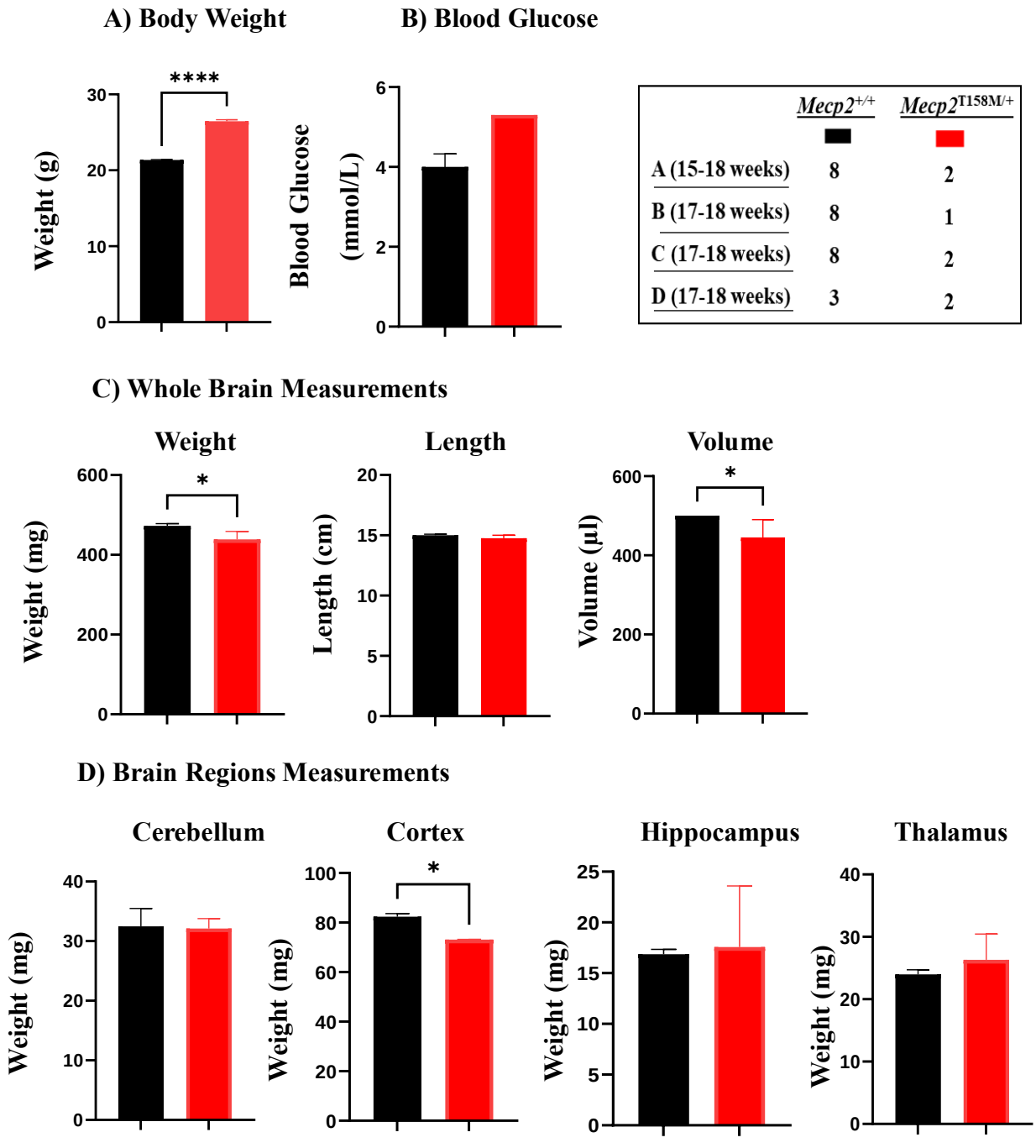

Figure 3.12. The Evaluation of Phenotypic Characterization of *Mecp2*$^{+/+}$ and *Mecp2*$^{T158M/+}$ Female Mice at the Basal Level. **A**) The *Mecp2*$^{T158M/+}$ mice significantly showed a higher level of A) average body weight, **C**) reduced level of whole brain weight, the smaller size of brain volume, and **D**) lower level of cortex weight compared with that of sex- and age-matched *Mecp2*$^{+/+}$ mice. All the statistical analysis was completed by unpaired t-test, and the level of differences are *$p < 0.05$ and ****$p < 0.000$. All the values are shown as mean ± SEM.

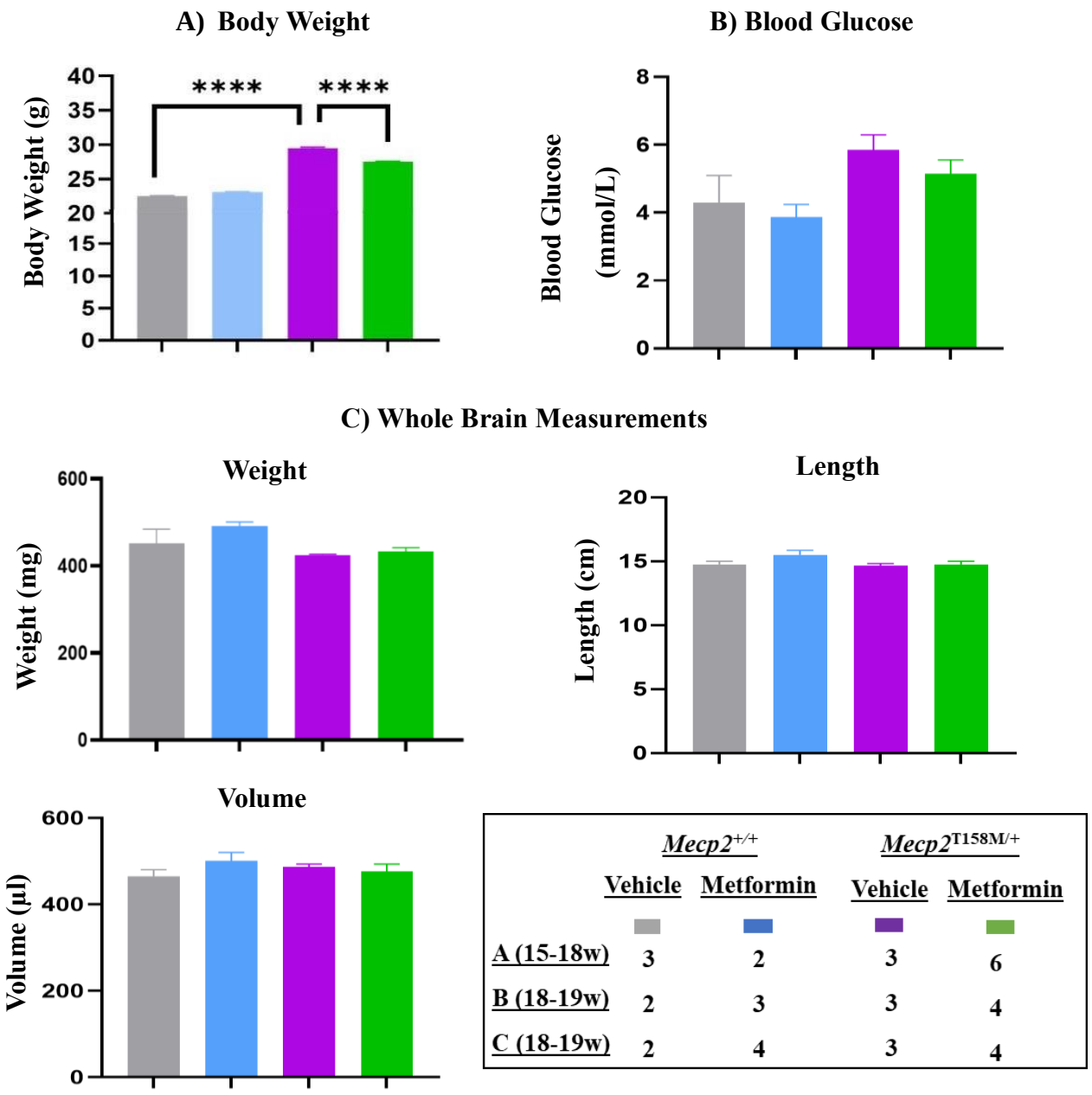

	Mecp2$^{+/+}$		*Mecp2*$^{T158M/+}$	
	Vehicle	Metformin	Vehicle	Metformin
A (15-18w)	3	2	3	6
B (18-19w)	2	3	3	4
C (18-19w)	2	4	3	4

Figure 3.13. The Effect of Metformin on the Phenotypic Characterization of *Mecp2*$^{+/+}$ and *Mecp2*$^{T158M/+}$ Female Mice. A) The control *Mecp2*$^{T158M/+}$ female mice were significantly weighed heavier compared with control *Mecp2*$^{+/+}$ female mice (vehicle). Metformin reduced the **A**) average body weight of *Mecp2*$^{T158M/+}$ female mice compared with control *Mecp2*$^{T158M/+}$ female mice, but it did not affect any phenotypical characterization including **B**) blood glucose level, and **C**) brain measurements of *Mecp2*$^{+/+}$ and *Mecp2*$^{T158M/+}$ female mice. All the statistical analysis was completed by unpaired t-test and the level of difference is $***p < 0.001$. All the values are shown as mean ± SEM.

3.8. The Evaluation of Phenotypic Scoring of *Mecp2*^{T158M} *Mice*

According to the literature, the evaluation of phenotypic scoring, which assesses a range of RTT-like phenotypes, involving gait defects, motor deficits, and breathing was performed on *Mecp2*$^{T158M/y}$ mice at 4-12 weeks of age. Also, the characterization of RTT-like phenotypes in heterozygous females as clinically pertinent mouse models were completed [280]. Even though the hemizygous *Mecp2*$^{T158M/y}$ male mice and heterozygous *Mecp2*$^{T158M/+}$ female mice represent comparable RTT-like phenotypes, the severity, and progression are milder in females and have a longer lifespan, but have premature death as compared to WT. Therefore, both male and female *Mecp2*^{T158M} mice exhibit similar phenotypes to those of *Mecp2*-null mice and several neurological deficits similar to RTT [37, 43]. To evaluate the metformin-mediated improvement of RTT-like phenotypes in *Mecp2*$^{T158M/y}$ male mice (5-9 weeks of age) and *Mecp2*$^{T158M/+}$ female mice (15-19 weeks of age), I completed the daily phenotypic scoring of *Mecp2*^{T158M} mice before and after metformin treatment in six categories including, activity, gait, hind-limb clasping, tremor, breathing, and general condition as previously mentioned [281]. Furthermore, to avoid bias, the blind daily scoring was completed by CACS staff for some mice during weekdays.

3.8.1 The Effect of Metformin on the Phenotypic Scoring of *Mecp2*^{T158M} Male and Female Mice

To investigate the severity of RTT-like symptoms at the basal level, the evaluation of scoring of *Mecp2*$^{T158M/y}$ and *Mecp2*$^{+/y}$ male and sham mice was completed. The results showed an age-dependent increase in the severity of symptoms in the *Mecp2*$^{T158M/y}$ male mice compared with *Mecp2*$^{+/y}$ male mice in 6 categories (activity, gait, hind-limb clasping, tremor, breathing, and general condition) as shown in **Figure 3.14**. The effect of metformin on the improvement of RTT-like phenotypes in *Mecp2*$^{T158M/y}$ and *Mecp2*$^{+/y}$ male mice was evaluated in 6 categories. Animals were given a score of 0, 1, or 2 for each category, corresponding to the sign being absent, present, or severe, respectively. The results showed that metformin tends to improve the severity of RTT-like symptoms, which in the case of activity, general condition, and breathing abnormalities is significant and age-dependent (**Figure 3.15**). The results of scoring in females showed the improvement of tremor scores and breathing abnormalities in an age-dependent manner (**Figure 3.16**).

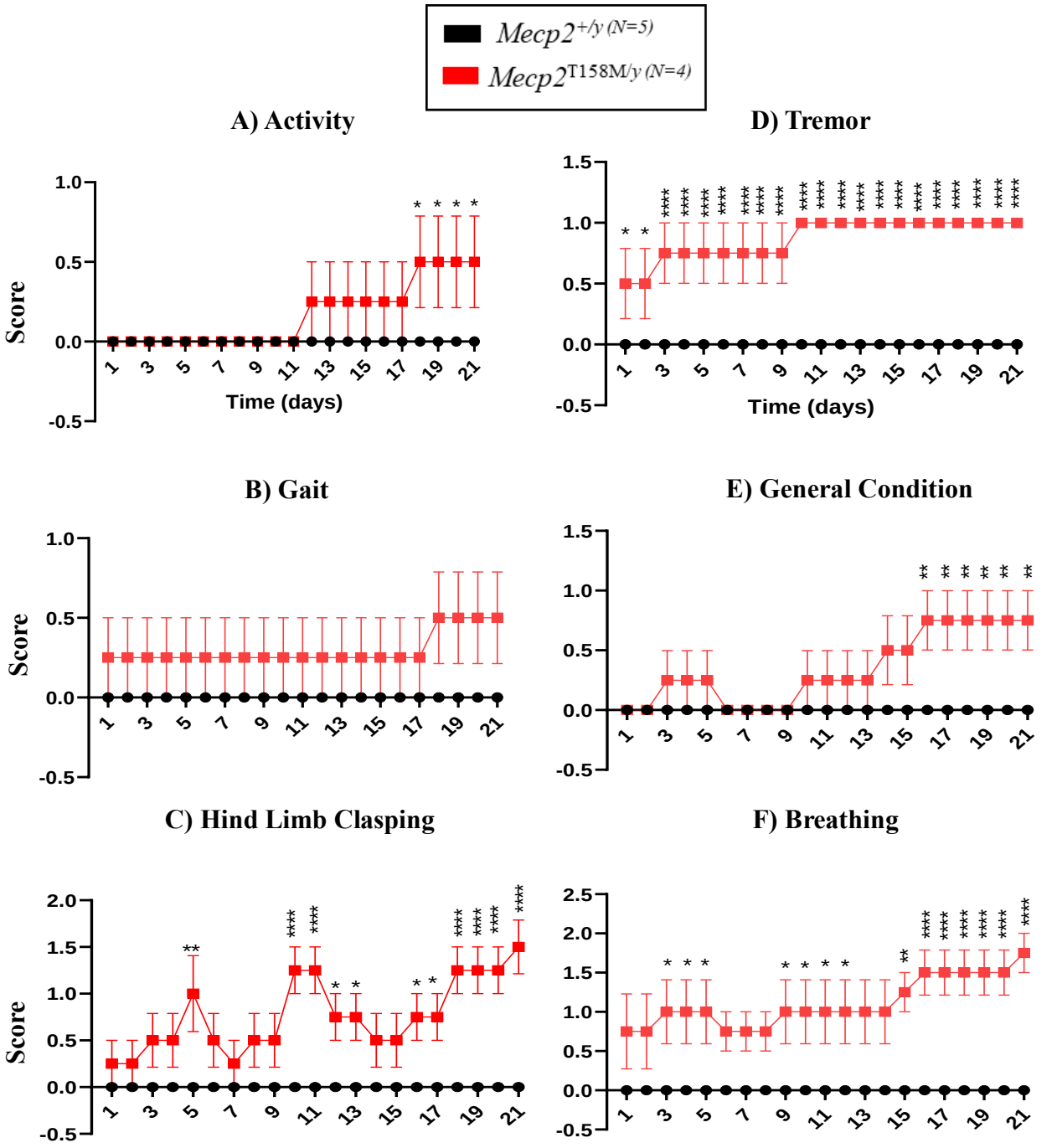

Figure 3.14. The Evaluation of Phenotypic Scoring in Sham *Mecp2*$^{T158M/y}$ Male Mice. The *Mecp2*$^{T158M/y}$ male mice exhibited defects in an age-dependent manner compared with their age and sex-matched *Mecp2*$^{+/y}$ male mice, which are shown in 6 categories including **A**) activity **B**) gait, **C**) hind limb clasping, **D**) tremor, **E**) general condition, and **F**) breathing. All statistical analysis was completed by two-way ANOVA followed by Šídák's multiple comparisons tests. The level of difference is $*p < 0.05$, $**p < 0.01$, $***p<0.001$, and $****p < 0.0001$. All the values are shown as mean ± SEM.

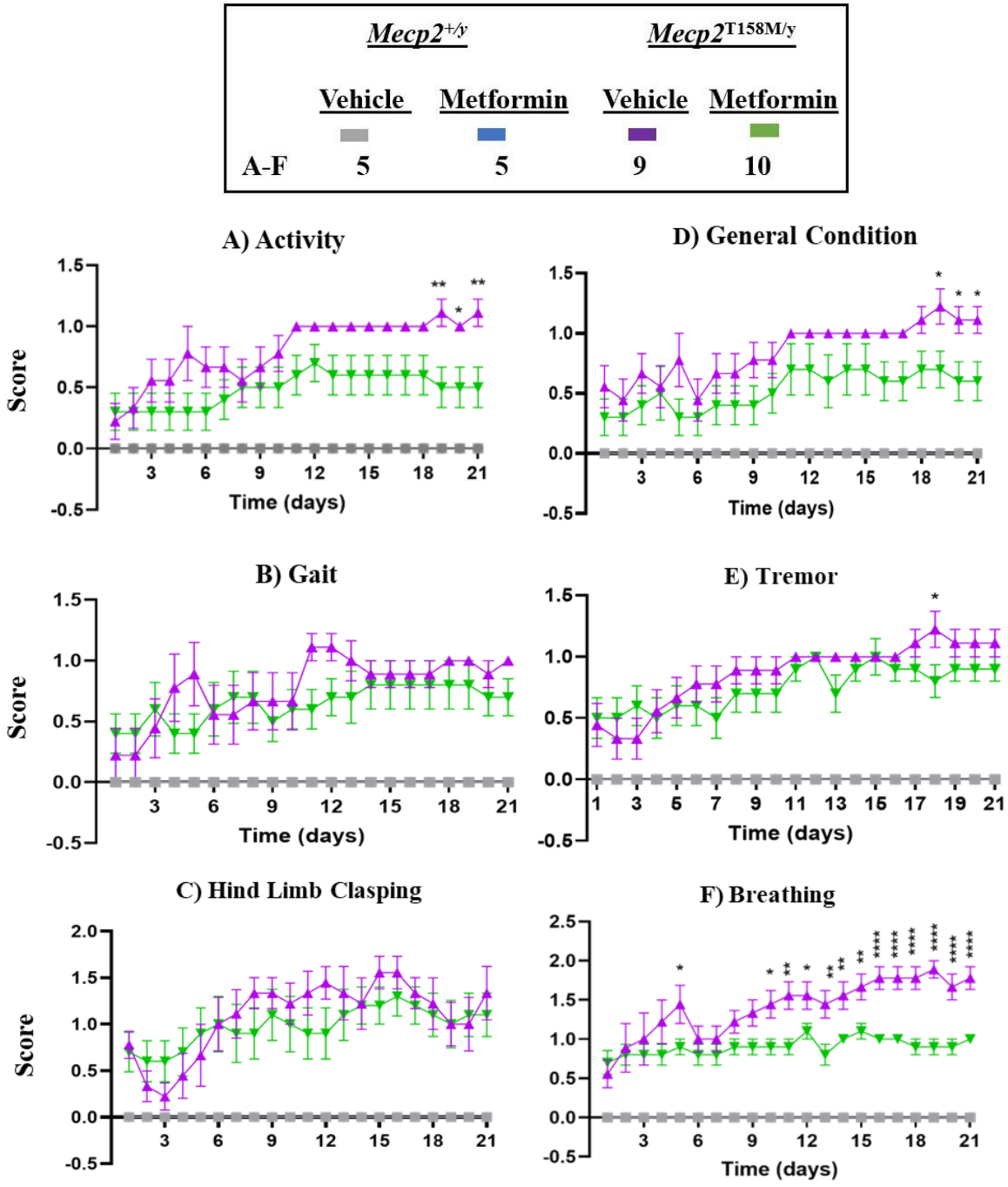

Figure 3.15. The Effect of Metformin on the RTT-like Symptoms of *Mecp2*$^{T158M/y}$ Male Mice. The analysis of phenotypic scoring showed improvement in the symptom's severity of metformin-treated *Mecp2*$^{T158M/y}$ male mice compared with control *Mecp2*$^{+/y}$ male mice, which in case of activity, general condition, and breathing is significant in an age-dependent manner. Statistical analysis was completed with two-way ANOVA followed by Tukey's multiple comparisons tests. The level of significance is *$p < 0.05$, **$p < 0.01$, ***$p < 0.001$, and ****$p < 0.0001$. All the values are shown as mean ± SEM.

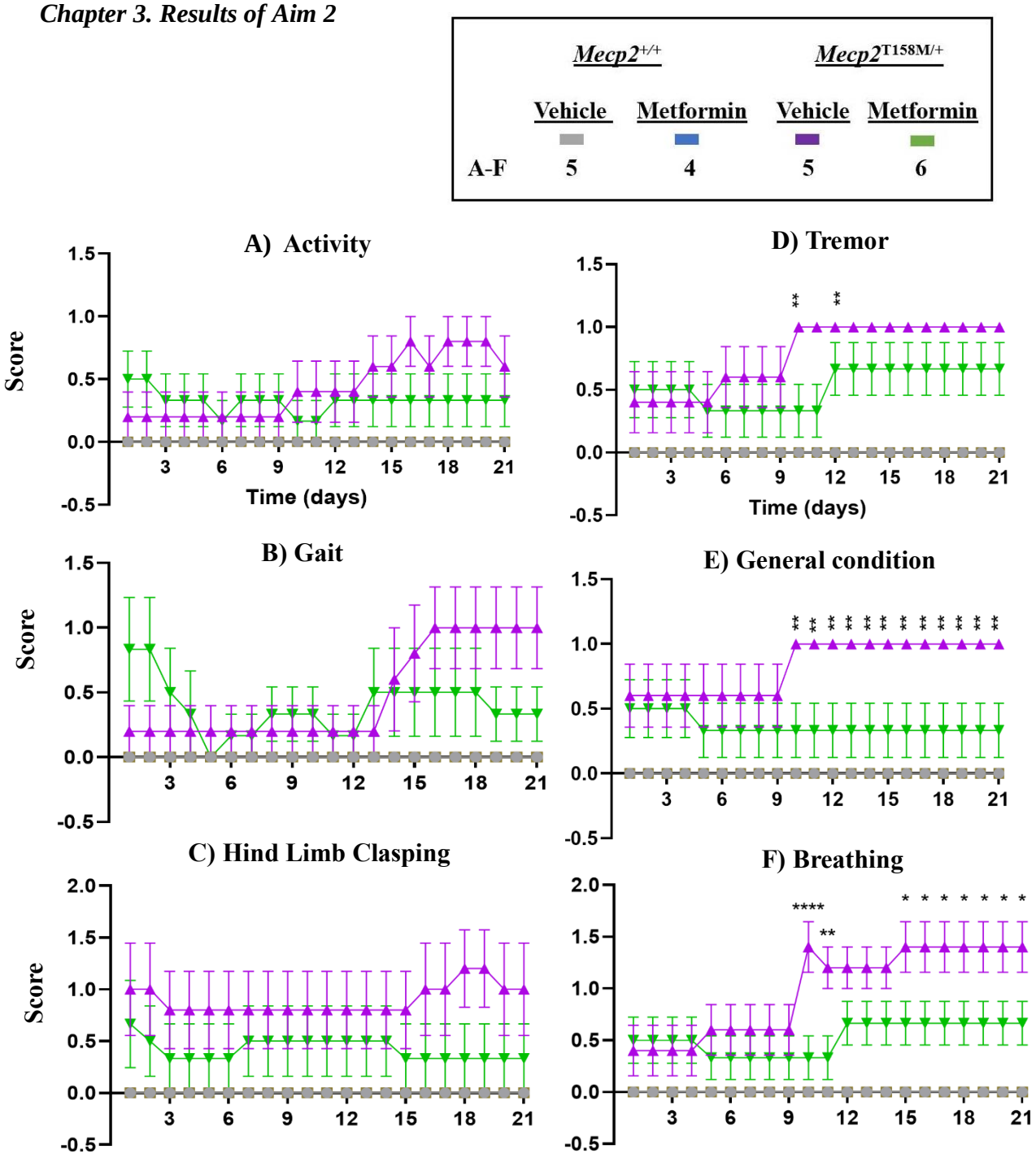

Figure 3.16. The Effect of Metformin on the RTT-like Symptoms of *Mecp2*$^{T158M/+}$ and *Mecp2*$^{+/+}$ Female Mice. The *Mecp2*$^{T158M/+}$ and *Mecp2*$^{+/+}$ (15-18 weeks) mice were assessed by a semi-quantitative approach to measuring RTT-like phenotypes in 6 categories: activity, gait, hind-limb clasping, tremor, breathing, and general condition. An improvement in **E**) general condition and **F**) breathing abnormalities of *Mecp2*$^{T158M/+}$ female mice was detected after 10 days of IP injections. The analysis was completed by two-way ANOVA followed by Tukey's multiple comparison tests and the level of significance is shown by $*p < 0.05$, $**p < 0.01$, $***p < 0.001$, and $****p < 0.0001$. All the values are shown as mean ± SEM.

3.9. The Evaluation of RTT-like Behavioral Abnormalities of *Mecp2*^{T158M} Mice

To evaluate the effect of metformin on the RTT-like behavioral deficits, *Mecp2*^{T158M} male and female mice and their age and sex-matched WT mice were exposed to a series of behavioral tests including Open Filed Test (OFT), New Objective Recognition (NOR), and Elevated Plus Maze (EPM) before and after metformin treatment.

3.9.1. The Effect of Metformin on Motor Function and Anxiety-like Behavior of *Mecp2*$^{T158M/y}$ Mice

To evaluate the motor function and anxiety-related behavior, OFT was completed (**Figure 3. 18**) in *Mecp2*$^{T158M/y}$ male mice and their age- and sex-matched *Mecp2*$^{+/y}$ male mice at the basal level. Representative traces of diverse groups of mice display a 10-min assay of total distance moved and time in zones (**Figure 3.17.A**). The lower total distance traveled and lower velocity in *Mecp2*$^{T158M/y}$ male mice compared with *Mecp2*$^{+/y}$ male mice indicate motor abnormalities in agreement with other studies in *Mecp2*^{T158M} mice [71] (**Figure 3.17.B**). To investigate the anxiety-associated behavior, the time spent in the zones of the open field was measured, which equal time between both genotypes indicating no effect of genotype on anxiety in OFT. As previously mentioned, metformin can treat neurodevelopmental disorders such as Autism Spectrum Disorder (ASD) [178, 190] and Fragile X Syndrome (FXS) [178]. Therefore, we studied the possible effect of metformin on the behavioral abnormalities of *Mecp2*$^{T158M/y}$ male mice *via* OFT (**Figure 3.18**). A representative trace (**Figure 3.18.A**) of 4 groups of diverse genotype and treatment group mice displays a 10-min assay of total distance moved and time in zones. Metformin did not affect the total distance traveled, velocity (the speed of movement in a specific direction), and time spent (**Figure 3.18.C**) in the corner or center zones of either genotype of mice. Consequently, metformin did not show any effect on the locomotion or anxiety-related behaviors in *Mecp2*$^{T158M/y}$ or *Mecp2*$^{+/y}$ male mice. In conclusion, since motor dysfunction is a leading symptom of RTT, all *Mecp2*^{T158M} mice models have been subjected to a series of behavioral tests including OFT. Our results are consistent with previous in *Mecp2*-null and MeCP2 T158A–knock-in (*Mecp2T158A*) mice [282] since *Mecp2*^{T158M} mice indicate considerably decreased movement compared with their WT littermates. In contrast, genetically modified *Mecp2*$^{T158M/y}$ T158M–Tg animals demonstrated noticeable progress in locomotion, as evaluated by the overall number of distances traveled and average velocity in the open field arena compared with *Mecp2*^{T158M} mice [69].

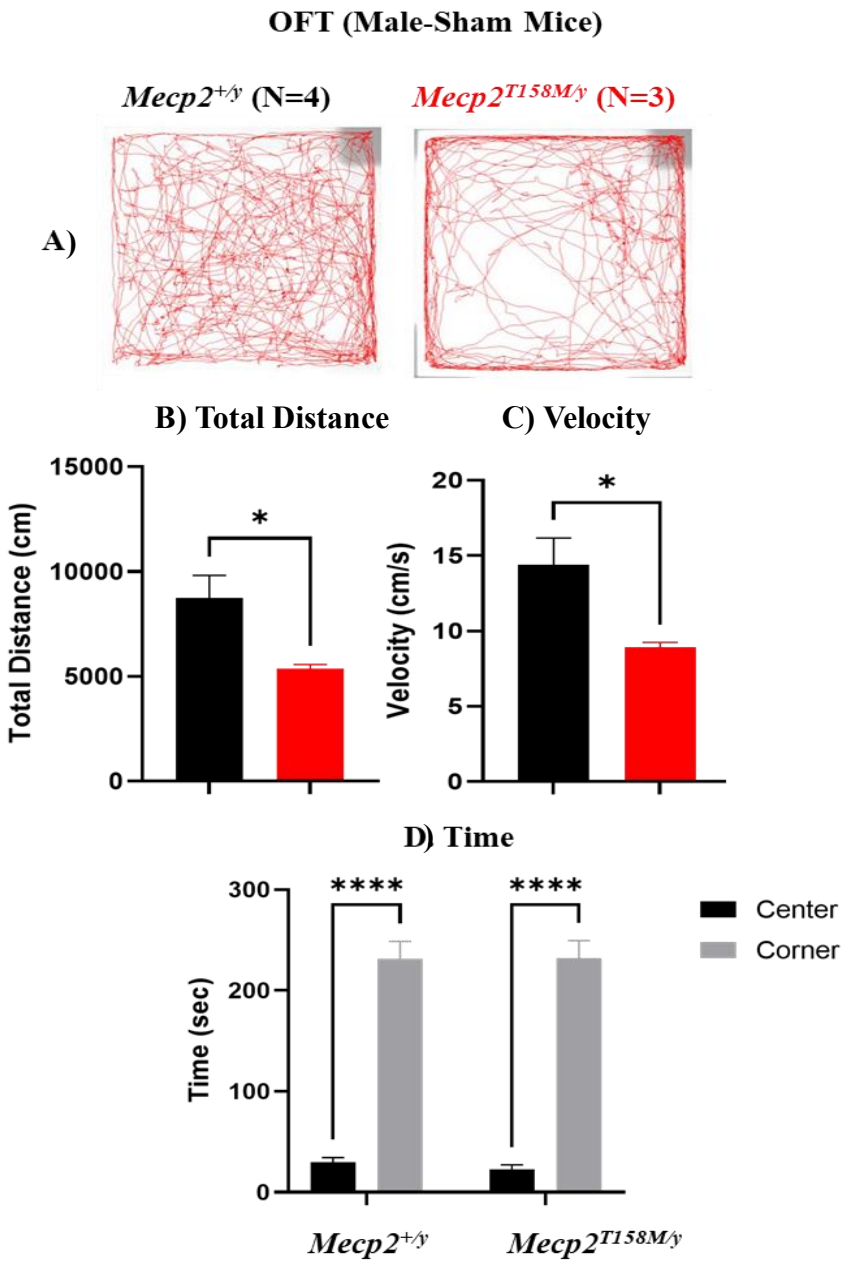

Figure 3.17. The *Mecp2*$^{T158M/y}$ Male Mice Showed Motor Deficits. A) Representative trace of a diverse group of mice displays a 10 min assay of the total distance moved and time in the zones. **B**) The *Mecp2*$^{T158M/y}$ mice showed lower traveled distance and **C**) velocity compared with *Mecp2*$^{+/y}$ mice, which is the indicator of locomotion abnormalities. **D**) Within each group of mice, corner zone time is significantly higher compared with center time; however, no effect of genotype was detected on the spent time in zones. The statistical analysis was completed by unpaired t-test and two-way ANOVA followed by Šídák's multiple comparisons tests. The level of differences is shown by *$p < 0.05$, and ****$p < 0.0001$, and all the values are shown as mean ± SEM.

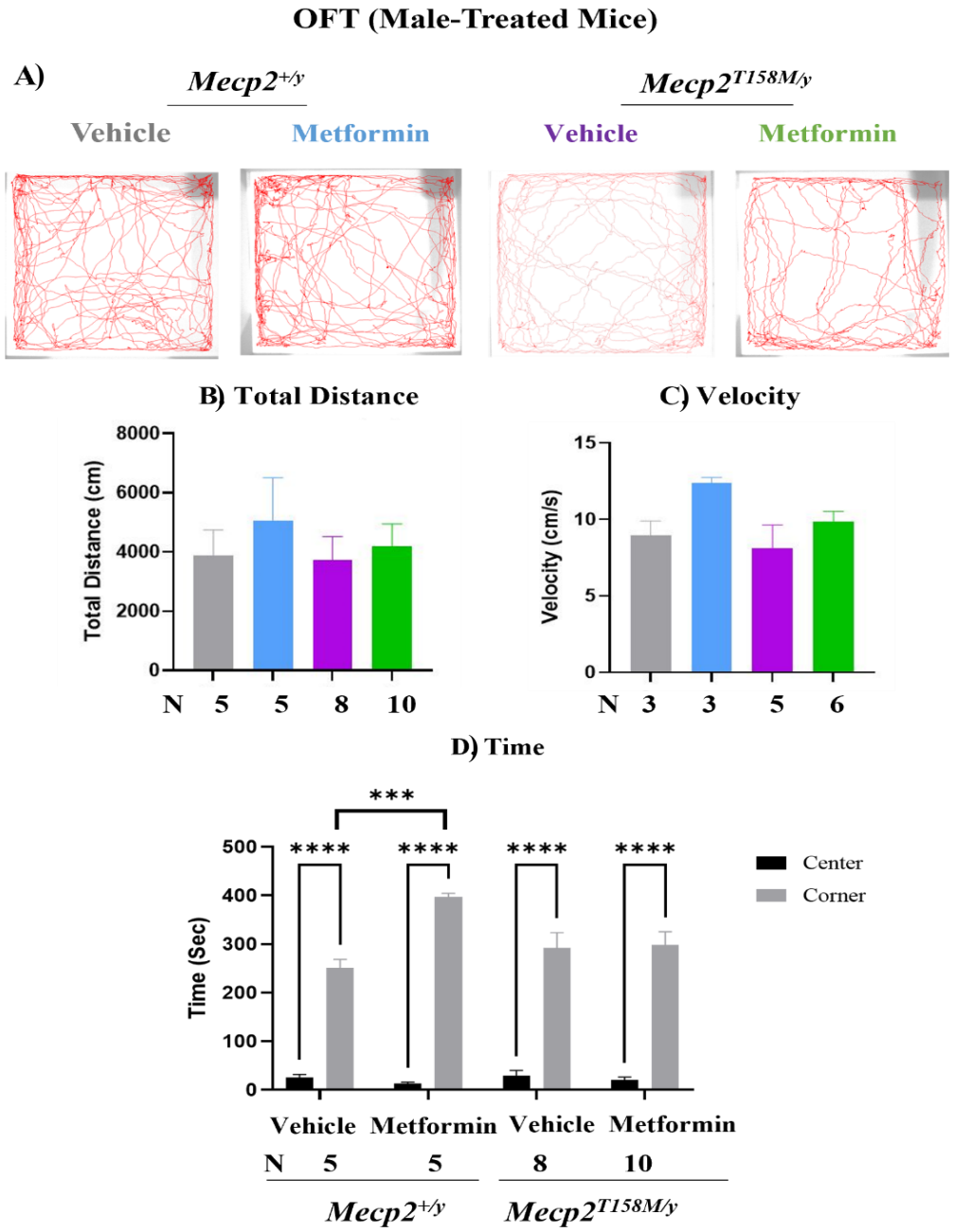

Figure 3.18. Metformin Did not Affect the Locomotion and Anxiety-like Behavior of *Mecp2*$^{T158M/y}$ Male Mice. A) A representative trace of 4 groups of diverse genotype and treatment mice displays a 10-min assay of total distance moved and time in zones (center and corner). **B**) In the case of mobility, no genotype or drug effect on the total distance traveled and velocity were detected. **C**) In all 4 groups, mice spent significantly more time in the corner and metformin increased the spent time in the corner of *Mecp2*$^{+/y}$ male mice compared with age and sex-matched control. The statistical analysis was completed by unpaired t-test and two-way ANOVA followed by Šídák's multiple comparisons tests. The level of difference is shown by ***$p < 0.001$ and ****$p < 0.0001$, and the values are presented as mean ± SEM.

3.9.2. The Effect of Metformin on Motor Function and Anxiety-like Behavior of *Mecp2*$^{T158M/+}$ Mice

Given that RTT is predominantly a female disorder, we then analyzed whether pharmacological intervention with metformin could improve RTT-associated behavior such as reduced mobility and anxiety in *Mecp2*^{T158M} female mice using OFT. Metformin treatment did not alter the exploratory locomotion and anxiety of *Mecp2*$^{T158M/+}$ or *Mecp2*$^{+/+}$ female mice compared with the vehicle. Consequently, no genotype or drug effect was detected on locomotion or anxiety (**Figure 3.19**).

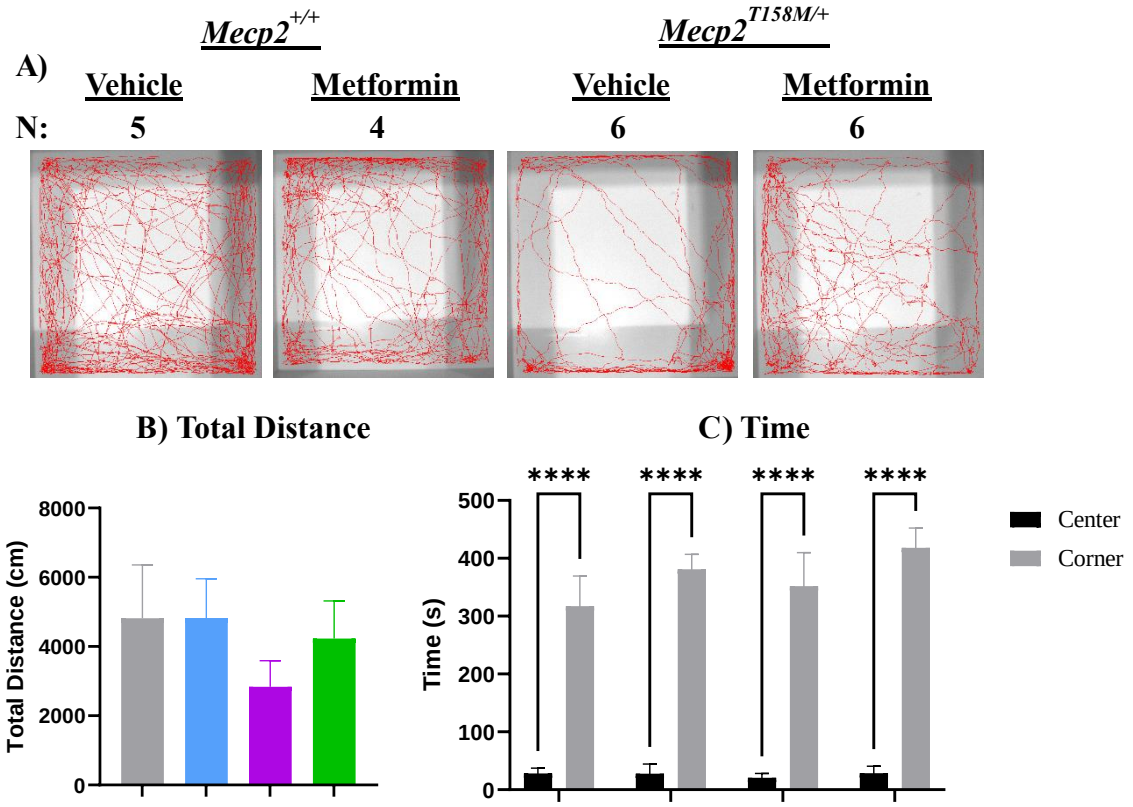

Figure 3.19. Metformin Did not Influence the Locomotion or Anxiety-like Behavior of *Mecp2*$^{T158M/+}$ Female Mice. **A**) A rrepresentative trace of a diverse group of mice in OFT displays a 10-min assay of total distance moved and time in zones. Metformin did not affect the **B**) total distance and **C**) time spent in zones of *Mecp2*$^{T158M/+}$ and *Mecp2*$^{T158M/+}$ female mice and consequently, it did not affect the locomotion and anxiety-like behavior of mice. The statistical analysis was completed by unpaired t-test and two-way ANOVA followed by Šídák's multiple comparisons tests. The level of difference is shown by ***$p < 0.001$. All the values are shown as mean ± SEM.

3.9.3. The Effect of Metformin on the Social Deficits of *Mecp2*$^{T158M/y}$ Male Mice

To evaluate social deficits in *Mecp2*^{T158M} mice at the basal level, the *Mecp2*$^{+/y}$ *and Mecp2*$^{T158M/y}$ male mice were exposed to NOR tests in 3 steps and 2 days. On the first day and at the same time with OFT, mice were habituated to the open field for 10 minutes. The next day, NOR was completed in 2 steps (as mentioned in Chapter 2). In sham mice, the time spent exploring the 2 objects in the familiarization trial and time exploring the novel against the familiar objects was the same in both *Mecp2*$^{+/y}$ and *Mecp2*$^{T158M/y}$ male mice (**Figure 3.20**). At the basal level, the Preference Index (PI) of *Mecp2*$^{+/y}$ male mice was slightly higher than 50% chance indicating that Wt mice did not have memory deficits. Nevertheless, that of the *Mecp2*$^{T158M/y}$ male mice was slightly lower than 50 % representing memory impairment.

In the treated experimental groups of mice, the time spent exploring the two objects in the familiarization trial and time exploring the novel against the familiar objects was similar, except that in *Mecp2*$^{T158M/y}$ male mice, and metformin tends to slightly increase time spent with a novel object. The PIs of all experimental groups were insignificantly higher than 50% chance, suggesting that mice did not have memory deficits. However, that of the metformin-treated *Mecp2*$^{+/y}$ male mice group was insignificantly lower (**Figure 3.21**).

In conclusion, these discoveries uncover that treatment with metformin could have various effects depending on the genotype of the mice since it tends to increase PI in *Mecp2*$^{T158M/y}$ male mice, while metformin tends to reduce the novel object recognition ability of *Mecp2*$^{+/y}$ male.

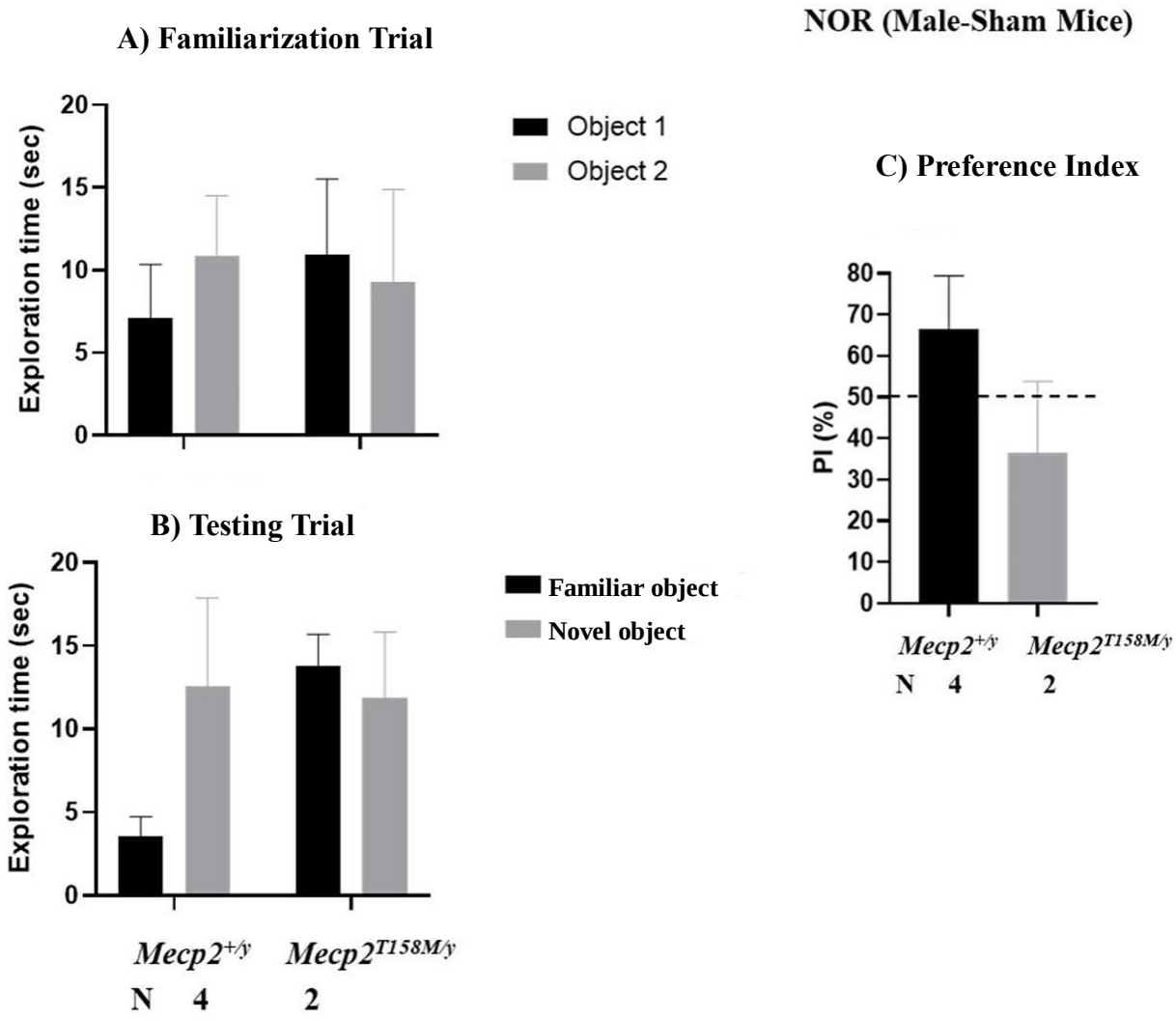

Figure 3.20. The *Mecp2*$^{T158M/y}$ Male Mice May Have Memory Impairment at the Basal Level. Both groups of mice should same exploration time in **A**) the familiarization trial and **B**) the testing trial. **C**) The PI of *Mecp2*$^{T158M/y}$ male mice was higher and that of *Mecp2*$^{+/y}$ male mice was lower than 50 % which is an indication of memory deficits in *Mecp2*$^{T158M/y}$ male mice. The statistical analysis was completed by unpaired t-test and two-way ANOVA followed by Šídák's multiple comparisons test and the values are presented as mean ± SEM.

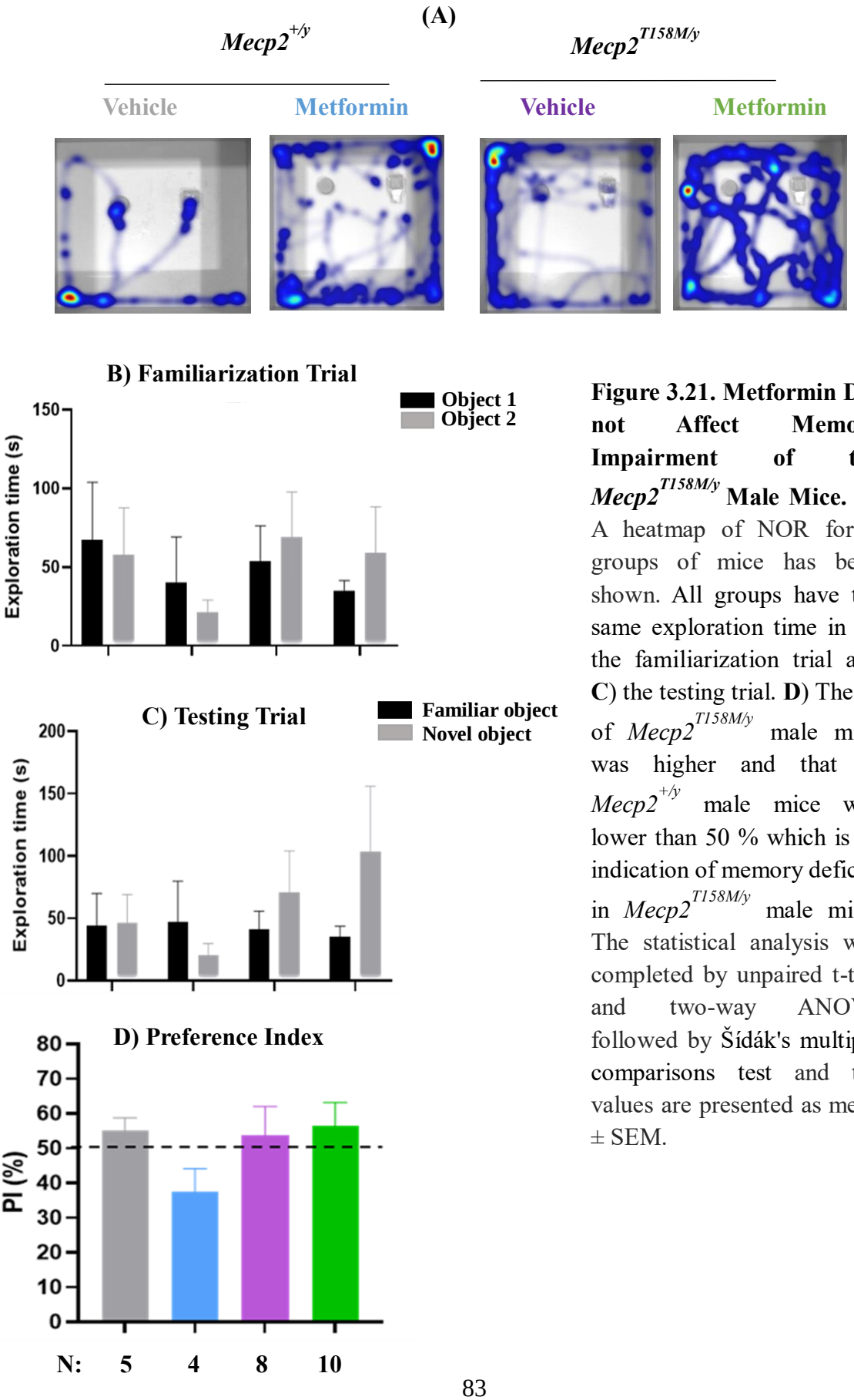

Figure 3.21. Metformin Did not Affect Memory Impairment of the *Mecp2*$^{T158M/y}$ Male Mice. **A**) A heatmap of NOR for 4 groups of mice has been shown. All groups have the same exploration time in **B**) the familiarization trial and **C**) the testing trial. **D**) The PI of *Mecp2*$^{T158M/y}$ male mice was higher and that of *Mecp2*$^{+/y}$ male mice was lower than 50 % which is an indication of memory deficits in *Mecp2*$^{T158M/y}$ male mice. The statistical analysis was completed by unpaired t-test and two-way ANOVA followed by Šídák's multiple comparisons test and the values are presented as mean ± SEM.

3.9.4. The Effect of Metformin on the Social Deficits of *Mecp2*$^{T158M/+}$ Female Mice

To evaluate the effect of metformin on social deficits in *Mecp2*$^{T158M+y}$ Female Mice, NOR test was completed in 4 groups of female mice and no genotype of drug treatment was detected in spent time in either familiarization or testing step of NOR (**Figure 3.22**).

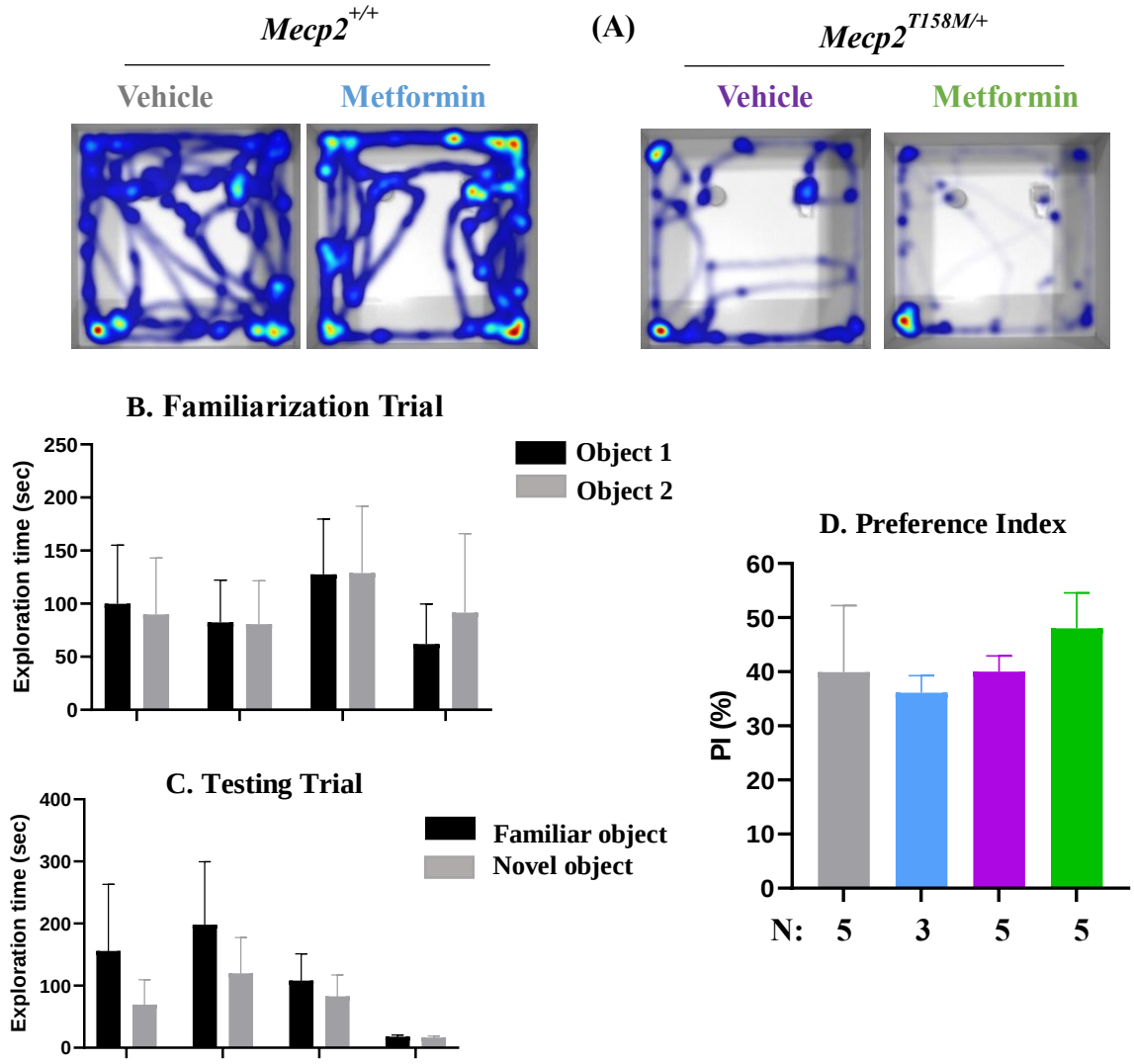

Figure 3.22. Metformin Did not Affect the NOR Criteria in the *Mecp2*$^{T158M/+}$ Female Mice. **A**) A heatmap of NOR for 4 groups of mice has been shown. All mice have the same exploration time in **B**) the familiarization and **C**) the testing trial. **D**) The PI of all mice was insignificantly lower than 50 % which is an indication of possible memory deficits in mice. However, metformin tends to slightly induce the novel object recognition ability of *Mecp2*$^{T158M/+}$ female mice. The statistical analysis was completed by unpaired t-test and two-way ANOVA followed by Šídák's multiple comparisons test and the values are shown as mean ± SEM.

3.9.5. The Effect of Metformin on the Anxiety-like Behavior of *Mecp2*$^{T158M/y}$ Mice

Anxiety testing in MeCP2 deficient mouse models has mainly revealed declines in anxiety-like behaviors in relation to WT performance [283, 284]. As a result, EPM was applied to investigate anxiety-related behaviors in *Mecp2*$^{T158M/y}$ and *Mecp2*$^{+/y}$ male mice at the basal level (sham) and after metformin treatment. At the basal level, *Mecp2*$^{+/y}$ male mice spent more time in closed arms and metformin did not affect the spent time in the arms of 4 groups of male mice (**Figure 3.23**).

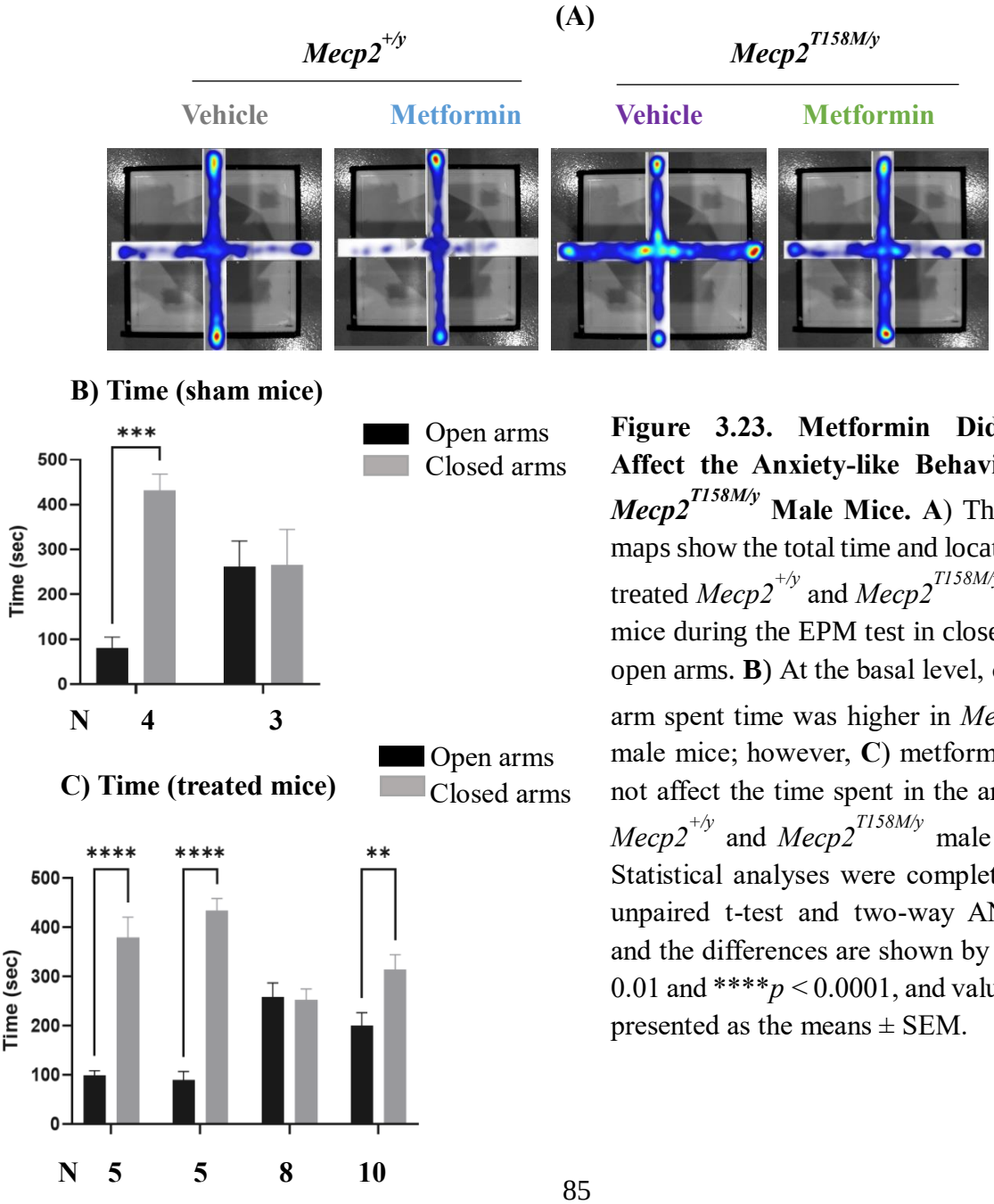

Figure 3.23. Metformin Did not Affect the Anxiety-like Behavior of *Mecp2*$^{T158M/y}$ Male Mice. A) The heat maps show the total time and location in treated *Mecp2*$^{+/y}$ and *Mecp2*$^{T158M/y}$ male mice during the EPM test in closed and open arms. **B**) At the basal level, closed arm spent time was higher in *Mecp2*$^{+/y}$ male mice; however, **C**) metformin did not affect the time spent in the arms in *Mecp2*$^{+/y}$ and *Mecp2*$^{T158M/y}$ male mice. Statistical analyses were completed by unpaired t-test and two-way ANOVA and the differences are shown by $^{**}p < 0.01$ and $^{****}p < 0.0001$, and values are presented as the means ± SEM.

3.9.6. The Effect of Metformin on Anxiety-like Behavior of *Mecp2*$^{T158M/+}$ Female Mice

To evaluate the effect of metformin on anxiety-like behavior, the *Mecp2*$^{+/+}$ and *Mecp2*$^{T158M/+}$ female mice were exposed to EPM (**Figure 3.24**). At the basal level, in *Mecp2*$^{+/+}$ female mice, spent time in the corner was higher than time in the center. Within all experimental groups and control mice, the spent time in the corner compared with the center was higher except in metformin-treated *Mecp2*$^{+/+}$ female mice. Although, metformin did not affect spent time in zones.

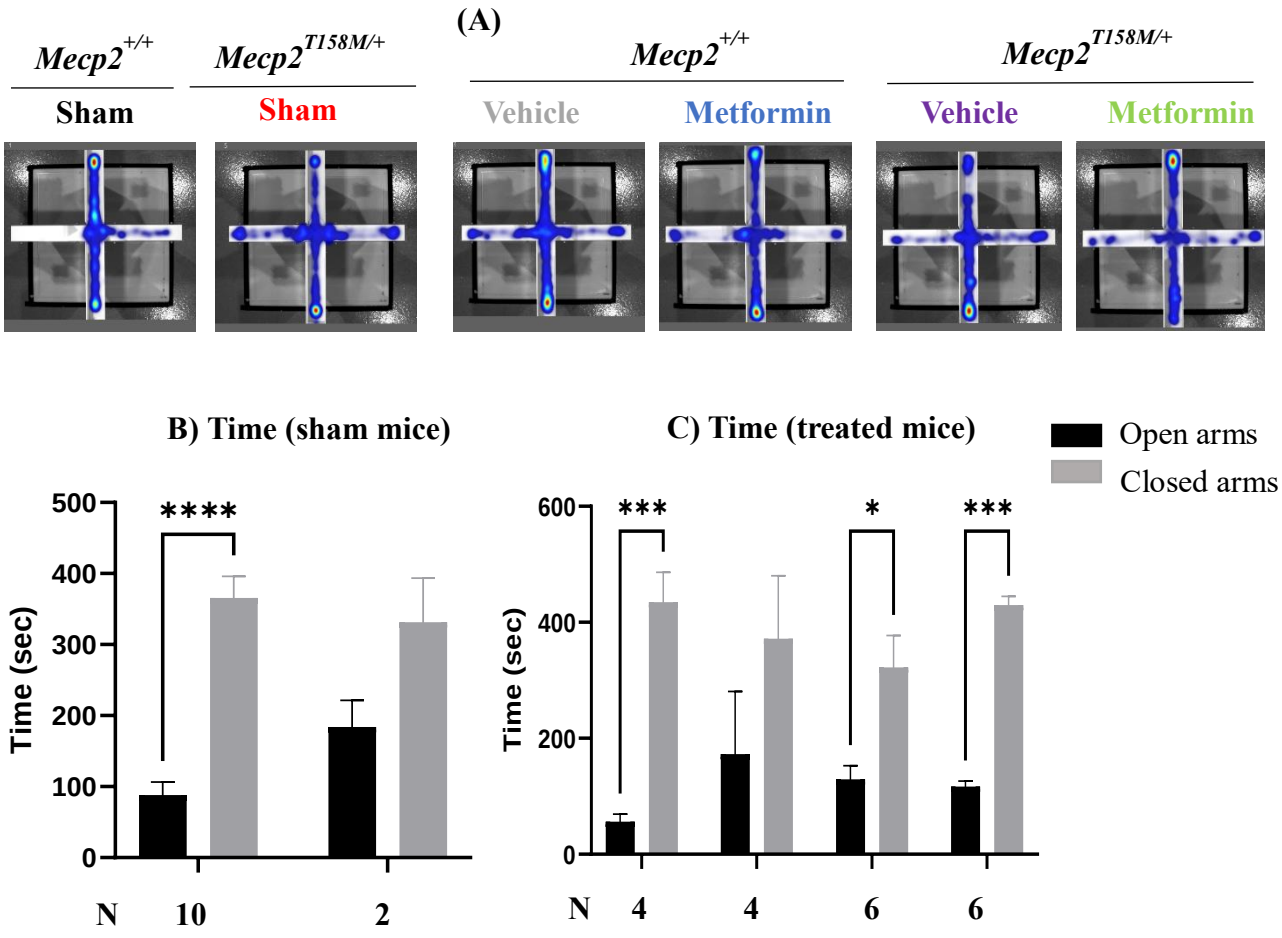

Figure 3.24. Metformin Did not Affect the Anxiety-like Behavior of *Mecp2*$^{T158/+}$ Female Mice. **A**) The heat maps show the total time and location in treated *Mecp2*$^{+/+}$ and *Mecp2*$^{T158M/+}$ female mice during the EPM test in closed and open arms. **B-C**) The time spent in closed arms was higher in all groups of mice compared with time spent in open arms spent time, except in sham *Mecp2*$^{T158M/+}$ and metformin-treated *Mecp2*$^{T158M/+}$ female mice. Statistical analyses were completed by unpaired t-test and two-way ANOVA and the differences are shown by *$p < 0.05$ and ****$p < 0.0001$, and values are presented as the means ± SEM.

Table 3.1. Summary of Mice Experimental Groups and Numbers.

Approaches (Phenotypical and behavioral)	**Sex and Genotype**			
	Male (5-9 weeks)		**Female (15-22 weeks)**	
	***Mecp2*$^{+/y}$**	***Mecp2*$^{T158M/y}$**	***Mecp2*$^{+/+}$**	***Mecp2*$^{T158M/+}$**
Sham				
Characterization	4-5	3-7	8	2
Scoring	5	4	-	-
Behavioral tests	4	2-3	10	2
Vehicle				
Characterization	3-5	5-9	2-5	3-5
Scoring	5	9	5	5
Behavioral test	3-5	5-8	5	6

Metformin				
Characterization	4-5	5-10	3-4	4-6
Scoring	5	10	4	6
Behavioral tests	3-5	6-10	4	6

3.10. Summary of Aim 2 Results. A pre-clinical study

To study the effect of metformin on the improvement of RTT-like symptoms *in vivo*.

1. Both sexes of the *Mecp2*^{T158M} mouse model showed RTT-like phenotypes in terms of body weight and brain size.
2. A metformin-mediated, sex- and genotype-dependent reduction of body weight and blood glucose level was detected in *Mecp2*^{T158M} mice.
3. A metformin-mediated and age-dependent improvement of RTT-like phenotypes including tremor, general condition, and breathing abnormalities) was detected in both sexes of the *Mecp2*^{T158M} mouse model with the highest improvement in breathing abnormalities.
4. Metformin did not affect the hindlimb clasping and gait abnormalities in either sex of mice.
5. Metformin-mediated improvement of RTT-like symptoms is age- and sex-dependent with significant phenotypical improvement and partial behavioral improvement.

Chapter 4. Discussion

In this study, the effect of metformin was assessed at the molecular, phenotypical, and behavioral levels *in vivo* to test our hypothesis that metformin not only could have a possible regulatory effect on murine brain MeCP2/BDNF, and S6 at the protein level but also could improve the RTT-associated abnormalities *in vivo* at the phenotypical and behavioral. The molecular analysis of the metformin (200 mg/kg/day) effect was focused on the assessment of the following proteins: MeCP2-BDNF, AMPK, S6, and p-S6 (235/236)/S6) in the brain and liver tissues of a WT mouse (C57BL/6). However, the phenotypical and behavioral analysis was focused on metformin (250 mg/kg/day) effects on the improvement of RTT-like symptoms in a knock-in RTT mouse model (*Mecp2*^{T158M}). In terms of the first aim of my thesis, frozen liver and brain tissues of C57BL/6 mice were used for protein evaluations through the Western Blot technique. While, in my second aim, we used 3 complementary approaches (characterization of phenotypes and evaluation of phenotypic scoring and 3 types of behavioral tests) for the assessment of RTT-like symptoms of *Mecp2*^{T158M} male and female mice and their age- and sex-matched controls, at the basal level as well as after metformin treatment. Likewise, metformin effects on MeCP2 and BDNF in different brain regions of mice were studied. My results showed sex- and region-dependent effects of metformin in mice that improve some RTT-like symptoms which are significant at the phenotypical level and partial at the behavioral level.

4.1. A Pilot Study Approved the Safety of Metformin IP Injections

To address our hypothesis regarding the possible metformin-mediated MeCP2-BDNF and AMPK activation and mTOR pathway inhibition at the dosage of 200 mg/kg/day, a pilot study was completed. The results of the study did not show any adverse effect of metformin on the average body weight and blood glucose level of male and female C57BL/6 mice compared with their age- and sex-matched control. As a result, due to the lack of side effects on mice's health status, the safety, and tolerability of metformin treatment at 200 mg/kg/day dosage along with the IP injections were approved, which corresponds with the prior studies in mice on regular diets [243]. In contrast, a study in HFD-Fed C57BL/6J mice showed metformin-mediated body weight loss and improved glucose intolerance [289]. Accordingly, in some studies, the effects of metformin treatment are attributed to calorie restriction, including increased physical performance, enhanced sensitivity of insulin, and decreased cholesterol levels regardless of caloric intake reduction [285].

In conclusion, the antihyperglycemic effect of metformin could be attributed to the ability of metformin to inhibit hepatic gluconeogenesis or improve glucose sensitivity in the HFD in Diabetic patients or mice, but it is not effective in normoglycemic mice on standard Diet (SD) [286, 287].

4.2. The Effect of Metformin *In Vivo* is Sex- and Region-Specific at the Protein Level

It is shown that at a molecular level, stimulation of AMPK is the main mechanism of metformin action leading to anti-oxidative and anti-inflammatory effects, which could explain the favorable effects of metformin on the improvement of male mice's lifespan. These results agree with existing data and increase the probability of drug treatment with metformin to improve aging. The related dosage to these useful effects was tolerable in mice but result in higher serum levels compared with those commonly used in diabetes patients [288]. Therefore, regardless of metformin pleiotropic effect *in vivo*, its central mechanism of action has not been known yet and different parameters need to be considered in rodents studies including the metformin's dosage, timing, and route of delivery along with the rodent's age and sex [287, 289]. The dosages used in animal studies change broadly with both useful and harmful impacts throughout the widespread scale of metformin dosages [287]. The male and female C57BL/6 mice in our study underwent 200 mg/kg/day of metformin treatment which is similar to the dosage in former studies to be a strong inhibitor of hepatic mTORC1 activity, indicated by phosphorylation of the S6K1 and S6, which is beneficial to test our hypothesis regarding metformin-mediated inhibition of hepatic mTOR pathway [222]. Regarding the length of metformin treatment, a substantial number of reports used shorter times, but the higher metformin dose was presented to be primarily efficient at generating useful metabolic and cognitive impacts [287]. Nonetheless, long-lasting use eventually led to harmful effects, probably owing to declined levels of neurotrophic factors, which are significant for neuronal plasticity and survival. In addition, the initial age for mice treatment possibly had a large effect on the consequences since late-age treatment reduces the ability of metformin to expand the male mice's lifespan [290]. Additional studies on the age, dose, and duration of metformin treatment are required to discover any age-linked effects of metformin use that may result in changes in brain biochemistry in a way that generates bigger susceptibility of the CNS [287].

In this study, we have examined RTT-related abnormalities including compromised *MECP2-BDNF* transcripts and mTOR pathway in human RTT brain [114, 152] at the basal level and after metformin treatment in the brain tissues of C57BL/6 male and female mice. Due to the possible stimulatory effect of metformin on the *MECP2E1/BDNF* transcripts [138], and AMPK activity, while its inhibitory effect on mTORC1 [222], this study could provide a solid foundation for the metformin-mediated therapeutic approaches of RTT in pre-clinical studies. To fulfill this aim, our lab reports have been reviewed as the basis of my hypothesis and the aim of my thesis.

A study from our lab has investigated the components of the *MECP2-BDNF-miR132* feedback regulatory loop in the RTT patient's brain and the results showed impaired transcript levels of those elements in 4 brain regions including the amygdala, frontal cortex, cerebellum, and hippocampus. However, according to the correlation studies, MeCP2E1/E2-BDNF protein levels did not follow their corresponding transcript trends [114]. So, our theory was derived from this study whether metformin could affect the protein level of MeCP2-BDNF in both sexes of C57BL/6 mice brain tissues and what would be the probable consequences on its potential downstream targets including S6 which is important for protein synthesis [152]. Furthermore, our lab showed the metformin-mediated posttranscriptional induction of *MECP2E1* and *BDNF* transcripts whereas transcriptional inhibition of *MECP2E2* transcripts in a time and dose-dependent manner [138]. Interestingly, this could be a part of the mechanism of metformin action to activate the atypical protein kinase C (aPKC)-CBP pathway (downstream of AMPK) in neural stem cells and enhance neurogenesis in mice [246].

Along with *in vitro* studies, our *in vivo* studies tend to evaluate the metformin effect on the protein level of MeCP2-BDNF in different brain regions (cerebellum, cortex, hippocampus, and thalamus) of C57BL/6 mice models. Furthermore, another study from our lab has reported compromised nucleolin-*rRNA*-mTOR-P70S6K signaling in the human RTT brain with several spots of variation from the control tissues leading to unusual ribosome biogenesis in the RTT brain. Consequently, one of our hypotheses of targeting mTOR pathways at the basal level through metformin treatment could be offered as a therapeutic approach, which is important for RTT without any current cure [152].

According to a study in C57BL/6 mice, metformin effectively inhibits the hepatic mTORC1 and its downstream protein synthesis in a dose-dependent manner like other effects of metformin [173, 291]. In fact, metformin has been shown a biphasic response, which in low doses is AMPK and TSC-dependent, while in higher doses is independent of AMPK and TSC. Along with the suggested mechanistic of the metformin effect on crucial pathways and functions in the liver, our discoveries about the dose-dependent effects of metformin reveal a probable clarification for the inconsistency among earlier studies with contradictory conclusions about the metformin-mediated mTORC1 inhibition, which could be extended to its effect in brain regions to some extend. Regardless of the known stimulatory effect of metformin on AMPK and its inhibitory effect on mTORC1 in mice liver, the metformin effect on different brain regions of mice has not been well-known, which brings me to our hypothesis of whether the same results are feasible *in vivo*. Consequently, to study the effect of metformin at the molecular level, and particularly the protein level, mice tissues underwent Western blot analysis.

Initially, as a proof of principle on the inhibitory effect of metformin, the detection of mice hepatic p-S6 (235/236)/S6 was completed and regardless of the detected significant variation between the p-S6 (235/236) protein level in both sexes of C57BL/6 mice, a metformin-mediated and sex-dependent inhibitory effect of p-S6 (235/236) and p-S6 (235/236)/S6 ratio led to the normalization of protein level in mice liver [292]. Simultaneously, the detection of AMPK as a positive control for the stimulatory effect of metformin was completed, however, the detection of p-AMPK was not successful and needs further investigation in future studies. Although AMPK was detected in 4 brain regions, since p-AMPK is critical for the measurement of AMPK activity, further studies are required to be able to reach a precise conclusion.

In the next step, protein analysis of mice brain tissues showed a metformin-mediated increase of MeCP2 and mBDNF in the hippocampus of C57BL/6 male mice, and a decrease in the level of mBDNF in the thalamus.

Ultimately, we concluded that the metformin effect in the liver and brain of C57BL6 mice is sex- and region-dependent at the protein level. Our results are consistent with prior studies which have approved the influences of treatment on activity throughout the AMPK/mTOR signaling pathway were both sex and age-dependent [287].

In conclusion, our study of the mice brain tissues is an attempt about addressing metformin effects on MeCP2, BDNF, p-S6 (235/236)/S6, and p-AMP/AMPK in the mice brain tissues. Considering other probable factors such as age, timing, and handling of samples that may control the effect of metformin, further protein studies in the case of mTORC1 components are required to suggest a possible mechanism of action for metformin in mice brain tissues.

Due to the MeCP2 significance in normal brain function, the connection between MeCP2 dysfunction and neurological irregularities of RTT patients is essential [153]. Studies have demonstrated that the major identified anomaly in the CNS structure is the reduction of the entire brain and single neuron size [292]. Studies have confirmed that the brain size of RTT patients decreased by about 12-34% compared with the age-matched controls without any signs of inflammation, atrophy, or deterioration [293].

These findings indicate the neurodevelopmental nature of RTT disease instead of a neurodegenerative disorder. Conversely, degeneration of the cortex and cerebellum has been displayed to increasingly happen in an age-dependent manner in RTT patients [12]. Therefore, microcephaly is spread through the brain and influences white and grey matter in diverse regions [292, 294]. Likewise, diminished neuronal cell density in cortical neurons is suggested to trigger breakdown to develop dendritic connections between neurons and decreased synaptic output [295]. The cerebellum is also significantly reduced in RTT patients [12]. Neuropathological irregularities in other areas contain neuronal size reduction in the hippocampus, amygdala, and thalamus. Nevertheless, in the hippocampus, neuronal cell packing increase has been detected contrary to reduced cortical packing [293].

Studies in the hippocampus have discovered the benefits of metformin treatment on different RTT-associated abnormalities including molecular and behavioral performances, formation of memory, and neuronal plasticity. Additionally, in ischaemic and metformin-treated rats, improvement of short-term memory following an increase of BDNF and p-P70S6K levels *via* AMPK activation proposes the AMPK/BDNF/P70S6K pathway, which requires further examinations [315].

In conclusion, due to the importance of controlling the RNA and protein level of *MECP2*/MeCP2, and *BDNF*/BDNF in X-lined disorders such as RTT, our findings would help to broaden our horizon on RTT pathobiology, and possible drug treatment with metformin in pre-clinical studies.

4.3. Metformin is Beneficial for the Improvement of RTT-like Phenotypes of *Mecp2*^{T158M} Mice

As previously mentioned, MeCP2 T158M is the most common missense mutation identified in individuals with classical RTT [17]. In my second aim and in consistent with other studies, to screen RTT-like symptoms before and after metformin treatment, 2 approaches were used including phenotypic characterization and evaluation of phenotypic scoring.

Furthermore, according to prior discoveries of insulin resistance in *Mecp2*$^{NULL/Y}$ mice, RTT has been considered a metabolic Syndrome with irregular systemic and brain glucose metabolism including insulin resistance. So, we expected to see elevated blood glucose levels in *Mecp2*$^{T158M/y}$ male and female mice compared with their WT littermates. However, regardless of our theory, no difference was found in the blood glucose levels of mice at the basal level, but metformin reduced its level in *Mecp2*$^{T158M/y}$ males in a sex-dependent manner.

Then, we checked both sexes of *Mecp2*^{T158M} mice for the development of RTT-like symptoms *via* phenotypic scoring, which measures a range of RTT-like phenotypes derived from *Mecp2* mutations. The scoring of experimental mice (metformin-treated and control) was measured and recorded in 6 categories of symptoms including loss of mobility, irregular gait, the existence of a hindlimb clasp, enhanced tremors, breathing problems, and total decline in general condition. The age of our studied male mice was 5-9 weeks, which is approximately close to the range of *Mecp2*$^{T158M/y}$ mice's age mentioned in similar studies (4–12 weeks). According to our expectation, a significant increase was detected in the phenotypic scoring of *Mecp2*$^{T158M/y}$ male mice in an age-dependent manner resulting in an early death at about 7-8 weeks in some of them. Due to the clinical relation of the *Mecp2*$^{T158M/+}$ female mouse model to RTT, we additionally monitored their RTT-like phenotypes, and like male mice, a significant increase in scoring was detected in 3 categories (hind limb clasping, breathing abnormalities, and general condition) in an age-dependent manner. However, due to the limitation in the number of *Mecp2*$^{T158M/+}$ female mice, analysis of other scoring criteria needs further mice at the basal level, and it is worth mentioning that, unlike male mice, the age of our studied female mice was 15-19 weeks due to the late onset of symptoms [255].

In agreement with similar studies [71], like hemizygous *Mecp2*$^{T158M/y}$ male mice, heterozygous *Mecp2*$^{T158M/+}$ female mice displayed RTT-like phenotypes, although they were milder and had late progress.

In conclusion, at the phenotypical level, our utilized approaches including phenotypic characterization and phenotypic scoring [71] confirmed RTT-like symptoms in *Mecp2*^{T158M} male and female mice like symptoms found in *Mecp2*-null and other types of RTT-associated mice models [37, 43].

It is shown that the genetic or pharmacological elevation of the MeCP2 T158M protein expression or stability has been a beneficial therapeutic approach in the reduction of RTT-like phenotypes in the *Mecp2*^{T158M} mice model. Consequently, like the results of other pre-clinical studies [71], we expected to detect improvement in the RTT-like phenotypes in both sexes of our *Mecp2*^{T158M} mice models after metformin treatment. Likewise, our results indicated a slight and age-dependent improvement after metformin treatment (250 mg/kg/day dosage for 21 days) in *Mecp2*$^{T158M/y}$ males and *Mecp2*$^{T158M/+}$ females mice. Although, in terms of breathing abnormalities (males and females) and general conditions (females), a significant improvement was detected after day 10 of IP injections.

We concluded that in general, metformin could have a beneficial effect on the improvement of RTT-like phenotypes, however, different factors need to be considered while metformin treatment including the dosage, time and duration of treatment, route of drug delivery, sex, age, and type of mouse model, along with phenotypic variation in female mice. Also, at the molecular level, possible metformin of metformin action is the elevation of MeCP2 T158M protein level or stability by partial improvement of its binding ability, but further studies are required for understanding the exact mechanism of metformin action in the improvement of RTT-like phenotypes.

4.4. Metformin Partially Improved Locomotion and Anxiety of *Mecp2*^{T158M} Mice at the Behavioral Level

To test the beneficial effect of metformin on the improvement of RTT-associated locomotor and anxiety-like behavior, *Mecp2*^{T158M} Mouse Model underwent OFT and EPM tests. As we expected, a significantly lower total distance and velocity were detected in *Mecp2*$^{T158M/y}$ males compared with their age- and sex-matched *Mecp2*$^{+/y}$ male mice during the 10 min of habituation, suggesting motor deficits that agree with other studies in *Mecp2*$^{T158M/y}$ mice models [71]. The analysis with two-way ANOVA indicated no drug or genotype effect after metformin treatment for the total distance and velocity. In the case of anxiety, both *Mecp2*$^{+/y}$ and *Mecp2*$^{T158M/y}$ male mice showed more time spent in corners of an open field during the habituation period, indicating higher levels of anxiety. However, no significant genotype-based difference was detected between them. Contrary to other studies, a metformin-mediated stimulation of corner time was detected in *Mecp2*$^{+/y}$ male mice.

In conclusion, according to the OFT results, 3 weeks of metformin treatment did not affect the locomotion and anxiety-like behavior of *Mecp2*$^{T158M/y}$ male mice. Like males, *Mecp2*$^{+/+}$ and *Mecp2*$^{T158M/+}$ female mice spent more time in corners of an open field, but metformin did not affect the total distance and time spent in zones, suggesting no effect of metformin on the locomotion and anxiety-like behavior of female mice.

Furthermore, despite our expectation, the EPM test did not show any anxiety-like behavior in *Mecp2*$^{T158M/y}$ male and *Mecp2*$^{T158M/+}$ female mice, and metformin did not affect it.

In conclusion, these results show that 3 weeks of metformin treatment did not change the overall anxiety-like behaviors in OFT and EPM tests in *Mecp2*$^{T158M/y}$ males and *Mecp2*$^{T158M/+}$ female mice but showed anxiogenic effects in *Mecp2*$^{+/y}$ male mice in OFT.

Our results of the NOR test showed a slight reduction in the percentage of PI in *Mecp2*$^{T158M/y}$ male mice compared with *Mecp2*$^{T158M/+}$ control mice, indicating possible cognitive and memory impairment. However, metformin did not affect the PI of any 4 groups of male or female mice, which could be reasonable due to the controversial role of metformin in the improvement of intellectual abnormalities.

Although some studies in T2DM patients have recommended useful effects [296], others have considered the continuing consumption of metformin as a risk factor in the progress of cognitive impairment [297]. Likewise, in nondiabetic patients with mild AD-related dementia, metformin did not improve cognitive function. In high-fat diet animal models, the metformin effect is debated, with 3 studies indicating the mitigation of cognitive defects and one study does not report any beneficial effect. So, the total effects of metformin appeared to alter in various disorder circumstances, and attractively, an earlier study in a mouse model proposed that metformin treatment in aged mice results in memory deficit.

The inconsistency between the previous studies and our findings probably displays differences in the intervention time, the dosage, the occurrence/length of administration, and the type of conducted tests. Primary, the onset of metformin treatment might have distinct effects since the range of neuronal impairments enhances gradually in an age-dependent manner in the brain. Consequently, it is reasonable that beginning metformin treatment at an early age could apply useful effects, contrary to the start of metformin treatment in old age, a period at which neuronal dysfunction has proceeded to considerably higher levels.

Chapter 5. Conclusion

5.1. Strength, Challenges, Limitations

5.1.1. Strength and Significance

This study presents proof of metformin-mediated changes at the molecular, phenotypical, and behavioral levels *in vivo*, using different techniques and approaches including Western blot, phenotypic scoring, and behavioral tests analysis. These include sex- and region-dependent changes in terms of p-S6 (235/236) (increase in the male liver and decrease in the female liver), MeCP2 (increase in the male hippocampus), BDNF (increase in the male hippocampus and decrease in the thalamus), and AMPK (increase in female thalamus) protein levels in C57BL/6 mice along with improvement of RTT-like phenotypes, and without a remarkable effect on the behavior of *Mecp2*^{T158M} mice model. Although our data relatively advocate earlier pre-clinical and clinical research, besides *in vitro* models, important changes have been emphasized in this study. Additionally, we indicated a significant increase of MeCP2 and BDNF protein levels in the hippocampus of C57BL/6 male mice, while a reduction of BDNF in males and AMPK protein levels in the thalamus of females. Furthermore, the increase of p-S6 (235/236) and p-S6 (235/236)/S6 ratio in male mice, while the decrease of p-S6 (235/236) showed the sex- and region-dependent effect of metformin. Although most of our discoveries have been approved for the sex and region-specific effects of metformin treatment on mice tissues, phenotypes, and behavior, the exact mechanism of metformin action needs further investigation.

Ultimately, our discoveries would assist to shed some light on the effect of metformin *in vivo* in the mice's brains by offering a new vision regarding the multiple effects of metformin (molecular, phenotypical, and behavioral levels) provides a better understanding of the RTT etiology at the basal level. Also, these results are significant as an attempt to convert the huge amount of data from *in vitro* models of RTT to preclinical and clinical studies. Besides RTT, other MeCP2-associated conditions like MDS, ASD, and FASD, would take advantage of the results of our study.

5.1.2. Limitations and Challenges

At the molecular level, the detection of our protein of interest was completed by Western blot. However, the detection of phospho-proteins was tricky, particularly in the case of p-S6 in the cortex and p-AMPK in 4 brain regions (cerebellum, cortex, hippocampus, and thalamus) was unsuccessful, which could be attributed to the quality of samples and/or instability of phospho-proteins. Additionally, the collection of female mice samples compared with males was harder and more time-consuming, since females were not only used for breeding purposes but also showed milder and later symptoms.

5.2. Future Direction

In the case of my first aim, the results of this thesis have been focused on the analyzing effects of metformin on the pan and phosphorylated protein levels of MeCP2, BDNF, AMPK, and S6. However, further studies could focus on more proteins related to the metformin-targeted pathways including the mTOR pathway as well as RNA levels to generate a clear correlation between the metformin mechanism of action *in vivo*. Besides, using fresh samples with a higher concentration of total extracts could be beneficial for the detection of phosphoproteins.

In the case of my second aim, to study the origin of RTT-associated abnormalities in the *Mecp2*^{T158M} mouse model, mice brain tissues could be analyzed at the protein and RNA levels. Consequently, increasing the number of an experimental group of *Mecp2*^{T158M} mice, particularly *Mecp2*$^{T158M/+}$ female mice to undergo various behavioral tests, could be beneficial in finding metformin effect in the improvement of RTT- associated abnormalities.

Finally, the different dosages of the drug, time, and duration of treatment, along with various ages and mice models of RTT could be tested in future pre-clinical studies to approve the feasibility of metformin treatments in clinical studies.

References

1. Haas, R.H., *The history and challenge of Rett syndrome.* J Child Neurol, 1988. **3 Suppl**: p. S3-5.
2. Singh, J., E. Lanzarini, and P. Santosh, *Autonomic dysfunction and sudden death in patients with Rett syndrome: a systematic review.* J Psychiatry Neurosci, 2020. **45**(3): p. 150-181.
3. Amir, R.E., et al., *Rett syndrome is caused by mutations in X-linked MECP2, encoding methyl-CpG-binding protein 2.* Nat Genet, 1999. **23**(2): p. 185-8.
4. Vashi, N. and M.J. Justice, *Treating Rett syndrome: from mouse models to human therapies.* Mamm Genome, 2019. **30**(5-6): p. 90-110.
5. Kyle, S.M., N. Vashi, and M.J. Justice, *Rett syndrome: a neurological disorder with metabolic components.* Open Biol, 2018. **8**(2).
6. Hagberg, B., *Clinical manifestations and stages of Rett syndrome.* Ment Retard Dev Disabil Res Rev, 2002. **8**(2): p. 61-5.
7. Motil, K.J., et al., *Gastrointestinal and nutritional problems occur frequently throughout life in girls and women with Rett syndrome.* J Pediatr Gastroenterol Nutr, 2012. **55**(3): p. 292-8.
8. Shapiro, J.R., et al., *Bone mass in Rett syndrome: association with clinical parameters and MECP2 mutations.* Pediatr Res, 2010. **68**(5): p. 446-51.
9. Haas, R.H., et al., *Osteopenia in Rett syndrome.* J Pediatr, 1997. **131**(5): p. 771-4.
10. Menachem, S., et al., *Scoliosis in RETT Syndrome: A National Referral Centre Experience.* Clin Spine Surg, 2023. **36**(2): p. E75-E79.
11. Ward, C.S., et al., *Loss of MeCP2 Causes Urological Dysfunction and Contributes to Death by Kidney Failure in Mouse Models of Rett Syndrome.* PLoS One, 2016. **11**(11): p. e0165550.
12. Young, D., et al., *Sleep problems in Rett syndrome.* Brain and Development, 2007. **29**(10): p. 609-616.
13. Laurvick, C.L., et al., *Rett syndrome in Australia: a review of the epidemiology.* J Pediatr, 2006. **148**(3): p. 347-52.

14. Ramirez, J.M., C.S. Ward, and J.L. Neul, *Breathing challenges in Rett syndrome: lessons learned from humans and animal models.* Respir Physiol Neurobiol, 2013. **189**(2): p. 280-7.
15. Acampa, M. and F. Guideri, *Cardiac disease and Rett syndrome.* Arch Dis Child, 2006. **91**(5): p. 440-3.
16. Bienvenu, T., et al., *MECP2 mutations account for most cases of typical forms of Rett syndrome.* Hum Mol Genet, 2000. **9**(9): p. 1377-84.
17. Neul, J.L., et al., *Specific mutations in methyl-CpG-binding protein 2 confer different severity in Rett syndrome.* Neurology, 2008. **70**(16): p. 1313-21.
18. Bianciardi, L., et al., *MECP2 missense mutations outside the canonical MBD and TRD domains in males with intellectual disability.* J Hum Genet, 2016. **61**(2): p. 95-101.
19. Xi, C.Y., et al., *Analysis of MECP2 gene copy number in boys with autism.* J Child Neurol, 2011. **26**(5): p. 570-3.
20. Quaderi, N.A., et al., *Genetic and physical mapping of a gene encoding a methyl CpG binding protein, Mecp2, to the mouse X chromosome.* Genomics, 1994. **22**(3): p. 648-51.
21. Adler, D.A., et al., *The X-linked methylated DNA binding protein, Mecp2, is subject to X inactivation in the mouse.* Mamm Genome, 1995. **6**(8): p. 491-2.
22. Reichwald, K., et al., *Comparative sequence analysis of the MECP2-locus in human and mouse reveals new transcribed regions.* Mamm Genome, 2000. **11**(3): p. 182-90.
23. Kriaucionis, S. and A. Bird, *The major form of MeCP2 has a novel N-terminus generated by alternative splicing.* Nucleic Acids Res, 2004. **32**(5): p. 1818-23.
24. Mnatzakanian, G.N., et al., *A previously unidentified MECP2 open reading frame defines a new protein isoform relevant to Rett syndrome.* Nat Genet, 2004. **36**(4): p. 339-41.
25. Liyanage, V.R. and M. Rastegar, *Rett syndrome and MeCP2.* Neuromolecular Med, 2014. **16**(2): p. 231-64.
26. Lewis, J.D., et al., *Purification, sequence, and cellular localization of a novel chromosomal protein that binds to methylated DNA.* Cell, 1992. **69**(6): p. 905-14.
27. Nan, X., F.J. Campoy, and A. Bird, *MeCP2 is a transcriptional repressor with abundant binding sites in genomic chromatin.* Cell, 1997. **88**(4): p. 471-81.
28. Chandler, S.P., et al., *The methyl-CpG binding transcriptional repressor MeCP2 stably associates with nucleosomal DNA.* Biochemistry, 1999. **38**(22): p. 7008-18.

29. Bin Akhtar, G., M. Buist, and M. Rastegar, *MeCP2 and transcriptional control of eukaryotic gene expression.* Eur J Cell Biol, 2022. **101**(3): p. 151237.
30. Jones, P.L., et al., *Methylated DNA and MeCP2 recruit histone deacetylase to repress transcription.* Nat Genet, 1998. **19**(2): p. 187-91.
31. Delcuve, G.P., D.H. Khan, and J.R. Davie, *Roles of histone deacetylases in epigenetic regulation: emerging paradigms from studies with inhibitors.* Clin Epigenetics, 2012. **4**(1): p. 5.
32. Chahrour, M., et al., *MeCP2, a key contributor to neurological disease, activates and represses transcription.* Science, 2008. **320**(5880): p. 1224-9.
33. Kishi, N. and J.D. Macklis, *MECP2 is progressively expressed in post-migratory neurons and is involved in neuronal maturation rather than cell fate decisions.* Mol Cell Neurosci, 2004. **27**(3): p. 306-21.
34. Liyanage, V.R., R.M. Zachariah, and M. Rastegar, *Decitabine alters the expression of Mecp2 isoforms via dynamic DNA methylation at the Mecp2 regulatory elements in neural stem cells.* Mol Autism, 2013. **4**(1): p. 46.
35. Pejhan, S. and M. Rastegar, *Role of DNA Methyl-CpG-Binding Protein MeCP2 in Rett Syndrome Pathobiology and Mechanism of Disease.* Biomolecules, 2021. **11**(1).
36. Olson, C.O., et al., *Brain region-specific expression of MeCP2 isoforms correlates with DNA methylation within Mecp2 regulatory elements.* PloS one, 2014. **9**(3): p. e90645.
37. Guy, J., et al., *A mouse Mecp2-null mutation causes neurological symptoms that mimic Rett syndrome.* Nat Genet, 2001. **27**(3): p. 322-6.
38. Szczesna, K., et al., *Improvement of the Rett syndrome phenotype in a MeCP2 mouse model upon treatment with levodopa and a dopa-decarboxylase inhibitor.* Neuropsychopharmacology, 2014. **39**(12): p. 2846-56.
39. Yazdani, M., et al.,*Disease modeling using embryonic stem cells: MeCP2 regulates nuclear size and RNA synthesis in neurons.* Stem Cells, 2012. **30**(10): p. 2128-39.
40. Ezeonwuka, C.D. and M. Rastegar, *MeCP2-Related Diseases and Animal Models.* Diseases, 2014. **2**(1): p. 45-70.
41. Calfa, G., A.K. Percy, and L. Pozzo-Miller, *Experimental models of Rett syndrome based on Mecp2 dysfunction.* Exp Biol Med (Maywood), 2011. **236**(1): p. 3-19.

42. Hendrich, B. and S. Tweedie, *The methyl-CpG binding domain and the evolving role of DNA methylation in animals.* Trends Genet, 2003. **19**(5): p. 269-77.
43. Chen, R.Z., et al., *Deficiency of methyl-CpG binding protein-2 in CNS neurons results in a Rett-like phenotype in mice.* Nature genetics, 2001. **27**(3): p. 327-331.
44. Young, J.I. and H.Y. Zoghbi, *X-chromosome inactivation patterns are unbalanced and affect the phenotypic outcome in a mouse model of rett syndrome.* Am J Hum Genet, 2004. **74**(3): p. 511-20.
45. Samaco, R.C., et al., *Female Mecp2(+/-) mice display robust behavioral deficits on two different genetic backgrounds providing a framework for pre-clinical studies.* Hum Mol Genet, 2013. **22**(1): p. 96-109.
46. Samaco, R.C., et al., *A partial loss of function allele of methyl-CpG-binding protein 2 predicts a human neurodevelopmental syndrome.* Hum Mol Genet, 2008. **17**(12): p. 1718-27.
47. Shahbazian, M., et al., *Mice with truncated MeCP2 recapitulate many Rett syndrome features and display hyperacetylation of histone H3.* Neuron, 2002. **35**(2): p. 243-54.
48. Hagberg, B. and I. Witt-Engerström, *Rett syndrome: a suggested staging system for describing impairment profile with increasing age towards adolescence.* Am J Med Genet Suppl, 1986. **1**: p. 47-59.
49. Chahrour, M. and H.Y. Zoghbi, *The story of Rett syndrome: from clinic to neurobiology.* Neuron, 2007. **56**(3): p. 422-37.
50. Elefant, C. and T. Wigram, *Learning ability in children with Rett syndrome.* Brain Dev, 2005. **27 Suppl 1**: p. S97-S101.
51. Moretti, P., et al., *Learning and memory and synaptic plasticity are impaired in a mouse model of Rett syndrome.* J Neurosci, 2006. **26**(1): p. 319-27.
52. Tropea, D., et al., *Partial reversal of Rett Syndrome-like symptoms in MeCP2 mutant mice.* Proc Natl Acad Sci U S A, 2009. **106**(6): p. 2029-34.
53. Orefice, L.L., et al., *Peripheral Mechanosensory Neuron Dysfunction Underlies Tactile and Behavioral Deficits in Mouse Models of ASDs.* Cell, 2016. **166**(2): p. 299-313.
54. Goffin, D. and Z.J. Zhou, *The neural circuit basis of Rett syndrome.* Front Biol (Beijing), 2012. **7**(5): p. 428-435.

55. Buchovecky, C.M., et al., *A suppressor screen in Mecp2 mutant mice implicates cholesterol metabolism in Rett syndrome.* Nat Genet, 2013. **45**(9): p. 1013-20.
56. Segatto, M., et al., *Cholesterol metabolism is altered in Rett syndrome: a study on plasma and primary cultured fibroblasts derived from patients.* PLoS One, 2014. **9**(8): p. e104834.
57. Shulyakova, N., et al., *Mitochondrial Dysfunction in the Pathogenesis of Rett Syndrome: Implications for Mitochondria-Targeted Therapies.* Front Cell Neurosci, 2017. **11**: p. 58.
58. De Felice, C., et al., *Oxidative brain damage in Mecp2-mutant murine models of Rett syndrome.* Neurobiol Dis, 2014. **68**(100): p. 66-77.
59. Hara, M., et al., *Disturbance of cardiac gene expression and cardiomyocyte structure predisposes Mecp2-null mice to arrhythmias.* Sci Rep, 2015. **5**: p. 11204.
60. Cuddapah, V.A., et al., *Methyl-CpG-binding protein 2 (MECP2) mutation type is associated with disease severity in Rett syndrome.* J Med Genet, 2014. **51**(3): p. 152-8.
61. Brown, K., et al., *The molecular basis of variable phenotypic severity among common missense mutations causing Rett syndrome.* Hum Mol Genet, 2016. **25**(3): p. 558-70.
62. Shevkoplyas, D., et al., *The Chromatin Structure at the.* Int J Mol Sci, 2022. **23**(24).
63. Yasui, D.H., et al., *Mice with an isoform-ablating Mecp2 exon 1 mutation recapitulate the neurologic deficits of Rett syndrome.* Hum Mol Genet, 2014. **23**(9): p. 2447-58.
64. Itoh, M., et al., *Methyl CpG-binding protein isoform MeCP2_e2 is dispensable for Rett syndrome phenotypes but essential for embryo viability and placenta development.* J Biol Chem, 2012. **287**(17): p. 13859-67.
65. Tao, J., et al., *Phosphorylation of MeCP2 at Serine 80 regulates its chromatin association and neurological function.* Proc Natl Acad Sci U S A, 2009. **106**(12): p. 4882-7.
66. Cohen, S., et al., *Genome-wide activity-dependent MeCP2 phosphorylation regulates nervous system development and function.* Neuron, 2011. **72**(1): p. 72-85.
67. Lawson-Yuen, A., et al., *Ube3a mRNA and protein expression are not decreased in Mecp2R168X mutant mice.* Brain Res, 2007. **1180**: p. 1-6.
68. Rangasamy, S., et al., *Reduced neuronal size and mTOR pathway activity in the Mecp2 A140V Rett syndrome mouse model.* F1000Res, 2016. **5**: p. 2269.
69. Jentarra, G.M., et al., *Abnormalities of cell packing density and dendritic complexity in the MeCP2 A140V mouse model of Rett syndrome/X-linked mental retardation.* BMC Neurosci, 2010. **11**: p. 19.

70. Li, H., et al., *Loss of activity-induced phosphorylation of MeCP2 enhances synaptogenesis, LTP and spatial memory.* Nat Neurosci, 2011. **14**(8): p. 1001-8.
71. Lamonica, J.M., et al., *Elevating expression of MeCP2 T158M rescues DNA binding and Rett syndrome-like phenotypes.* J Clin Invest, 2017. **127**(5): p. 1889-1904.
72. Fyffe, S.L., et al., *Deletion of Mecp2 in Sim1-expressing neurons reveals a critical role for MeCP2 in feeding behavior, aggression, and the response to stress.* Neuron, 2008. **59**(6): p. 947-58.
73. Samaco, R.C., et al., *Loss of MeCP2 in aminergic neurons causes cell-autonomous defects in neurotransmitter synthesis and specific behavioral abnormalities.* Proc Natl Acad Sci U S A, 2009. **106**(51): p. 21966-71.
74. Chao, H.T., et al., *Dysfunction in GABA signalling mediates autism-like stereotypies and Rett syndrome phenotypes.* Nature, 2010. **468**(7321): p. 263-9.
75. Maezawa, I., et al., *Rett syndrome astrocytes are abnormal and spread MeCP2 deficiency through gap junctions.* J Neurosci, 2009. **29**(16): p. 5051-61.
76. Ballas, N., et al., *Non-cell autonomous influence of MeCP2-deficient glia on neuronal dendritic morphology.* Nat Neurosci, 2009. **12**(3): p. 311-7.
77. Maezawa, I. and L.W. Jin, *Rett syndrome microglia damage dendrites and synapses by the elevated release of glutamate.* J Neurosci, 2010. **30**(15): p. 5346-56.
78. Shahbazian, M.D., et al., *Insight into Rett syndrome: MeCP2 levels display tissue- and cell-specific differences and correlate with neuronal maturation.* Hum Mol Genet, 2002. **11**(2): p. 115-24.
79. Jung, B.P., et al., *The expression of methyl CpG binding factor MeCP2 correlates with cellular differentiation in the developing rat brain and in cultured cells.* J Neurobiol, 2003. **55**(1): p. 86-96.
80. Stiles, J. and T.L. Jernigan, *The basics of brain development.* Neuropsychol Rev, 2010. **20**(4): p. 327-48.
81. Sidman, R.L. and P. Rakic, *Neuronal migration, with special reference to developing human brain: a review.* Brain Res, 1973. **62**(1): p. 1-35.
82. Waites, C.L., A.M. Craig, and C.C. Garner, *Mechanisms of vertebrate synaptogenesis.* Annu Rev Neurosci, 2005. **28**: p. 251-74.

83. Mullaney, B.C., M.V. Johnston, and M.E. Blue, *Developmental expression of methyl-CpG binding protein 2 is dynamically regulated in the rodent brain.* Neuroscience, 2004. **123**(4): p. 939-49.
84. Nicholson, J.L. and J. Altman, *Synaptogenesis in the rat cerebellum: effects of early hypo- and hyperthyroidism.* Science, 1972. **176**(4034): p. 530-2.
85. Altman, J., *Postnatal development of the cerebellar cortex in the rat. I. The external germinal layer and the transitional molecular layer.* J Comp Neurol, 1972. **145**(3): p. 353-97.
86. Ross, P.D., et al., *Exclusive expression of MeCP2 in the nervous system distinguishes between brain and peripheral Rett syndrome-like phenotypes.* Hum Mol Genet, 2016. **25**(20): p. 4389-4404.
87. Ronnett, G.V., et al., *Olfactory biopsies demonstrate a defect in neuronal development in Rett's syndrome.* Ann Neurol, 2003. **54**(2): p. 206-18.
88. Guy, J., et al., *The role of MeCP2 in the brain.* Annu Rev Cell Dev Biol, 2011. **27**: p. 631-52.
89. Glaze, D.G., *Neurophysiology of Rett syndrome.* J Child Neurol, 2005. **20**(9): p. 740-6.
90. Moser, S.J., P. Weber, and J. Lütschg, *Rett syndrome: clinical and electrophysiologic aspects.* Pediatr Neurol, 2007. **36**(2): p. 95-100.
91. Oldfors, A., et al., *Rett syndrome: cerebellar pathology.* Pediatr Neurol, 1990. **6**(5): p. 310-4.
92. Heydel, J.M., et al., *UDP-glucuronosyltransferases (UGTs) in neuro-olfactory tissues: expression, regulation, and function.* Drug Metab Rev, 2010. **42**(1): p. 74-97.
93. Ehrhart, F., et al., *Rett syndrome - biological pathways leading from MECP2 to disorder phenotypes.* Orphanet J Rare Dis, 2016. **11**(1): p. 158.
94. Deaton, A.M. and A. Bird, *CpG islands and the regulation of transcription.* Genes Dev, 2011. **25**(10): p. 1010-22.
95. Rastegar, M., et al., *MECP2 isoform-specific vectors with regulated expression for Rett syndrome gene therapy.* PLoS One, 2009. **4**(8): p. e6810.
96. Liyanage, V.R.B., et al., *DNA Methylation Contributes to the Differential Expression Levels of.* Int J Mol Sci, 2019. **20**(8).

97. Renthal, W., et al., *Characterization of human mosaic Rett syndrome brain tissue by single-nucleus RNA sequencing.* Nat Neurosci, 2018. **21**(12): p. 1670-1679.
98. Castro, J., N. Mellios, and M. Sur, *Mechanisms and therapeutic challenges in autism spectrum disorders: insights from Rett syndrome.* Curr Opin Neurol, 2013. **26**(2): p. 154-9.
99. Van Esch, H., et al., *Duplication of the MECP2 region is a frequent cause of severe mental retardation and progressive neurological symptoms in males.* Am J Hum Genet, 2005. **77**(3): p. 442-53.
100. Nagel-Wolfrum, K., et al., *Targeting Nonsense Mutations in Diseases with Translational Read-Through-Inducing Drugs (TRIDs).* BioDrugs, 2016. **30**(2): p. 49-74.
101. Bhatnagar, S., et al., *Genetic and pharmacological reactivation of the mammalian inactive X chromosome.* Proc Natl Acad Sci U S A, 2014. **111**(35): p. 12591-8.
102. Carrette, L.L.G., et al., *A mixed modality approach towards Xi reactivation for Rett syndrome and other X-linked disorders.* Proc Natl Acad Sci U S A, 2018. **115**(4): p. E668-E675.
103. Gadalla, K.K., M.E. Bailey, and S.R. Cobb, *MeCP2 and Rett syndrome: reversibility and potential avenues for therapy.* Biochem J, 2011. **439**(1): p. 1-14.
104. Foust, K.D., et al., *Intravascular AAV9 preferentially targets neonatal neurons and adult astrocytes.* Nat Biotechnol, 2009. **27**(1): p. 59-65.
105. Gonçalves, M.A., *Adeno-associated virus: from defective virus to effective vector.* Virol J, 2005. **2**: p. 43.
106. Hinderer, C., et al., *Severe Toxicity in Nonhuman Primates and Piglets Following High-Dose Intravenous Administration of an Adeno-Associated Virus Vector Expressing Human SMN.* Hum Gene Ther, 2018. **29**(3): p. 285-298.
107. Armstrong, D.D., *The neuropathology of the Rett syndrome.* Brain Dev, 1992. **14 Suppl**: p. S89-98.
108. Zanella, S., et al., *Oral treatment with desipramine improves breathing and life span in Rett syndrome mouse model.* Respir Physiol Neurobiol, 2008. **160**(1): p. 116-21.
109. Mancini, J., et al., *Effect of desipramine on patients with breathing disorders in RETT syndrome.* Ann Clin Transl Neurol, 2018. **5**(2): p. 118-127.

110. Brunkhorst, R., et al., *FTY720 treatment in the convalescence period improves functional recovery and reduces reactive astrogliosis in photothrombotic stroke.* PLoS One, 2013. **8**(7): p. e70124.

111. Itoh, M., et al., *Methyl CpG-binding protein 2 (a mutation of which causes Rett syndrome) directly regulates insulin-like growth factor binding protein 3 in mouse and human brains.* J Neuropathol Exp Neurol, 2007. **66**(2): p. 117-23.

112. Chen, W.G., et al., *Derepression of BDNF transcription involves calcium-dependent phosphorylation of MeCP2.* Science, 2003. **302**(5646): p. 885-9.

113. Amaral, M.D. and L. Pozzo-Miller, *TRPC3 channels are necessary for brain-derived neurotrophic factor to activate a nonselective cationic current and to induce dendritic spine formation.* J Neurosci, 2007. **27**(19): p. 5179-89.

114. Pejhan, S., M.R. Del Bigio, and M. Rastegar, *The MeCP2E1/E2-BDNF-miR132 homeostasis regulatory network is region-dependent in the human brain and is impaired in rett syndrome patients.* Frontiers in Cell and Developmental Biology, 2020: p. 763.

115. Yi, X., et al., *Serum mBDNF and ProBDNF Expression Levels as Diagnosis Clue for Early Stage Parkinson's Disease.* Frontiers in Neurology, 2021. **12**: p. 680765.

116. Graham, D.L., et al., *Dynamic BDNF activity in nucleus accumbens with cocaine use increases self-administration and relapse.* Nat Neurosci, 2007. **10**(8): p. 1029-37.

117. Chang, Q., et al., *The disease progression of Mecp2 mutant mice is affected by the level of BDNF expression.* Neuron, 2006. **49**(3): p. 341-8.

118. Pejhan, S., et al., *Differential brain region-specific expression of MeCP2 and BDNF in Rett Syndrome patients: a distinct grey-white matter variation.* Neuropathol Appl Neurobiol, 2020. **46**(7): p. 735-750.

119. Radziejewski, C., et al., *Dimeric structure and conformational stability of brain-derived neurotrophic factor and neurotrophin-3.* Biochemistry, 1992. **31**(18): p. 4431-6.

120. Mowla, S.J., et al., *Biosynthesis and post-translational processing of the precursor to brain-derived neurotrophic factor.* J Biol Chem, 2001. **276**(16): p. 12660-6.

121. Seidah, N.G., et al., *Mammalian subtilisin/kexin isozyme SKI-1: A widely expressed proprotein convertase with a unique cleavage specificity and cellular localization.* Proc Natl Acad Sci U S A, 1999. **96**(4): p. 1321-6.

122. Lee, R., et al., *Regulation of cell survival by secreted proneurotrophins.* Science, 2001. **294**(5548): p. 1945-8.

123. Matsuda, N., et al., *Differential activity-dependent secretion of brain-derived neurotrophic factor from axon and dendrite.* J Neurosci, 2009. **29**(45): p. 14185-98.

124 Dieni, S., et al., *BDNF and its pro-peptide are stored in presynaptic dense core vesicles in brain neurons.* J Cell Biol, 2012. **196**(6): p. 775-88.

125. Nagappan, G., et al., *Control of extracellular cleavage of ProBDNF by high frequency neuronal activity.* Proc Natl Acad Sci U S A, 2009. **106**(4): p. 1267-72.

126. Ballas, N., et al., *REST and its corepressors mediate plasticity of neuronal gene chromatin throughout neurogenesis.* Cell, 2005. **121**(4): p. 645-657.

127. Zhou, Z., et al., *Brain-specific phosphorylation of MeCP2 regulates activity-dependent Bdnf transcription, dendritic growth, and spine maturation.* Neuron, 2006. **52**(2): p. 255-69.

128. Li, W., et al., *Activity-dependent BDNF release and TRPC signaling is impaired in hippocampal neurons of Mecp2 mutant mice.* Proc Natl Acad Sci U S A, 2012. **109**(42): p. 17087-92.

129. Li, W. and L. Pozzo-Miller, *BDNF deregulation in Rett syndrome.* Neuropharmacology, 2014. **76 Pt C**(0 0): p. 737-46.

130. Gonzales, M.L., et al., *Phosphorylation of distinct sites in MeCP2 modifies cofactor associations and the dynamics of transcriptional regulation.* Mol Cell Biol, 2012. **32**(14): p. 2894-903.

131. Wu, H., et al., *Genome-wide analysis reveals methyl-CpG-binding protein 2-dependent regulation of microRNAs in a mouse model of Rett syndrome.* Proc Natl Acad Sci U S A, 2010. **107**(42): p. 18161-6.

132. Katz, D.M., *Brain-derived neurotrophic factor and Rett syndrome.* Handb Exp Pharmacol, 2014. **220**: p. 481-95.

133. Kim, J.W., et al., *Sustained effects of rapidly acting antidepressants require BDNF-dependent MeCP2 phosphorylation.* Nat Neurosci, 2021. **24**(8): p. 1100-1109.

134. Huang, L., et al., *The role of MeCP2 and the BDNF/TrkB signaling pathway in the stress resilience of mice subjected to CSDS.* Psychopharmacology (Berl), 2022. **239**(9): p. 2921-2929.

135. Justice, M.J., et al., *A role for metabolism in Rett syndrome pathogenesis: New clinical findings and potential treatment targets.* Rare Dis, 2013. **1**: p. e27265.
136. Puglielli, L., R.E. Tanzi, and D.M. Kovacs, *Alzheimer's disease: the cholesterol connection.* Nat Neurosci, 2003. **6**(4): p. 345-51.
137. Tint, G.S., et al., *Defective cholesterol biosynthesis associated with the Smith-Lemli-Opitz syndrome.* N Engl J Med, 1994. **330**(2): p. 107-13.
138. Gold, W.A., et al., *Mitochondrial dysfunction in the skeletal muscle of a mouse model of Rett syndrome (RTT): implications for the disease phenotype.* Mitochondrion, 2014. **15**: p. 10-7.
139. Kriaucionis, S., et al., *Gene expression analysis exposes mitochondrial abnormalities in a mouse model of Rett syndrome.* Mol Cell Biol, 2006. **26**(13): p. 5033-42.
140. Eeg-Olofsson, O., et al., *Abnormal mitochondria in the Rett syndrome.* Brain Dev, 1988. **10**(4): p. 260-2.
141. Schon, E.A. and G. Manfredi, *Neuronal degeneration and mitochondrial dysfunction.* J Clin Invest, 2003. **111**(3): p. 303-12.
142. Haas, R.H., et al., *Oxidative metabolism in Rett syndrome: 1. Clinical studies.* Neuropediatrics, 1995. **26**(2): p. 90-4.
143. Mochel, F., et al., *Pyruvate carboxylase deficiency: clinical and biochemical response to anaplerotic diet therapy.* Mol Genet Metab, 2005. **84**(4): p. 305-12.
144. Roe, C.R., et al., *Treatment of cardiomyopathy and rhabdomyolysis in long-chain fat oxidation disorders using an anaplerotic odd-chain triglyceride.* J Clin Invest, 2002. **110**(2): p. 259-69.
145. Buist, M., D. Fuss, and M. Rastegar, *Transcriptional Regulation of MECP2E1-E2 Isoforms and BDNF by Metformin and Simvastatin through Analyzing Nascent RNA Synthesis in a Human Brain Cell Line.* Biomolecules, 2021. **11**(8): p. 1253.
146. Villemagne, P.M., et al., *Brain glucose metabolism in Rett Syndrome.* Pediatr Neurol, 2002. **27**(2): p. 117-22.
147. Sevastre-Berghian, A.C., et al., *Targeting Oxidative Stress Reduction and Inhibition of HDAC1, MECP2, and NF-kB Pathways in Rats With Experimentally Induced Hyperglycemia by Administration of.* Front Pharmacol, 2020. **11**: p. 581470.

148. Krishnan, N., et al., *PTP1B inhibition suggests a therapeutic strategy for Rett syndrome.* J Clin Invest, 2015. **125**(8): p. 3163-77.
149. Vuu, Y.M., C.T. Roberts, and M. Rastegar, *MeCP2 Is an Epigenetic Factor That Links DNA Methylation with Brain Metabolism.* Int J Mol Sci, 2023. **24**(4).
150. Kuroda, A., et al., *Insulin gene expression is regulated by DNA methylation.* PLoS One, 2009. **4**(9): p. e6953.
151. Pitcher, M.R., et al., *Insulinotropic treatments exacerbate metabolic syndrome in mice lacking MeCP2 function.* Hum Mol Genet, 2013. **22**(13): p. 2626-33.
152. Ricciardi, S., et al., *Reduced AKT/mTOR signaling and protein synthesis dysregulation in a Rett syndrome animal model.* Hum Mol Genet, 2011. **20**(6): p. 1182-96.
153. Na, E.S. and L.M. Monteggia, *The role of MeCP2 in CNS development and function.* Horm Behav, 2011. **59**(3): p. 364-8.
154. Marzban, H., et al., *Cellular commitment in the developing cerebellum.* Front Cell Neurosci, 2014. **8**: p. 450.
155. Klauck, S.M., et al., *A mutation hot spot for nonspecific X-linked mental retardation in the MECP2 gene causes the PPM-X syndrome.* Am J Hum Genet, 2002. **70**(4): p. 1034-7.
156. Cooke, D.W., et al., *Abnormalities of thyroid function and glucose control in subjects with Rett syndrome.* Horm Res, 1995. **43**(6): p. 273-8.
157. Matsuishi, T., et al., *Abnormal carbohydrate metabolism in cerebrospinal fluid in Rett syndrome.* J Child Neurol, 1994. **9**(1): p. 26-30.
158. Can, K., et al., *Neuronal Redox-Imbalance in Rett Syndrome Affects Mitochondria as Well as Cytosol, and Is Accompanied by Intensified Mitochondrial O.* Front Physiol, 2019. **10**: p. 479.
159. Olson, C.O., et al., *MECP2 mutation interrupts nucleolin–mTOR–P70S6K signaling in Rett syndrome patients.* Frontiers in Genetics, 2018. **9**: p. 635.
160. Saxton, R.A. and D.M. Sabatini, *mTOR Signaling in Growth, Metabolism, and Disease.* Cell, 2017. **169**(2): p. 361-371.
161. Buist, M., et al., *Differential Sensitivity of the Protein Translation Initiation Machinery and mTOR Signaling to.* Cells, 2022. **11**(9).
162. Magnuson, B., B. Ekim, and D.C. Fingar, *Regulation and function of ribosomal protein S6 kinase (S6K) within mTOR signalling networks.* Biochem J, 2012. **441**(1): p. 1-21.

163. Ruvinsky, I., et al., *Ribosomal protein S6 phosphorylation is a determinant of cell size and glucose homeostasis.* Genes Dev, 2005. **19**(18): p. 2199-211.
164. Lazarus, M.B., R.S. Levin, and K.M. Shokat, *Discovery of new substrates of the elongation factor-2 kinase suggests a broader role in the cellular nutrient response.* Cell Signal, 2017. **29**: p. 78-83.
165. Li, Y., et al., *Global transcriptional and translational repression in human-embryonic-stem-cell-derived Rett syndrome neurons.* Cell Stem Cell, 2013. **13**(4): p. 446-58.
166. Slipczuk, L., et al., *BDNF activates mTOR to regulate GluR1 expression required for memory formation.* PLoS One, 2009. **4**(6): p. e6007.
167. Liu, J. and U. Francke, *Identification of cis-regulatory elements for MECP2 expression.* Hum Mol Genet, 2006. **15**(11): p. 1769-82.
168. Mihaylova, M.M. and R.J. Shaw, *The AMPK signalling pathway coordinates cell growth, autophagy and metabolism.* Nat Cell Biol, 2011. **13**(9): p. 1016-23.
169. McGee, S.L., et al., *Normal hypertrophy accompanied by phosphoryation and activation of AMP-activated protein kinase alpha1 following overload in LKB1 knockout mice.* J Physiol, 2008. **586**(6): p. 1731-41.
170. Lira, V.A., et al., *Nitric oxide increases GLUT4 expression and regulates AMPK signaling in skeletal muscle.* Am J Physiol Endocrinol Metab, 2007. **293**(4): p. E1062-8.
171. Toloe, J., et al., *Metabolic differences in hippocampal 'Rett' neurons revealed by ATP imaging.* Mol Cell 23, 2014. **59**: p. 47-56.
172. Golubiani, G., et al., *Metabolomic Fingerprint of Mecp2-Deficient Mouse Cortex: Evidence for a Pronounced Multi-Facetted Metabolic Component in Rett Syndrome.* Cells, 2021. **10**(9).
173. Foretz, M., et al., *Metformin: from mechanisms of action to therapies.* Cell Metab, 2014. **20**(6): p. 953-66.
174. DeFronzo, R.A. and A.M. Goodman, *Efficacy of metformin in patients with non-insulin-dependent diabetes mellitus. The Multicenter Metformin Study Group.* N Engl J Med, 1995. **333**(9): p. 541-9.
175. Paudel, Y.N., et al., *Emerging neuroprotective effect of metformin in Parkinson's disease: A molecular crosstalk.* Pharmacol Res, 2020. **152**: p. 104593.

176. Correll, C.U., et al., *Metformin add-on vs. antipsychotic switch vs. continued antipsychotic treatment plus healthy lifestyle education in overweight or obese youth with severe mental illness: results from the IMPACT trial.* World Psychiatry, 2020. **19**(1): p. 69-80.
177. Arnoux, I., et al., *Metformin reverses early cortical network dysfunction and behavior changes in Huntington's disease.* Elife, 2018. **7**.
178. Gantois, I., et al., *Metformin ameliorates core deficits in a mouse model of fragile X syndrome.* Nature medicine, 2017. **23**(6): p. 674-677.
179. Cao, G., et al., *Mechanism of metformin regulation in central nervous system: Progression and future perspectives.* Biomedicine & Pharmacotherapy, 2022. **156**: p. 113686.
180. Dy, A.B.C., et al., *Metformin as targeted treatment in fragile X syndrome.* Clin Genet, 2018. **93**(2): p. 216-222.
181. Kessing, L.V., et al., *Antidiabetes Agents and Incident Depression: A Nationwide Population-Based Study.* Diabetes Care, 2020. **43**(12): p. 3050-3060.
182. Zemdegs, J., et al., *Metformin Promotes Anxiolytic and Antidepressant-Like Responses in Insulin-Resistant Mice by Decreasing Circulating Branched-Chain Amino Acids.* J Neurosci, 2019. **39**(30): p. 5935-5948.
183. Herzig, S. and R.J. Shaw, *AMPK: guardian of metabolism and mitochondrial homeostasis.* Nat Rev Mol Cell Biol, 2018. **19**(2): p. 121-135.
184. Patil, S.P., et al., *Neuroprotective effect of metformin in MPTP-induced Parkinson's disease in mice.* Neuroscience, 2014. **277**: p. 747-54.
185. Mor, D.E., et al., *Metformin rescues Parkinson's disease phenotypes caused by hyperactive mitochondria.* Proc Natl Acad Sci U S A, 2020. **117**(42): p. 26438-26447.
186. Tayara, K., et al., *Divergent Effects of Metformin on an Inflammatory Model of Parkinson's Disease.* Front Cell Neurosci, 2018. **12**: p. 440.
187. Koenig, A.M., et al., *Effects of the Insulin Sensitizer Metformin in Alzheimer Disease: Pilot Data From a Randomized Placebo-controlled Crossover Study.* Alzheimer Dis Assoc Disord, 2017. **31**(2): p. 107-113.
188. Scherrer, J.F., et al., *Metformin and Sulfonylurea Use and Risk of Incident Dementia.* Mayo Clin Proc, 2019. **94**(8): p. 1444-1456.
189. Farr, S.A., et al., *Metformin Improves Learning and Memory in the SAMP8 Mouse Model of Alzheimer's Disease.* J Alzheimers Dis, 2019. **68**(4): p. 1699-1710.

190. Wang, L., Y. Cai, and X. Fan, *Metformin administration during early postnatal life rescues autistic-like behaviors in the BTBR T+ Itpr3tf/J mouse model of autism.* Frontiers in behavioral neuroscience, 2018. **12**: p. 290.
191. Zuliani, I., et al., *The Anti-Diabetic Drug Metformin Rescues Aberrant Mitochondrial Activity and Restrains Oxidative Stress in a Female Mouse Model of Rett Syndrome.* J Clin Med, 2020. **9**(6).
192. Jellinger, K.A., *Basic mechanisms of neurodegeneration: a critical update.* J Cell Mol Med, 2010. **14**(3): p. 457-87.
193. Kalia, L.V. and A.E. Lang, *Parkinson's disease.* Lancet, 2015. **386**(9996): p. 896-912.
194. Abdelaziz, D.H., et al., *Metformin reduces prion infection in neuronal cells by enhancing autophagy.* Biochem Biophys Res Commun, 2020. **523**(2): p. 423-428.
195. Stavoe, A.K.H. and E.L.F. Holzbaur, *Autophagy in Neurons.* Annu Rev Cell Dev Biol, 2019. **35**: p. 477-500.
196. Komatsu, M., et al., *Loss of autophagy in the central nervous system causes neurodegeneration in mice.* Nature, 2006. **441**(7095): p. 880-4.
197. Hara, T., et al., *Suppression of basal autophagy in neural cells causes neurodegenerative disease in mice.* Nature, 2006. **441**(7095): p. 885-9.
198. Kim, Y.C. and K.L. Guan, *mTOR: a pharmacologic target for autophagy regulation.* J Clin Invest, 2015. **125**(1): p. 25-32.
199. Jeon, S.M., *Regulation and function of AMPK in physiology and diseases.* Exp Mol Med, 2016. **48**(7): p. e245.
200. Kim, J., et al., *Differential regulation of distinct Vps34 complexes by AMPK in nutrient stress and autophagy.* Cell, 2013. **152**(1-2): p. 290-303.
201. Kim, J., et al., *AMPK and mTOR regulate autophagy through direct phosphorylation of Ulk1.* Nat Cell Biol, 2011. **13**(2): p. 132-41.
202. Benito-Cuesta, I., L. Ordóñez-Gutiérrez, and F. Wandosell, *AMPK activation does not enhance autophagy in neurons in contrast to MTORC1 inhibition: different impact on β-amyloid clearance.* Autophagy, 2021. **17**(3): p. 656-671.
203. Barini, E., et al., *Metformin promotes tau aggregation and exacerbates abnormal behavior in a mouse model of tauopathy.* Mol Neurodegener, 2016. **11**: p. 16.

204. Li, J., et al., *Metformin attenuates Alzheimer's disease-like neuropathology in obese, leptin-resistant mice.* Pharmacol Biochem Behav, 2012. **101**(4): p. 564-74.
205. Eskens, B.J., et al., *Effects of two weeks of metformin treatment on whole-body glycocalyx barrier properties in db/db mice.* Cardiovasc Diabetol, 2013. **12**: p. 175.
206. Ghadernezhad, N., et al., *Metformin pretreatment enhanced learning and memory in cerebral forebrain ischaemia: the role of the AMPK/BDNF/P70SK signalling pathway.* Pharmaceutical biology, 2016. **54**(10): p. 2211-2219.
207. Wang, Y., et al., *Metformin ameliorates synaptic defects in a mouse model of AD by inhibiting Cdk5 activity.* Frontiers in cellular neuroscience, 2020. **14**: p. 170.
208. Fang, W., et al., *Metformin ameliorates stress-induced depression-like behaviors via enhancing the expression of BDNF by activating AMPK/CREB-mediated histone acetylation.* Journal of affective disorders, 2020. **260**: p. 302-313.
209. Xiao, H., et al., *Metformin attenuates cardiac fibrosis by inhibiting the TGFβ1–Smad3 signalling pathway.* Cardiovascular research, 2010. **87**(3): p. 504-513.
210. Liu, B., et al., *Dendrobium nobile Lindl alkaloid and metformin ameliorate cognitive dysfunction in senescence-accelerated mice via suppression of endoplasmic reticulum stress.* Brain Res, 2020. **1741**: p. 146871.
211. Teo, E., et al., *Metabolic stress is a primary pathogenic event in transgenic.* Elife, 2019. **8**.
212. Peralta, S., et al., *Metformin delays neurological symptom onset in a mouse model of neuronal complex I deficiency.* JCI Insight, 2020. **5**(21).
213. Matassa, D.S., et al., *Oxidative metabolism drives inflammation-induced platinum resistance in human ovarian cancer.* Cell Death Differ, 2016. **23**(9): p. 1542-54.
214. Houtkooper, R.H., et al., *Mitonuclear protein imbalance as a conserved longevity mechanism.* Nature, 2013. **497**(7450): p. 451-7.
215. Mouchiroud, L., et al., *The NAD(+)/Sirtuin Pathway Modulates Longevity through Activation of Mitochondrial UPR and FOXO Signaling.* Cell, 2013. **154**(2): p. 430-41.
216. Docrat, T.F., et al., *The protective effect of metformin on mitochondrial dysfunction and endoplasmic reticulum stress in diabetic mice brain.* Eur J Pharmacol, 2020. **875**: p. 173059.
217. Hawley, S.A., et al., *Use of cells expressing gamma subunit variants to identify diverse mechanisms of AMPK activation.* Cell Metab, 2010. **11**(6): p. 554-65.

218. Zhou, G., et al., *Role of AMP-activated protein kinase in mechanism of metformin action.* J Clin Invest, 2001. **108**(8): p. 1167-74.
219. Miller, R.A., et al., *Biguanides suppress hepatic glucagon signalling by decreasing production of cyclic AMP.* Nature, 2013. **494**(7436): p. 256-60.
220. Kim, Y.D., et al., *Metformin ameliorates IL-6-induced hepatic insulin resistance via induction of orphan nuclear receptor small heterodimer partner (SHP) in mouse models.* Diabetologia, 2012. **55**(5): p. 1482-94.
221. He, L., et al., *Metformin and insulin suppress hepatic gluconeogenesis through phosphorylation of CREB binding protein.* Cell, 2009. **137**(4): p. 635-46.
222. Howell, J.J., et al., *Metformin Inhibits Hepatic mTORC1 Signaling via Dose-Dependent Mechanisms Involving AMPK and the TSC Complex.* Cell Metab, 2017. **25**(2): p. 463-471.
223. Kovacic, S., et al., *Akt activity negatively regulates phosphorylation of AMP-activated protein kinase in the heart.* J Biol Chem, 2003. **278**(41): p. 39422-7.
224. Duca, F.A., et al., *Metformin activates a duodenal Ampk-dependent pathway to lower hepatic glucose production in rats.* Nat Med, 2015. **21**(5): p. 506-11.
225. Foretz, M., et al., *Metformin inhibits hepatic gluconeogenesis in mice independently of the LKB1/AMPK pathway via a decrease in hepatic energy state.* J Clin Invest, 2010. **120**(7): p. 2355-69.
226. Madiraju, A.K., et al., *Metformin suppresses gluconeogenesis by inhibiting mitochondrial glycerophosphate dehydrogenase.* Nature, 2014. **510**(7506): p. 542-6.
227. Kalender, A., et al., *Metformin, independent of AMPK, inhibits mTORC1 in a rag GTPase-dependent manner.* Cell Metab, 2010. **11**(5): p. 390-401.
228. Li, N., T. Zhou, and E. Fei, *Actions of Metformin in the Brain: A New Perspective of Metformin Treatments in Related Neurological Disorders.* Int J Mol Sci, 2022. **23**(15).
229. Banks, W.A., *From blood-brain barrier to blood-brain interface: new opportunities for CNS drug delivery.* Nat Rev Drug Discov, 2016. **15**(4): p. 275-92.
230. Łabuzek, K., et al., *Quantification of metformin by the HPLC method in brain regions, cerebrospinal fluid and plasma of rats treated with lipopolysaccharide.* Pharmacol Rep, 2010. **62**(5): p. 956-65.

231. Chen, Y., et al., *Antidiabetic drug metformin (GlucophageR) increases biogenesis of Alzheimer's amyloid peptides via up-regulating BACE1 transcription.* Proc Natl Acad Sci U S A, 2009. **106**(10): p. 3907-12.

232. Liang, D., et al., *Cytotoxic edema: mechanisms of pathological cell swelling.* Neurosurg Focus, 2007. **22**(5): p. E2.

233. Nath, N., et al., *Metformin attenuated the autoimmune disease of the central nervous system in animal models of multiple sclerosis.* J Immunol, 2009. **182**(12): p. 8005-14.

234. Sharma, S., et al., *Repurposing metformin to treat age-related neurodegenerative disorders and ischemic stroke.* Life Sci, 2021. **274**: p. 119343.

235. Tucker, G.T., et al., *Metformin kinetics in healthy subjects and in patients with diabetes mellitus.* Br J Clin Pharmacol, 1981. **12**(2): p. 235-46.

236. Samodelov, S.L., et al., *Organic Cation Transporters in Human Physiology, Pharmacology, and Toxicology.* Int J Mol Sci, 2020. **21**(21).

237. Liang, X., et al., *Metformin Is a Substrate and Inhibitor of the Human Thiamine Transporter, THTR-2 (SLC19A3).* Mol Pharm, 2015. **12**(12): p. 4301-10.

238. Vialou, V., et al., *Altered aminergic neurotransmission in the brain of organic cation transporter 3-deficient mice.* J Neurochem, 2008. **106**(3): p. 1471-82.

239. Cui, M., et al., *The organic cation transporter-3 is a pivotal modulator of neurodegeneration in the nigrostriatal dopaminergic pathway.* Proc Natl Acad Sci U S A, 2009. **106**(19): p. 8043-8.

240. Chaves, C., et al., *An Interspecies Molecular and Functional Study of Organic Cation Transporters at the Blood-Brain Barrier: From Rodents to Humans.* Pharmaceutics, 2020. **12**(4).

241. Du, Y., et al., *Metformin in therapeutic applications in human diseases: its mechanism of action and clinical study.* Mol Biomed, 2022. **3**(1): p. 41.

242. Owen, M.R., E. Doran, and A.P. Halestrap, *Evidence that metformin exerts its anti-diabetic effects through inhibition of complex 1 of the mitochondrial respiratory chain.* Biochem J, 2000. **348 Pt 3**(Pt 3): p. 607-14.

243. Li, W., et al., *Metformin Alters Locomotor and Cognitive Function and Brain Metabolism in Normoglycemic Mice.* Aging Dis, 2019. **10**(5): p. 949-963.

244. Engber, D., *The mouse trap.* Slate Magazine, 2011. **15**.

245. Lyst, M.J., et al., *Rett syndrome mutations abolish the interaction of MeCP2 with the NCoR/SMRT co-repressor.* Nature neuroscience, 2013. **16**(7): p. 898-902.

246. Wang, J., et al., *Metformin activates an atypical PKC-CBP pathway to promote neurogenesis and enhance spatial memory formation.* Cell Stem Cell, 2012. **11**(1): p. 23-35.

247. Gkogkas, C.G., et al., *Pharmacogenetic inhibition of eIF4E-dependent Mmp9 mRNA translation reverses fragile X syndrome-like phenotypes.* Cell Rep, 2014. **9**(5): p. 1742-1755.

248. Hou, L., et al., *Dynamic translational and proteasomal regulation of fragile X mental retardation protein controls mGluR-dependent long-term depression.* Neuron, 2006. **51**(4): p. 441-54.

249. Deng, W., et al., *Effect of metformin in autistic BTBR T + Itpr3tf/J mice administered a high-fat diet.* Brain Res Bull, 2022. **183**: p. 172-183.

250. Mehrabi, S., et al., *Evaluation of metformin effects in the chronic phase of spontaneous seizures in pilocarpine model of temporal lobe epilepsy.* Metab Brain Dis, 2018. **33**(1): p. 107-114.

251. Yang, A.J.T., S. Frendo-Cumbo, and R.E.K. MacPherson, *Resveratrol and Metformin Recover Prefrontal Cortex AMPK Activation in Diet-Induced Obese Mice but Reduce BDNF and Synaptophysin Protein Content.* J Alzheimers Dis, 2019. **71**(3): p. 945-956.

252. Rösen, P. and N.F. Wiernsperger, *Metformin delays the manifestation of diabetes and vascular dysfunction in Goto-Kakizaki rats by reduction of mitochondrial oxidative stress.* Diabetes Metab Res Rev, 2006. **22**(4): p. 323-30.

253. Tunc-Ozcan, E., et al., *Hippocampus-dependent memory and allele-specific gene expression in adult offspring of alcohol-consuming dams after neonatal treatment with thyroxin or metformin.* Mol Psychiatry, 2018. **23**(7): p. 1643-1651.

254. Achilly, N.P., et al., *Deleting Mecp2 from the cerebellum rather than its neuronal subtypes causes a delay in motor learning in mice.* Elife, 2021. **10**: p. e64833.

255. van den Berg, K.R. and R.C. Helmich, *The role of the cerebellum in tremor–evidence from neuroimaging.* Tremor and Other Hyperkinetic Movements, 2021. **11**.

256. Lalonde, R. and C. Strazielle, *Brain regions and genes affecting limb-clasping responses.* Brain research reviews, 2011. **67**(1-2): p. 252-259.

257. Boggio, E.M., et al., *Synaptic determinants of rett syndrome.* Frontiers in synaptic neuroscience, 2010. **2**: p. 28.

258. Dong, Q., et al., *An astrocytic influence on impaired tonic inhibition in hippocampal CA1 pyramidal neurons in a mouse model of Rett syndrome.* Journal of Neuroscience, 2020. **40**(32): p. 6250-6261.

259. Silvestre, M.F., et al., *The AMPK-SIRT signaling network regulates glucose tolerance under calorie restriction conditions.* Life Sci, 2014. **100**(1): p. 55-60.

260. Ma, X., et al., *Metformin restores hippocampal neurogenesis and learning and memory via regulating gut microbiota in the obese mouse model.* Brain Behav Immun, 2021. **95**: p. 68-83.

261. Rastegar, M., et al., *Sequential histone modifications at Hoxd4 regulatory regions distinguish anterior from posterior embryonic compartments.* Molecular and cellular biology, 2004. **24**(18): p. 8090-8103.

262. Zachariah, R.M., et al., *Novel MeCP2 isoform-specific antibody reveals the endogenous MeCP2E1 expression in murine brain, primary neurons and astrocytes.* PLoS One, 2012. **7**(11): p. e49763.

263. Sheikholeslami, K., et al., *Simvastatin induces apoptosis in medulloblastoma brain tumor cells via mevalonate cascade prenylation substrates.* Cancers, 2019. **11**(7): p. 994.

264. Amiri, S., J.R. Davie, and M. Rastegar, *Chronic ethanol exposure alters DNA methylation in neural stem cells: role of mouse strain and sex.* Molecular Neurobiology, 2020. **57**: p. 650-667.

265. Xu, W., et al., *Genome-wide transcriptome landscape of embryonic brain-derived neural stem cells exposed to alcohol with strain-specific cross-examination in BL6 and CD1 mice.* Scientific Reports, 2019. **9**(1): p. 206.

266. Liyanage, V.R.B., et al., *Ethanol deregulates Mecp2/MeCP2 in differentiating neural stem cells via interplay between 5-methylcytosine and 5-hydroxymethylcytosine at the Mecp2 regulatory elements.* Experimental neurology, 2015. **265**: p. 102-117.

267. Lueptow, L.M., *Novel object recognition test for the investigation of learning and memory in mice.* JoVE (Journal of Visualized Experiments), 2017(126): p. e55718.

268. Leger, M., et al., *Object recognition test in mice.* Nature protocols, 2013. **8**(12): p. 2531-2537.

269. Moazzam, S., et al., *Effects of high fat diet-induced obesity and pregnancy on prepartum and postpartum maternal mouse behavior.* Psychoneuroendocrinology, 2021. **126**: p. 105147.

270. Barber, B.A., et al., *Dynamic expression of MEIS1 homeoprotein in E14. 5 forebrain and differentiated forebrain-derived neural stem cells.* Annals of Anatomy-Anatomischer Anzeiger, 2013. **195**(5): p. 431-440.

271. Kushida, M., et al., *Dose-related induction of hepatic preneoplastic lesions by diethylnitrosamine in C57BL/6 mice.* Toxicologic pathology, 2011. **39**(5): p. 776-786.

272. Matsui, Y., et al., *Metformin reduces body weight gain and improves glucose intolerance in high-fat diet-fed C57BL/6J mice.* Biological and Pharmaceutical Bulletin, 2010. **33**(6): p. 963-970.

273. Bramble, M.S., N. Vashist, and E. Vilain, *Sex steroid hormone modulation of neural stem cells: a critical review.* Biology of sex Differences, 2019. **10**(1): p. 1-10.

274. Vial, G., D. Detaille, and B. Guigas, *Role of Mitochondria in the Mechanism(s) of Action of Metformin.* Front Endocrinol (Lausanne), 2019. **10**: p. 294.

275. Kim, J., et al., *AMPK activators: mechanisms of action and physiological activities.* Exp Mol Med, 2016. **48**(4): p. e224.

276. Rastegar, M., *Epigenetics and cerebellar neurodevelopmental disorders.* Development of the cerebellum from molecular aspects to diseases, 2017: p. 197-218.

277. Castro, J., et al., *Functional recovery with recombinant human IGF1 treatment in a mouse model of Rett Syndrome.* Proceedings of the National Academy of Sciences, 2014. **111**(27): p. 9941-9946.

278. Pitcher, M.R., et al., *Rett syndrome like phenotypes in the R255X Mecp2 mutant mouse are rescued by MECP2 transgene.* Human molecular genetics, 2015. **24**(9): p. 2662-2672.

279. Vogel Ciernia, A., et al., *Early motor phenotype detection in a female mouse model of Rett syndrome is improved by cross-fostering.* Human Molecular Genetics, 2017. **26**(10): p. 1839-1854.

280. Guy, J., et al., *Reversal of neurological defects in a mouse model of Rett syndrome.* Science, 2007. **315**(5815): p. 1143-1147.

281. Jorge-Torres, O.C., et al., *Inhibition of Gsk3b reduces Nfkb1 signaling and rescues synaptic activity to improve the Rett syndrome phenotype in Mecp2-knockout mice.* Cell Reports, 2018. **23**(6): p. 1665-1677.

282. Goffin, D., et al., *Rett syndrome mutation MeCP2 T158A disrupts DNA binding, protein stability and ERP responses.* Nature neuroscience, 2012. **15**(2): p. 274-283.

283. Patrizi, A., et al., *Chronic administration of the N-methyl-D-aspartate receptor antagonist ketamine improves Rett syndrome phenotype.* Biological Psychiatry, 2016. **79**(9): p. 755-764.

284. Stearns, N., et al., *Behavioral and anatomical abnormalities in Mecp2 mutant mice: a model for Rett syndrome.* Neuroscience, 2007. **146**(3): p. 907-921.

285. Napoleão, A., et al., *Effects of Calorie Restriction on Health Span and Insulin Resistance: Classic Calorie Restriction Diet vs. Ketosis-Inducing Diet.* Nutrients, 2021. **13**(4).

286. Correia, S., et al., *Mechanisms of action of metformin in type 2 diabetes and associated complications: an overview.* Mini Rev Med Chem, 2008. **8**(13): p. 1343-54.

287. Allard, J.S., et al., *Prolonged metformin treatment leads to reduced transcription of Nrf2 and neurotrophic factors without cognitive impairment in older C57BL/6J mice.* Behav Brain Res, 2016. **301**: p. 1-9.

288. Martin-Montalvo, A., et al., *Metformin improves healthspan and lifespan in mice.* Nat Commun, 2013. **4**: p. 2192.

289. LaMoia, T.E. and G.I. Shulman, *Cellular and Molecular Mechanisms of Metformin Action.* Endocr Rev, 2021. **42**(1): p. 77-96.

290. McNeilly, A.D., et al., *A high-fat-diet-induced cognitive deficit in rats that is not prevented by improving insulin sensitivity with metformin.* Diabetologia, 2012. **55**(11): p. 3061-70.

291. He, L. and F.E. Wondisford, *Metformin action: concentrations matter.* Cell Metab, 2015. **21**(2): p. 159-162.

292. Subramaniam, B., S. Naidu, and A.L. Reiss, *Neuroanatomy in Rett syndrome: cerebral cortex and posterior fossa.* Neurology, 1997. **48**(2): p. 399-407.

293. Armstrong, D.D., *Neuropathology of Rett syndrome.* J Child Neurol, 2005. **20**(9): p. 747-53.

294. Reiss, A.L., et al., *Neuroanatomy of Rett syndrome: a volumetric imaging study.* Ann Neurol, 1993. **34**(2): p. 227-34.

295. Kaufmann, W.E. and H.W. Moser, *Dendritic anomalies in disorders associated with mental retardation.* Cereb Cortex, 2000. **10**(10): p. 981-91.

296. Hsu, C.C., et al., *Incidence of dementia is increased in type 2 diabetes and reduced by the use of sulfonylureas and metformin.* J Alzheimers Dis, 2011. **24**(3): p. 485-93.

297. Imfeld, P., et al., *Metformin, other antidiabetic drugs, and risk of Alzheimer's disease: a population-based case-control study.* J Am Geriatr Soc, 2012. **60**(5): p. 916-21.